FORMULATION, CHARACTERIZATION AND EVALUATION OF NANOSPONGE-BASED DRUG DELIVERY SYSTEM FOR POORLY SOLUBLE DRUGS

Thesis Submitted for the Award of the Degree of

DOCTOR OF PHILOSOPHY

in

Pharmaceutics

By

Mohit Vij

Registration Number: 41800748

Supervised By

Dr. Pankaj Wadhwa (23400)

Department of Pharmaceutical Sciences (Associate Professor)
Lovely Professional University

LOVELY PROFESSIONAL UNIVERSITY
PUNJAB, INDIA
2023

DECLARATION

I, hereby declared that the presented work in the thesis entitled "**Formulation, characterization and evaluation of nanosponge-based drug delivery system for poorly soluble drugs**" in fulfilment of degree of **Doctor of Philosophy (Ph. D.)** is outcome of research work carried out by me under the supervision **Dr. Pankaj Wadhwa**, working as Associate Professor, in the Department of Pharmaceutical Sciences, Lovely Professional University, Punjab, India. In keeping with general practice of reporting scientific observations, due acknowledgements have been made whenever work described here has been based on findings of other investigator. This work has not been submitted in part or full to any other University or Institute for the award of any degree.

Mohit Vij
Registration No.: 41800748
Department of Pharmaceutical Sciences,
Lovely Professional University,
Punjab, India

CERTIFICATE

This is to certify that the work reported in the Ph.D. thesis entitled "**Formulation, characterization and evaluation of nanosponge-based drug delivery system for poorly soluble drugs**" submitted in fulfillment of the requirement for the reward of degree of **Doctor of Philosophy (Ph.D.)** in the Department of Pharmaceutical Sciences, is a research work carried out by **Mohit Vij**, 41800748, is bonafide record of his/her original work carried out under my supervision and that no part of thesis has been submitted for any other degree, diploma or equivalent course.

Supervisor
Dr. Pankaj Wadhwa
Associate Professor
Department of Pharmaceutical Sciences,
Lovely Professional University,
Punjab, India

ACKNOWLEDGEMENT

TABLE OF CONTENTS

LIST OF TABLES

LIST OF FIGURES

LIST OF ABBREVIATIONS

Abbreviation	Full form
µg	Microgram
µL	Microliter
ACN	Acetonitrile
ANOVA	Analysis of Variance
AUC	Area Under the Curve
BCS	Biopharmaceutical Classification System
CD	Cyclodextrin
CDI	Carbonyldiimidazole
CDNS	Cyclodextrin-Based Nanosponges
CIN	Cinnarizine
Cl	Clearance
Cm	Centimeter
Cmax	Maximum concentration
D/W	Distilled water
DMC	Dimethyl Carbonate
DMF	Dimethylformamide
DMSO	Dimethyl Sulfoxide
DOE	Design of Experiments
DOM	Domperidone
DPC	Diphenyl Carbonate
DSC	Differential Scanning Calorimetry
DTA	Differential Thermal Analysis
EDTA	Ethylene Diamine Tetraacetic Acid
FTIR	Fourier Transform-Infrared Spectroscopy
GIT	Gastrointestinal Tract
Gm	Gram
GRAS	Generally Regarded as Safe
HBV	Hepatitis B Virus
HETP	Height Equivalent to Theoretical Plate

Abbreviation	Full form
HIV	Human Immunodeficiency Virus
HPLC	High Performance Liquid Chromatography
HPβCD	Hydroxypropyl-β-Cyclodextrin
HQC	Higher Quality Control Standards
hr	Hour
ICH	International Council for Harmonization
IP	Indian pharmacopoeia
IRB	Irbesartan
IS	Internal Standard
IUPAC	International Union of Pure and Applied Chemistry
Kg	Kilogram
Ks	Binding constant
L	Liter
LOD	Limit of Detection
LOQ	Limit of Quantification
LQC	Lower Quality Control
Met	Methanol
min	Minute
mL	Milliliter
mM	Millimolar
MQC	Medium Quality Control
MRt	Mean Residence Time
MW	Microwave
MW-NS	Microwave-Assisted Nanosponges
MβCD	Methyl-β-Cyclodextrin
Nm	Nanometer
NMR	Nuclear Magnetic Resonance
NS	Nanosponge
ODT	Oral Dispersible Tablet
PDI	Polydispersity Index
PK	Pharmacokinetic

Abbreviation	Full form
PXRD	Powder X-ray Diffraction
RP-HPLC	Reverse Phase High Performance Liquid Chromatography
rpm	Rotations per minute
RSD	Relative Standard Deviation
SD	Standard Deviation
SEM	Scanning Electron Microscopy
t1/2	Half-life
TEM	Transmission Electron Microscopy
TGA	Thermogravimetric Analysis
tmax	Time for maximum absorption
US	Ultrasound
USFDA	United States Food and Drug Administration
US-NS	Ultrasound-Assisted Nanosponges
USP	United States Pharmacopoeia
UV	Ultraviolet
Vd	Volume of Distribution
W	Watt
XRPD	X-Ray Powder Diffraction
β-CD	Beta-Cyclodextrin
λmax	Absorbance maximum

LIST OF ANNEXURES	
Annexure Number	**Title**
Appendix I	Letter of Candidacy for Ph.D.
Appendix II	Publications
Appendix III	Poster presentation Certificates
Appendix IV	CPCSEA Approval Certificate

ABSTRACT

Highly cross-linked cyclodextrin polymers that have been nanostructured in three-dimensional networks make up cyclodextrin-based nanosponges. Nanosponges made of cyclodextrin can be complexed with a variety of hydrophilic and lipophilic compounds. Degradable materials can be preserved, weakly water-soluble compounds can be made more soluble in aqueous solutions, and new delivery mechanisms for pharmaceuticals, cosmetics, protein/peptide delivery, and diagnostics can be achieved by utilizing nanosponges. The conventional techniques of producing cyclodextrin-based nanosponges yield amorphous nanosponges with low entrapment efficiency, prolonged reaction durations, heat-induced instability, large solvent consumption, non-uniform reactions, complex preparative steps, and obstacles to bulk scaling. It was essential to employ new modern methods, such as microwave and ultrasonic-assisted synthesis of cyclodextrin-based nanosponges, and to investigate the effects of these cutting-edge synthetic techniques on the physical, morphological, and performance properties of nanosponges.

In order to improve the application of cyclodextrin-based nanosponges, the current study carried out to investigate these approaches for its preparation and to combination two drug such as domperidone and cinnarizine inside of its cavity. According to the results of the phase solubility study, both hydroxyl propyl β-cyclodextrin and β-cyclodextrin are suitable as the monomer to synthesise cyclodextrin-based nanosponges for the selected drugs. Due to the fact that the Box-Behnken design is excellent for studying quadratic response surfaces and developing second-order polynomial models., it was adopted as the methodology to improve the synthesis strategy. The yield and particle size were taken into account as the most key considerations in the optimization of both the microwave-assisted and ultrasonication-assisted procedures.

The developed nanosponges had a particle size ranging from 150 – 200 nm with a very narrow polydispersity index of 0.2 – 0.3. The zeta potential was found to be around -10 mV. The % entrapment efficiency of MW-NS was found to be 80% while that of the US-NS was found to be 61%. FTIR, DSC, and XRD studies proved that the drug was encapsulated within the cavities of the nanosponges as opposed to surface adsorption.

The SEM images revealed that the nanocarrier was porous. The hypothesis that these nanosponges could improve the aqueous solubility of weakly water-soluble drugs while also prolonging their drug release to ensure improved therapy and patient compliance was proven in vitro. Whereas the release of domperidone was found to be independent of the amount

remaining to be released, the release of cinnarizine from both nanosponges followed first-order kinetics. Both the nanosponges were successfully loaded into orally disintegrating tablets. The in-vivo pharmacokinetics investigation, which found that the bioavailability of domperidone increased by 2.75 times and that of cinnarizine by 4 times, further confirmed the hypothesis. The pharmacodynamic studies' findings showed that incorporating the drugs into nanosponges reduced the amount of kaolin that the animals consumed, indicating less GI distress/pica. This could be attributed to the improvement in solubility and overall bioavailability of both drugs.

Chapter 1
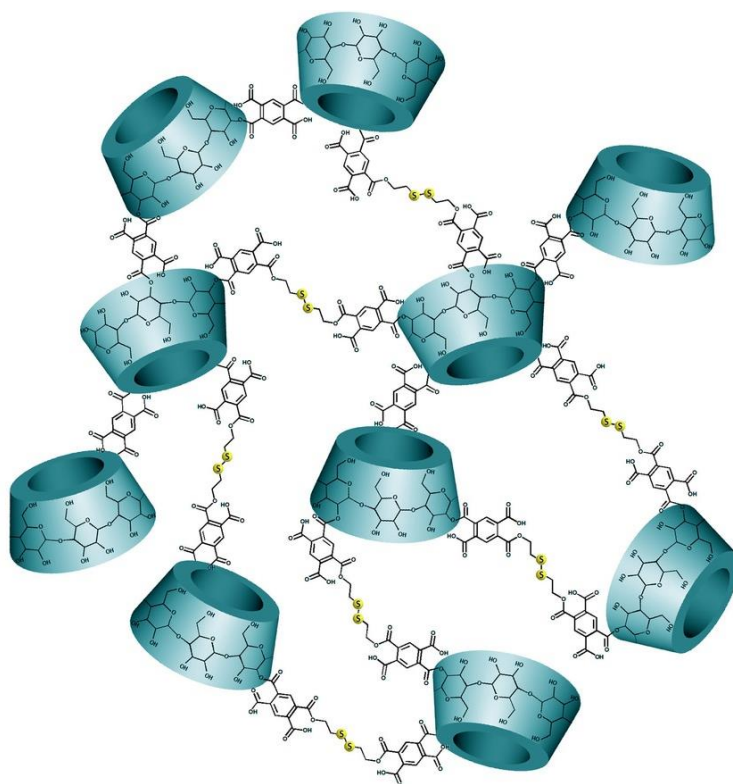
Introduction

1. INTRODUCTION

Oral administration remains the favoured way of administration used for the majority of medications, with more than 60% available as oral preparations [1]. The Biopharmaceutical Classification System (BCS) classifies drugs based on their solubility in water and their intestinal permeability, as illustrated in **Figure 1.1** [2]. It is reported that approximately 75% of chemical entities are low water-soluble, resulting in limited absorption and poor oral bioavailability. These pharmaceutical substances are categorised as BCS Class II and IV drugs. [3]. Oral administration of some drugs in their natural form is ineffective for a variety of reasons, including in vitro and in vivo instability, high first-pass metabolism, low membrane permeability and poor solubility, emphasising the significance of solubility and permeability in terms of bioavailability. Thus, active drug molecules must find a balance between hydrophilicity and lipophilicity to achieve optimum bioavailability [4].
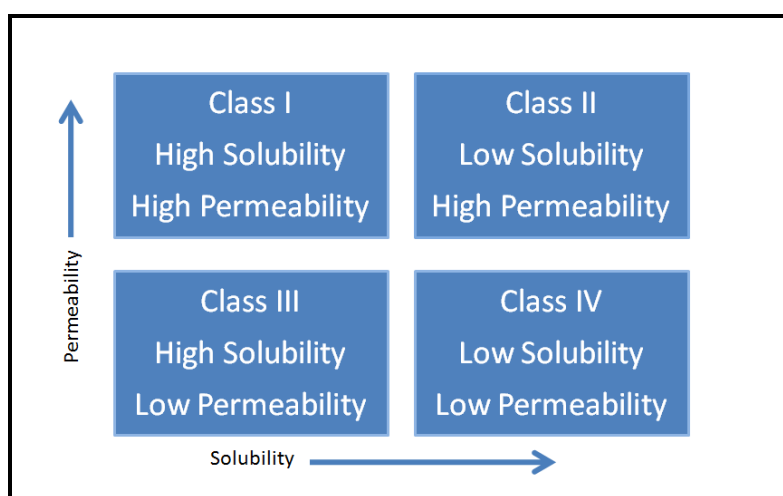
Figure 1.1: Representation of Biopharmaceutical Classification System of Drugs

Numerous strategies have been proposed and used to boost the marketability of drug candidates whose development is impeded by poor solubility or sluggish dissolution. Since hydrophobicity makes it simpler for drugs to enter the GIT, dissolution is the only thing that prevents hydrophobic drugs from entering the body. Structure-based and formulation-based approaches can both be used to improve a pharmaceutical's dissolution profile. The first method uses micronization, salt production, and prodrugs to change the physical or chemical structure [5]. The medication can also be integrated into a variety of

nanocarriers, such as hydrophilic polymers, cyclodextrins, cyclodextrin derivatives (nanosponges), nanosuspensions, nanoemulsions, and liposomes, resulting in a significant increase in solubility [6]. This technique is considered a novel delivery system because of the customized drug release and focused delivery features.

As an example, liposome-based formulations of poorly soluble drugs like docetaxel have shown a threefold increase in bioavailability [7,8]. Another report also describes an artemether nanoemulsion with enhanced solubility, stability, and oral bioavailability. Similar to the above, nanosponges can be used to increase telmisartan's intrinsic solubility and facilitate controlled release [9]. Nanosponges have also been demonstrated to have a sustained release of camptothecin in addition to improving oral bioavailability [10,11].

1.1 Solubility, dissolution, and dissolution rate

1.1.1 Basic consideration of solubility

International Union of Pure and Applied Chemistry (IUPAC) define solubility as the analytical configuration of a saturated solution expressed as a percentage of a specified solute in a specified solvent. It can also be expressed as ability of pharmaceuticals substances to dissolve in different types of solvent to produce a uniform solution of the solute in the solvent. The main factors that affects solubility are its solvent type, temperature, and pressure, respectively [12]. The strength of a chemical or drug substance in a solution does not rise when it reaches saturation in a suitable solvent. Solubility varies greatly, ranging from very soluble to poorly soluble substances. Insoluble compounds are those that dissolve very slowly or not at all in water. The dynamic balance between the processes of dissolving and phase joining is the source of solvability (e.g., precipitation of solids). When the two processes are occurring more frequently and at the identical rate, solubility equilibrium arises. Under certain conditions, it is plausible to exceed equilibrium solubility, leading to the formation of a metastable supersaturated solution [7]. Many different units are available for expressing solubility, such as concentration, molality, mole fractions, mole ratios, and so forth. Depending on the solubility of a solute in a given solvent under the specified conditions, one can calculate how much solute at equilibrium can be dissolved per unit amount of solvent. The descriptive terms for the approximate solubility are given in United States Pharmacopoeia (USP) and National Formulary substances as below in **Table 1.1**.

Table 1.1: Representing concepts of solubility

Parts of solvent required for each part of solute	Explanatory terminology
≤ 1	Very soluble
1 – 10	Freely soluble
10 – 30	Soluble
30 – 100	Sparingly soluble
100 – 1000	Slightly soluble
1000 – 10000	Very slightly soluble
≥ 10000	Practically insoluble or insoluble

1.1.2 Importance of Solubility

Drug molecules with limited aqueous solubility offer numerous challenges in pharmaceutical formulation development. When given orally, it can cause slow breakdown in bodily fluids, restricted and unpredictable systemic interaction, and sub-ideal effectiveness in individuals. Medication must be present in an aqueous solution to be absorbed in the absorption site. Dissolution of the drug in the blood is required for systemic distribution of medication following oral administration. Dissolution is dependent on the medicinal substance's solubility in the surrounding media. There is a general rule that polar medications are more soluble in water than in organic phases, but nonpolar solutes are just the contrary. Ionized species are more soluble in water than their non-ionized equivalents. As a result, the total solubility of acidic or basic compounds in an aqueous medium is pH-dependent. The oral absorption rate of drugs absorbed through passive diffusion is slower for those having a low aqueous solubility than for those having a high aqueous solubility. The aqueous solubility of pharmaceuticals has a significant impact on their pharmacokinetics (PK) and pharmacodynamics, which makes it an important characteristic for manufacturers [13,14].

1.1.3 Mechanism of Solubility

Drug dissolution is a process in which drug molecules migrate from a solid surface to a liquid medium. The process can be controlled by the affinity between the drug and the

dissolving medium. The dissolution will be greatly accelerated if the intermolecular forces between drug molecules are reduced as soon as possible. So, when a solvent can dislodge ions from its crystal lattice or structure, dissolution occurs. This process includes the dissolution of intermolecular or interionic bonds in the solvent, resulting in the production of holes. The crucial step in the process of solubilization is based on how the solute and solvent molecules bond together, as shown in **Figure 1.2**. Dipole interaction, London forces, hydrogen bonding, ionic bonding, and so on are the main types of bonds that make things solubilize [15]. Dissociation is the term used to describe the parting of ions caused by the engagement of a solvent. In general, molecules of polar solvents have the ability to dissolve ionic substances like salt by establishing bonds that are either polar or hydrogen. Positive ends of solvent molecules are attracted by negative ions of dissolved matter and vice versa. These ions are attracted to the slightly charged ends of water molecules. So as a consequence of this, the water molecules separate the ions and distribute them throughout the solution in equal amounts. A solution is formed when the separated solute molecules are incorporated into the solvent holes [16].
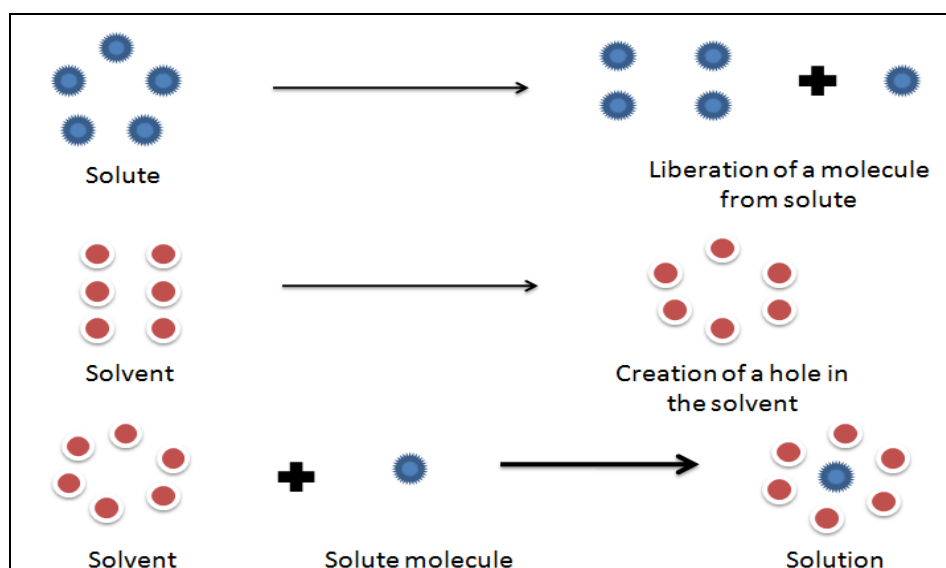
Figure 1.2: Representation of process of solubility

Dissolution of formulations is particularly critical for medications with a limited absorption window. The absorption of drugs via the gastrointestinal epithelia is dependent on the dissolution of the medication. The poor solubility of the medicine in water always leads to a sluggish rate of drug dissolution in coarse dispersion systems. Preparing dissolution-unconfined formulations for weakly water-soluble medications is a potential

method of increasing the oral absorption of these drugs. Several elements could potentially affect this process, including size, polymorphism, salt form, complexation, wettability, temperature, the concentration of the solute, and the dissolution rate constant. It can be used to improve the solubility of pharmaceuticals that are not easily dissolved in water. The ratio of the amount of drug ingredient that dissolves (dc) to the time interval (dt) under standardised temperature and solvent composition circumstances is referred to as the dissolution rate [17]. The variables such as solute-solvent attraction forces, temperature, polarities, ionisation and pH of the solvent can influence total solubility.

$$Dissolution\ rate = \frac{dC}{dt} \text{ -------------- Eq (1.1)}$$

Five basic physical phenomena cause drug dissolution, they are:

1. Wetting of drug.
2. Breaking of the drug's electrical attraction between cations and anions.
3. Drug molecules are solvated by water molecules.
4. Diffusion of drug particles.
5. Convection transports drug molecules, atoms and ions in a well-stirred bulk fluid.

The dissolving process involves two stages (as illustrated in **Figure 1.3**.) in which solute molecules are shifted by solvent molecules at the interface between the solute and solvent in the first phase. The second stage includes diffusion of solute molecules across the border layer, is the slower one.
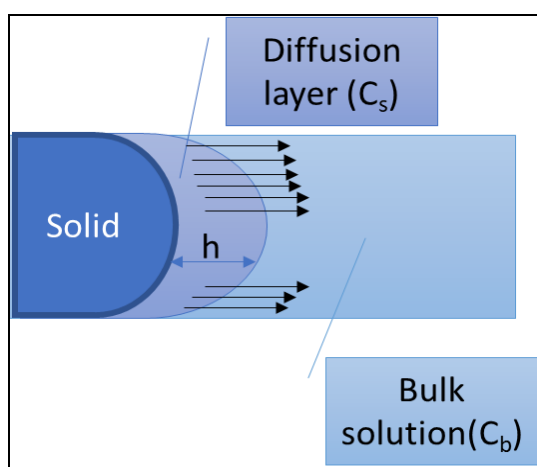
Figure 1.3: Schematic representation of the parameters of the Noyes – Whitney equation

Dissolution is a kinetic process by which a solute dissolves in a solvent to produce a solution. Solubility, on the other hand, is a thermodynamic process in which the system tries for the lowest potential energy (Gibbs free energy), which also happens to be the most thermodynamically stable situation. A solute's dissolving rate may be high even if it is weakly soluble in a solvent. Alternatively, some solutes are very soluble but take a long time to reach their saturation concentration [7]. During the formation of a homogeneous solution, between the two phases, a boundary layer forms. As the slowest step determines the dissolution rate overall, it is considered the rate-limiting step [18]. The dissolution process is described by the Noyes-Whitney equation, represented as equation 1.2.

$$\frac{dc}{dt} = \frac{DS(C_s - C_b)}{Vh}$$ ------------ Eq (1.2)

Here,

dc/dt =Dissolution rate; D = Diffusion coefficient; S = Surface area of the dissolving solid; V = Volume of the dissolution media; h = The diffusion layer's thickness; C_s = Solute concentration at the solid surface (saturated) and C_b = solute concentration in the bulk solution

1.2 Nanotechnology-based approaches for solubility enhancement

Nanotechnology offers a lot of promise in the pharmaceutical and medical fields. In recent years, numerous nanotechnology-based drug delivery systems that tackle the pharmacokinetic issues of various drugs have been developed. Nanotechnology-based drug delivery carriers having a size of less than 200 nm, are better than traditional methods in terms of controlled release, stability, and specificity. This technique, which includes carbon nanotubes, dendrimers, fullerenes, liposomes, nanosponges, nanosuspensions and many more, encapsulates pharmaceuticals spherically or as a surface coating and then releases them from their nanoparticles via degradation, diffusion, or swelling once they reach their target site of action [19].

A diverse range of routes for the administration of pharmaceuticals, as well as their capacity to transport both hydrophilic and lipophilic molecules, make them extremely versatile and popular in the pharmaceutical industry [20]. These nanomaterials are unique as their size and structure are related to biomolecules. Researchers are particularly interested in cyclodextrin-based nanosponges (CDNS) for tackling issues such as poor solubility, low dissolution, and inadequate stability of some therapeutics, as well as

improving their efficiency and reducing undesired adverse outcomes. This revolutionary system can also be available in a variety of dosage forms [21].

1.3 Cyclodextrin-based nanosponge (CDNS) as a prominent carrier

Nanotechnology has a long history of development. According to experts, there are no scientific barriers to the commercialization of nanomedicines. According to experts, there are no scientific barriers preventing nanomedicines from being commercialised. Until recently, innovations in pharmaceutical and health care were mostly evaluated based on their efficacy, safety, and quality, and cost-effectiveness was a secondary concern. The potential realization of pharmaceutical nanoparticles is limited by external factors, such as intellectual property rights, regulatory acceptance, industrial scalability, stability, clinical effectiveness, and toxicity [22,23]. Cyclodextrin-based nanoparticles, or nanosponges, may provide an answer to all of these problems since these nanoparticles are economic, non-mutagenic, non-irritating, non-toxic, and biodegradable. Unlike other nanomaterials, cyclodextrin-based nanosponges (CDNS) have an edge as cyclodextrin and its derivatives have wide regulatory acceptance [24]. This may make the regulatory path for CDNS easier compared to other systems. Due to the presence of inner hydrophobic cores and outer hydrophilic channels in CDNS, the devices can load both hydrophilic and hydrophobic drugs. This approach improves bioavailability and absorption in addition to its solubility and stability, minimizing the possibility of side effects, consequently, lowering the total quantity of the active component. Furthermore, this type of carrier makes sense for delivering therapeutics with a predictable release profile, such as extended-release pharmaceuticals. Changes in the ratio of their crosslinker component can modify their drug loading capacity and release profile [25]. CDNS have the capability of being used in different dosage forms. This intriguing carrying system, in contrast to the vast majority of conventional carriers, is able to maintain the molecular shape of the loaded drug even in the absence of surfactants. The carrier will be the same size and form as its non-complex equivalent [26]. There are numerous publications in the scientific literature on nanosponges, but the non-toxicity of CDNS makes them the most promising with in domain of drug delivery [27]. The advantages of cyclodextrin-based nanosponges have led researchers in the field of pharmaceutical nanotechnology to use these as a novel, versatile carrying system for poorly soluble drugs, thus improving their solubility [28,29].

β -cyclodextrin is one of the most regularly utilised cyclodextrins (CD) in nanosponges fabrication. α-, β- and γ-cyclodextrins are typical and natural agents for making hyper-crosslinked nanosponges with or without a cross-linking component. β-CD is the most extensively employed natural CD due to its highest complexation aptitude and permanency with cross-linking agents. It is likewise ideal for the preparation of nanosponges. β-CD is mainly preferred candidate due to their specific and appropriate cavity dimensions for a wide range of drugs, low production costs, higher production rates, and ready availability. Its candidature is strengthened by the United States Food and Drug Administration's (USFDA) affirmation that it is Generally Regarded as Safe (GRAS) for use in food. Practically it is found nontoxic when given in oral formulations [30,31].

The present study examines the development of cyclodextrin-based nanosponge carrier systems for drug delivery of two poorly soluble drugs in order to improve solubility while maintaining controlled release rate. Poorly soluble drugs with the same therapeutic effect, such as cinnarizine (BCS class II) and domperidone (BCS class II), are chosen for simultaneous loading. By using the nanocarrier, the solubility and eventually the bioavailability of the molecules can be increased [32]. A novel conception for nanosponges in combination drug therapy is to co-deliver two or more active compounds to boost therapeutic response when compared to a single medicine. The rationale of this method is to take advantage of a synergistic impact that occurs [33]. Furthermore, these dual delivery nanocarriers can reduce the number of drug administrations needed by patients and therefore improve their compliance.

The present chapter has given a detailed introduction about the concept of solubility, dissolution, and its significance in the area of drug delivery. The chapter has just hinted upon the use of nanotechnology, specifically cyclodextrin-based nanosponges in enhancing the said properties of a drug. The next chapter would cover the details about cyclodextrin-based nanosponges as a drug delivery carrier for poorly-water soluble drugs.

Chapter 2

Literature Review

2. LITERATURE REVIEW

The importance of solubility and dissolution rate to get optimum bioavailability of any drug molecule has been explained in the previous chapter. A large number of drugs being introduced today suffer from poor bioavailability on account of their insufficient water-solubility. One area that is finding prominence in rectifying the aforementioned problem is nanotechnology. The present chapter discusses nanotechnology, and more specifically, cyclodextrin-based nanosponges as the means to this end.

2.1. What are nanosponges?

Nanosponges (NS) are new category of materials either of organic or inorganic origin, natural or synthetic having at least a facet between 1 to 100 nm [34]. The overall size of nanosponges is usually less than 5μm or sometimes it may extend up to micrometers. But pores present with in the nanosponges are always in nanometer range. Treatments such as ultrasonication and homogenization could reduce the overall micrometer size of the nanosponge to the nanoscale [35]. Nanosponges are three-dimensional colloidal sponges that comprise solid small particles with nanosized interior cavities and mesh-like outside cavities to encapsulate a extensive range of pharmaceuticals of lipophilic as well as hydrophilic nature. Nanosponges may revolutionize the treatment of many diseases, because of their drug targeting, solubility improvement and tailored release characteristics. Early trials by researchers have proved that nanosponge-based treatment for cancer is around five times more effective than conventional methods [36]**.** They are a scaffold structure, made up of hyper-crosslinked polymers like hyper-crosslinked polystyrenes, cyclodextrins and their derivatives etc. Mostly these polymers are naturally degradable inside the body. When crosslinkers are put together with long-chain polymers in the presence of aprotic solvents, the crosslinkers will exhibit a special affinity for the specific site of the polymers. This outcomes in the development of a nanosponge with numerous inner and outer cavities for the storage of various drugs. As the scaffold structure of nanosponge is biodegradable, when it will break inside the body, drugs inside the nanocavities will be released at a scheduled time. Altered release from nanosponge can be achieved by changing the ratio between polymer and crosslinkers [37,38]. Nanosponges also facilitate drug targeting by showing attachment on the surface of desired target site while they move in the body and liberate the drug in a

regulated and predicted fashion [39, 40]. In comparison to other delivery systems, the nanosponge system is biocompatible, non-toxic, nanoporous and thermostable up to 300°C and has all the attributes, the prerequisite for a novel drug delivery system [41]. All of these attributes allowed us to finalize the nanosponge system as a potential carrier system for our drugs, Cinnarizine and Domperidone, which have limited aqueous solubility and consequently poor oral bioavailability. This nanosponge-based drug delivery will lead to high solubility and prolonged release of these poorly soluble drugs. They also have the potential to improve the bioavailability of actives by modifying their pharmacokinetic parameters.

Various nanosponges have found applications in the area of drug delivery and targeting, a comprehensive list is depicted in **Figure 2.1**. Out of the following NS, cyclodextrin-based NS has enjoyed maximum popularity.
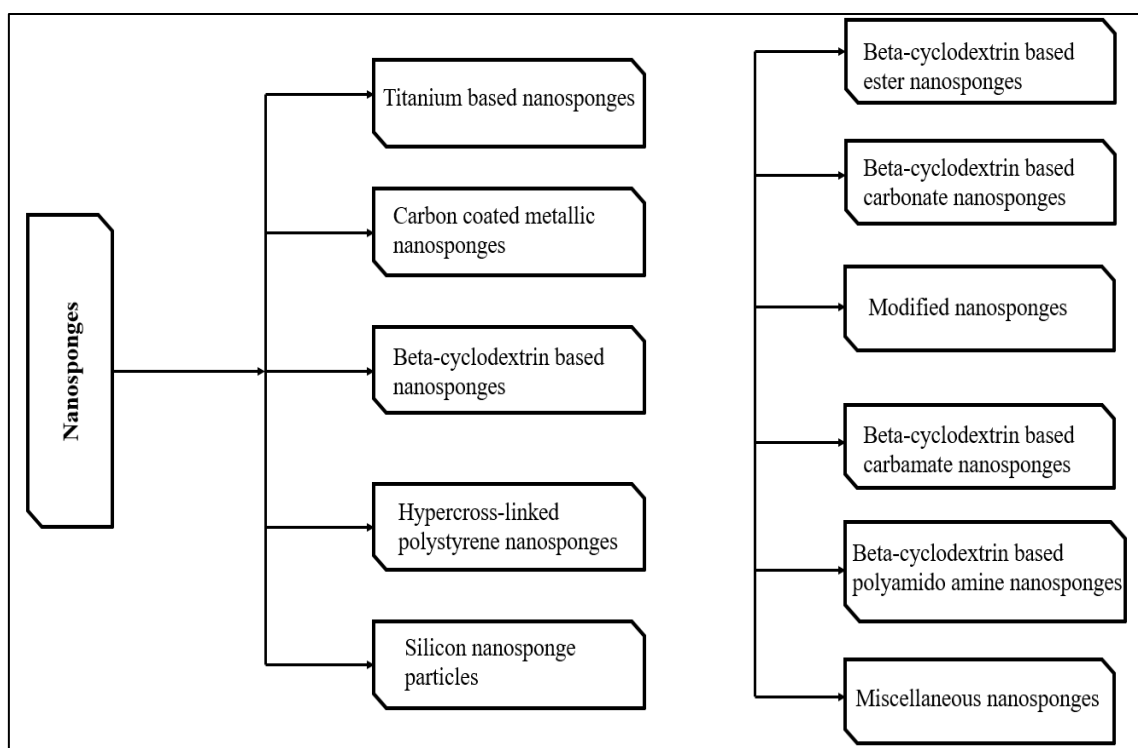
Figure 2.1: Types of nanosponges [42]

2.2. Cyclodextrin-Based Nanosponges (CDNS)

In contrast to other types of nanosponges, CDNS have a distinct advantage since cyclodextrin and all of its derivatives are non-toxic, biodegradable, and currently have widespread regulatory recognition in the pharmaceutical sector. Because of this, the regulatory process for CDNS based products may be easier compared to that of other nanosponges. In the pharmaceutical field, whenever the term 'nanosponge' is used, it is exclusively referred to as 'cyclodextrin-based nanosponges.'

Cyclodextrin-based nanosponges are multipurpose carriers, which can fit in both lipophilic and hydrophilic drugs in insertion and non- insertion complexes. Various drugs with low bioavailability due to limited solubility and dissolution rate, as well as active agents that were variable when revealed to light and external conditions, have been successfully prepared and administered by loading them in CDNS; a summary is shown in **Table 2.1**. Most drugs belonging to BCS class II and class IV have similar pharmacokinetic problems and can be delivered effectively with increased solubility, high bioavailability and fewer side effects when loaded in cyclodextrin-based nanosponges. The current study is driven on the design of a cyclodextrin-based nanosponge carrier system for dual drug delivery of poorly soluble drugs to improve the solubility and stability of actives with a controlled-release profile. Poorly soluble drugs, cinnarizine and domperidone of class II were selected as model drugs, having the same therapeutic response, to be loaded simultaneously in the same nanocarrier to increase their solubility and eventually bioavailability [32]. This novel idea of nanosponges for combination drug therapy consists of co-administration of two or more therapeutic molecules to enhance therapeutic response as opposed to the use of two systems to enhance the bioavailability of individual entities. The intention of this approach is to capitalize on the occurrence of a synergistic impact [33]. Furthermore, by reducing the number of drug administrations required, these dual delivery nanocarriers can increase patient compliance.

Table 2.1: List of drugs studied by complexation with cyclodextrin-based nanosponges

Drug classes	Name of drugs	CDNS Applications	References
Anticancer drugs	Curcumin and Resveratrol	Cyclodextrin nanosponges proved to be an effective nanocarrier for transdermal co-delivery of curcumin and resveratrol combination, result showed increase in cytotoxicity against breast cancer cells.	[43]
	Imatinib mesylate	Nanosponges are an efficient carrier for oral administration of anti-cancer pharmaceuticals because they encapsulate the drug and offer a prolonged release, avoiding unwanted exposure.	[44]
	Doxorubicin	High encapsulation efficiency and sustain profile for localized tumor treatment.	[45,46]
	Erlotinib	Nanosponge as a drug carrier increases bioavailability and reduces dose-related adverse effects.	[47]
	Tamoxifen	Protection from the acidic region and higher bioavailability (almost 1.5-fold) and cytotoxic activity against cancer cells.	[48]
	Paclitaxel	Improved drug solubility and physical stability for targeted delivery to cancer cells.	[49]
	Camptothecin	CDNS encapsulation improved drug solubility as well as stability.	[10]

	Tamoxifen	Protection from the acidic region and higher bioavailability (almost 1.5-fold) and cytotoxic activity against cancer cells.	[48]
Antifungal drugs	Griseofulvin	Successfully masked the bitter taste of the drug, improved dissolution rate and eventually enhanced oral bioavailability.	[50]
	Econazole	When applied topically, decreased dose frequency and dose-related topical adverse effects.	[51]
	Itraconazole	Itraconazole showed about 50 folds rise in water solubility with nanosponge delivery system.	[52]
Analgesic and Anti-inflammatory drugs	Meloxicam	Enhanced solubility and stability.	[53]
	Diclofenac	When drug was given as topical dosage form, it showed better localization of active drug in the subcutaneous and viable epidermis layer of skin.	[54]
	Acetylsalicylic acid	Sustained release with a longer half-life. Reduced undesired side effects.	[55]
	Dexamethasone	Enhanced solubility and slow-release profile.	[56]
	Flurbiprofen	Sustain release profile.	[57]
	Ibuprofen	Different molar ratios of CD to linker gave ibuprofen drug a customized release profile.	[58]
Antiviral drugs	Rilpivirine	Animal studies on cyclodextrin-based nanosponges, revealed high	[59]

		solubility and dissolution rate of rilpivirine up to 2-fold.	
	Efavirenz	The bioavailability of efavirenz was increased up to 2-fold by using a nanosponge-based carrier system as compared to plain drug.	[60]
	Acyclovir	Drug showed better loading, which eventually lead to prolonged release kinetics and improved antiviral activity.	[61]
	Nelfinavir	Improved drug solubility with the nanosponge-based carrier.	[62]
Antioxidant drugs	Ferulic acid	Compared to the pure drug, the encapsulated drug was 15-fold more soluble.	[63]
	Quercetin	Drug got improved dissolution parameters, when loaded into nanosponges, resulted into good bioavailability.	[64]
	Resveratrol	Solubility improvement and photostability of resveratrol.	[65]
Antihyperlipidemic drugs	Atorvastatin	Increase the bioavailability of the drug when complexed with CDNS.	[66]
Antidiabetic drugs	Repaglinide	Higher solubilization of repaglinide with CDNS.	[67]
Antiparkinsonian drugs	L-DOPA	The result is a controlled release of drug and also boosted the stability of the drugs in acidic, basic and neutral solutions as well.	[68]
Antimalarial drugs	Artemether and lumefantrine	Nanosponge formulation offered combinatory delivery of artemether	[32]

		and lumefantrine, with prolonged action and improved bioavailability.	
Antipsychotics	Paliperidone	Cyclodextrin-based nanosponges proved themselves as a insinuating carrier system for improving the solubility and dissolution of poorly soluble actives.	[69]
Antibacterial drug	Sulfamethoxazole	Nanosponges based on cyclodextrin have been developed and verified for their potential utility in antibacterial drug delivery. The findings show that nanosponges could improve drug bioavailability by allowing them to reach therapeutic plasma concentrations.	[70]

2.2.1. Components of CDNS

Polymers: The type of polymer employed can affect both the development and functioning of nanosponges. An important factor influencing the size of a nanosponges cavity is the type of polymer being used, which must be big enough to entrap a specific size drug molecule for complexation. Crosslinkers turn molecular nanocavities of polymers into three-dimensional, nanoporous structures. Commonly used polymers in formulation of nanosponges are hyper-crosslinked polystyrenes, cyclodextrins and their derivatives like beta-cyclodextrin (β-CD), methyl beta–cyclodextrin (Mβ-CD), hydroxypropyl beta-cyclodextrin (HPβ-CD), polymers like ethyl cellulose and polyvinyl alcohol, and copolymers like poly (Valero lactone-allyl Valero lactone) and poly (Valero lactone-allyl-Valero lactone oxepanedione) etc. Out of these polymers, cyclodextrins and their derivatives type polymers are very decisive here because of their versatile nature and wide regulatory acceptance.

Crosslinkers: The cross-linking agent helps in linking polymer molecules to form a cage-like structure of nanoscale and leads to the derivatization of these polymer molecules. Polymer tailored with different crosslinking agents shows dramatically modulation in some critical parameters like swellability and hydrophilicity/hydrophobicity. Commonly used crosslinkers are carbonyl crosslinkers, diisocyanate linkers, anhydride crosslinkers, and epichlorohydrin [71]. Out of these linkers, carbonyl-based linkers like diphenyl carbonate (DPC), dimethyl carbonate (DMC) and carbonyl diimidazole (CDI) are the first choices for cyclodextrin polymerization into nanosponges, by considering factors like time, cost, simple and straightforward processing stages with few input materials and acceptable physicochemical properties for nanosponges [72]. These carbonate-based nanosponges have shown good stability at 40°C and 75% relative humidity storage conditions [28].

Solvents: Solvents are required for the creation of nanosponges as well as for the loading of nanosponges with the drug. Commonly used solvents are dimethylformamide (DMF), dimethyl sulfoxide (DMSO), butanone, pyridine, dichloromethane, dimethyl acetamide, ethanol, water, etc. For the synthesis of nanosponges, aprotic solvents like DMF and DMSO are preferably used [73,74], because the substrate and aprotic solvents are unable to generate hydrogen bonds. These solvents are chemically inert and neutral in charge. Additionally, their dielectric constant is typically low.

2.2.2. Rational of cyclodextrin-based nanosponges

The fundamental notion underlying CDNS is to improve the physicochemical qualities of drugs and to function at the biotic level to enhance drug effects. These targets can be achieved because of 'versatile' cyclodextrin and 'intelligent' nanoparticles. This technology has proved much effective for delivering drugs in different illnesses as compared to conventional techniques [75, 76].

Drug molecules of any size and polarity can be entrapped by native cyclodextrins in their lipophilic cavity. However, they cannot capture some hydrophilic or big hydrophobic molecules. To improve the features of native CDs, many derivatives have been developed. CDs offer a wide range of potential as new drug carriers due to their knack to complex with an extensive selection of chemicals [56]. Hence chemical modification of these native CDs

has been reported to overcome these limitations and to make them versatile moiety. The chemical reaction of native cyclodextrins with crosslinking agents directed to the synthesis of CDNS [77]. Reactive primary hydroxyl groups present on the peripheral side of cyclodextrin molecule grant them to operate as multifunctional monomers, adept to be coupled with an assortment of crosslinkers including active carbonyl compounds, dianhydrides, diisocyanates, epoxides, carboxylic acids, etc. Consequently, formed an insoluble three-dimensional covalent network between cyclodextrin and linkers. The ultimate characteristic features of CDNS, such as solubility and crystallinity, are significantly impacted by the nature and ratio of the cross-linker employed and the degree of cross-linking that occurs [28]. The inner lipophilic central cavity of each monomer functions as the pore of a typical sponge with multiple intertwined outside hydrophilic microchannels and can incorporate things. This derivatization of native cyclodextrin makes them less soluble and more stable. CDNS have high efficiency towards enhancing solubility of weakly soluble drugs by their insertion and non-insertion accommodation behavior as compared to native cyclodextrins, demonstrating only the inclusion conduct. CDNS can be used for loading both hydrophilic and hydrophobic drugs due to the presence of inner hydrophobic cores and outer hydrophilic channels in its porous structure [78]. Nanosponges are the drug delivery system and their drug loading capability and drug liberation profile can be modified by simply changing the ratio of cyclodextrin and crosslinker. CDNS has been utilized in numerous disciplines, including biocatalysis, nanocarriers in pharmaceutical field, protective agents for active therapeutics, floriculture, fire engineering, environmental management, and effective gas carriers, as a result of its unique features.

2.2.3. Characteristic features of CDNS-based drug delivery systems

1. Nanosponges have a very small size range of about (1 μm or less) which gives a large effective surface area [35].
2. The resulting nanoporous polymer may be crystalline or paracrystalline. Because drug loading in nanosponges is directly proportional to the degree of crystallisation, a more crystalline structure of nanosponges is preferred [10].

3. Nanosponges are porous particles with a cavity of adjustable polarity and show stability up to 300 °C temperature [25].

4. Formulations of nanosponges show steadiness over the wide pH range and high temperatures up to 130 °C [79].

5. Nanosponges can be given in suspension dosage by using water as a vehicle and can be rejuvenated by processes like simple thermal desorption or extraction with solvents [80].

6. 3D structure of nanosponges has a variety of benefits like entrapment, transportation and selective release of drugs and their capacity to interact with several functional groups provides targeted pharmaceutical delivery. [81].

7. Magnetic properties can also be conferred on nanosponges by incorporating magnetic particles into the reaction mixture [82].

8. They can form insertion and non-insertion complexes with lipophilic and hydrophilic drugs individually or simultaneously [83].

2.2.4. Evolution of CDNS

Taking into mind their chemical makeup and properties, CDNS can be classified into four generations as depicted in **Figure 2.2**.
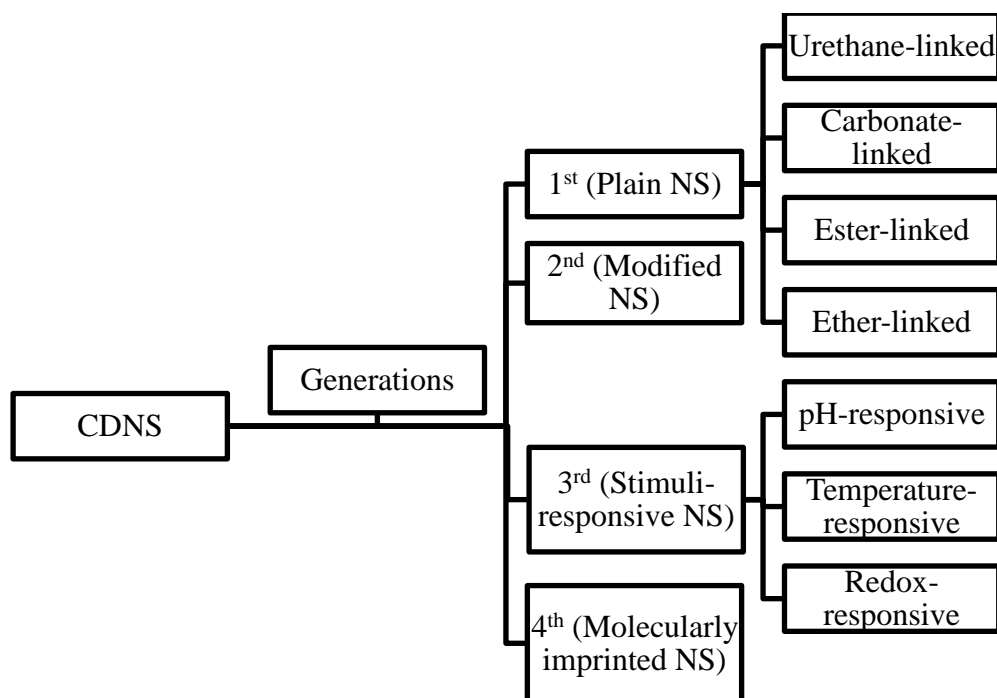
Figure 2.2: Evolution of cyclodextrin nanosponges [84]

The first generation of CDNS is plain nanosponges, which can be attributed to NS made by merely reacting cyclodextrins with a crosslinker. Based on the chemical composition of the functional group bonding the CD to the cross-linker, the earliest generations of NS can be classified into four distinct groups: urethane, carbonate, ester, and ether NS. In recent years, these first-generation CDNS especially carbonate-based nanosponges have been extensively used over conventional options for solubility enhancement and controlled release of numerous drugs. In **Table 2.2**, all subcategories of first-generation CDNS are discussed in depth, taking into account their practicality and relative ease of synthesis as compared to advanced generations.

Table 2.2: Subcategories of First-generation CDNS depending on the crosslinker used for nanosponges

Sr. No	Type of CDNS	Crosslinker	Functional group formed	Salient feature
1	CD-based carbonate nanosponges	Diphenyl carbonate, dimethyl carbonate, 1,1′ -Carbonyl diimidazole and triphosgene	Carbonate bond	The NS is tolerant to acidic and slightly alkaline pH and has a short cross-linking bridge with limited swelling ability. It also had great absorption capabilities for smaller molecules, and is most commonly used NS in drug delivery relevance. solubility enhancement capacity of these NS depends significantly on their degree of crystallinity [85].
2	CD-based urethane (carbamate) NS	Diisocyanates like toluene-2,4-diisocyanate (TDI) and hexamethylene diisocyanates	Carbamate bond	The structure is rigid, chemical resistance is good, swelling abilities are low, and the capacity of these nanosponges to attach to organic compounds has

Sr. No	Type of CDNS	Crosslinker	Functional group formed	Salient feature
		(HMDI)		led to their widespread use in water filtration [86].
3	CD-based ester NS	Dianhydride such as pyromellitic anhydride	Ester bond	Absorbs water around 25 times its weight, can form a hydrogel, has a crosslinking density that is inversely proportional to water intake, and is vulnerable to hydrolysis under aqueous circumstances [87].
4	CD-based ether NS	Epichlorohydrin, bisphenol A diglycidyl ether, ethylene glycol diglycidyl ether	Ether bond	High chemical resistance, variable swelling capacity, large surface area, and promising adsorption kinetics have all been demonstrated. When it came to removing organic contaminants, it performed admirably [88].

The second generation of CDNS is more complex and known as functionalized or modified nanosponges and has unique features such as fluorescence and electric charge. The stimuli-responsive CD polymers that make up the third generation of CDNS are capable of modulating their activity in response to their surroundings. External factors like pH and temperature, as well as oxidative/reducing conditions, might cause or improve the release of the loaded medicine from these nanocarriers. Fourth-generation CDNS, also known as molecularly imprinted CD polymers (MIPs), are created during the polymerization process when a template molecule, such as a drug, interacts with functional monomers in the presence of a cross-linking agent. After the reaction gets over, the template molecule can be removed, resulting in the formation of cavities that correspond to the target. On the basis of this imprint, these active drug molecules may then strategically rebind. These interactions are usually noncovalent and show a high level of selectivity and affinity for their targets [83], [84].

2.2.5. Factors influencing the formation of CDNS

The factors that can affect the formation of these CDNS and their expected effects have been briefly depicted in **Figure 2.3**. [82], [89], [90]. The factors that have been identified to have a profound effect on the synthetic route of CDNS are both related to the formulation, like the type of the drug, polymer, cross-linker, and the medium in which the reaction takes place; and to the process, such as the operating temperature and the method of preparation chosen.

Type of drug	• Aqueous solubility: < 10 mg/ml • Molecular weight: 100 to 400 g/mol • Should not have more than 5 condensed rings • Melting point: < 250°C
Type of polymers and crosslinkers	• Decides the quality and performance of NS • Changing the degree of crosslinking: change the hydrophilicity or hydrophobicity • Crosslinkers affect: rate of drug release, enhance permeation
Medium of interaction	• The interaction of nanosponges with drug is strongly depends upon medium used • Depends upon polarity, size and structural properties of drug
Temperature	• Affects the stability of nanosponges formulations • Increase in temperature decreases the stability
Method of preparation	• Affects complexation and drug loading
Degree of substitution	• The type, number and position of substituent on parent molecule can affect the nanosponges formation

Figure 2.3: Factors affecting the preparation and performance of CDNS

2.2.6. Advantages of CDNS

- Nanosponge allows for the capture of a wide range of substances with fewer side effects.
- Provides better stability, augmented grace and wide formulation flexibility.
- This delivery system can be used for extended-release with continuous action for 12 to 24 hours.
- Immiscible liquids can be incorporated into nanosponges and may be processed as powders.
- Drug targeting is also possible with new generation nanosponges [91].
- Nanosponge can entrap both lipophilic and hydrophilic drugs at the same time.
- Nanosponges can also be made magnetized when formulated in the presence of a composite having magnetic properties.
- Cyclodextrin-based nanosponges have a biodegradable structure that degrades gradually in the body [92].

2.2.7. Limitations of CDNS

- The cavity of nanoporous nanosponges can accommodate only small molecules.
- The efficiency of nanosponges is primarily determined by their drug loading capacity [10].
- NS can be of crystalline as well as para-crystalline nature. The degree of crystallization can impact the drug's loading into NS.
- The possibility of dose dumping exists.

  It is anticipated that alterations in the concentration of crosslinking agents and polymers will result in an increase in the loading of high molecular weight drug molecules into nanosponges. This approach appears to be effective to dodge above mentioned problems. Aside from that, 3D printing technology might be a useful tool in the production of NS, as it would allow us to customize them to meet our specific requirements [93].

Here, we have summarized the most commonly and successfully used polymer and linkers by the researchers in recent years in the field of nanosponge synthesis.

Table 2.3: Reported research work with β-CD polymer and linkers in the preparation of CDNS.

Sr. No	Drug	Polymer	Cross Linker	Polymer/ Linker ratio	Attributes	References
1	Piperine	B-CD	DPC	1:2,1:6,1:10	Improved crystallinity and loading capacity with a high degree of crosslinking	[94]
2	Curcumin	β-CD	DPC	1:4, 1:6,1:8	Compared to the curcumin β-cyclodextrin complex, curcumin in cross-linked β-cyclodextrin NS enhanced drug solubility and complexation stability more significantly	[95]
3	Gresiofulvin	B-CD	DPC	Ranging from1:2 to 1:6	Enhanced bioavailability and bitter taste masking	[50]
4	5-Fluorouracil	B-CD	DPC	1:2 to 1:10	Drug-loaded nanosponges with a 1:4 molar ratio	[96]

Sr. No	Drug	Polymer	Cross Linker	Polymer/ Linker ratio	Attributes	References
					showed the best result in terms of dissolution rate, complexation and entrapment efficiency.	
5	Lumefantrine	β-CD	CDI	1:12	Drug got controlled-release profile with enhanced solubility and stability.	[32]
6	Oxyresveratrol	β-CD	CDI	1:4	Complexed drug showed higher protection and stronger cell viability inhibition than the free drug.	[97]
7	Bortezomib	B-CD	CDI	Ranging from 1:2 to 1:4	The release profile slowed as the proportion of the crosslinker was increased	[98]
8	Sulfamethoxazole	B-CD	CDI	1:2 to 1:4	Using CDNS, the drug becomes 30 times more soluble.	[99]

Sr. No	Drug	Polymer	Cross Linker	Polymer/ Linker ratio	Attributes	References
9	Ferulic acid	B-CD	DPC	1:2 to 1:6	Solubility of the encapsulated drug was increased up to 15 times compared to the pure drug in the CDNS prepared by a 1:4 proportion	[100]
10	Paliperidone	β-CD	CDI	From 1:4 to 1:8	The drug's solubility was significantly increased, and in vitro studies showed that it was released from the CDNS for a longer period	[69]
11	Babchi Oil	B-CD	DPC	Ranging from 1:2 to 1:10	Encapsulation of active oil in nanosponge carrier system resulted into enhanced solubility by almost 5-times, with additional benefits likes	[101]

Sr. No	Drug	Polymer	Cross Linker	Polymer/ Linker ratio	Attributes	References
					photo-stability, safety and handling benefits.	
12	Atorvastatin calcium	β-CD	CDI	1:4	Improved dissolution and oral bioavailability	[102]
13	Rilpivirine HCl	β-CD	DPC	From 1:4 to 1:6	Increased solubility and oral bioavailability and reduction in dose and related side-effects.	[103]
14	Erlotinib	β-CD	CDI	1:4	Better solubility and oral bioavailability	[47]
15	Quercetin	β-CD	DPC	1:4 and 1:6	Solubility Enhancement	[104]
16	Acyclovir	β-CD	CDI	1:4	Enhanced solubility	[61]
17	Gamma-oryzanol	β-CD	DPC	1:4	Enhanced solubility and stability	[105]
18	Telmisartan	β-CD	DPC	1:4 and 1:8	Solubility enhancement	[9]
19	Curcumin	β-CD	Dimethyl carbonate	1:10	Enhanced activity and solubility	[106]

Sr. No	Drug	Polymer	Cross Linker	Polymer/ Linker ratio	Attributes	References
20	Tamoxifen	B-CD	CDI	1:2 and 1:8	Enhanced solubility	[48]
21	Dexamethasone	β-CD	DPC	1:4	Solubilization	[107]
22	Resveratrol	B-CD	CDI	Range 1:2 to 1:4	Enhanced permeation and stability	[65]
23	Camptothecin	B-CD	DPC	1:2, 1:4 and 1:8	Prolong release and increased solubility	[10]
24	Itraconazole	β-CD	DMC	1:10	Solubility enhancement	[52]
25	Doxorubicin	β-CD	DPC	1:4	Better stability and sustained drug release	[57]
26	Flurbiprofen	β-CD	DPC	1:4	Improved solubility and sustain release	[57]
27	Nelfinavir mesylate	B -CD	DPC	1:4	Enhanced drug solubility	[62]

2.2.8. Methods for Nanosponge preparation:

The methods of synthesis of CDNS have been classified based on the type of heating process undertaken. The conventional method relies on the traditional heating technique, whereas the newer wave-assisted methods employ modern equipment like a scientific microwave oven and a probe sonicator to serve the same purpose.
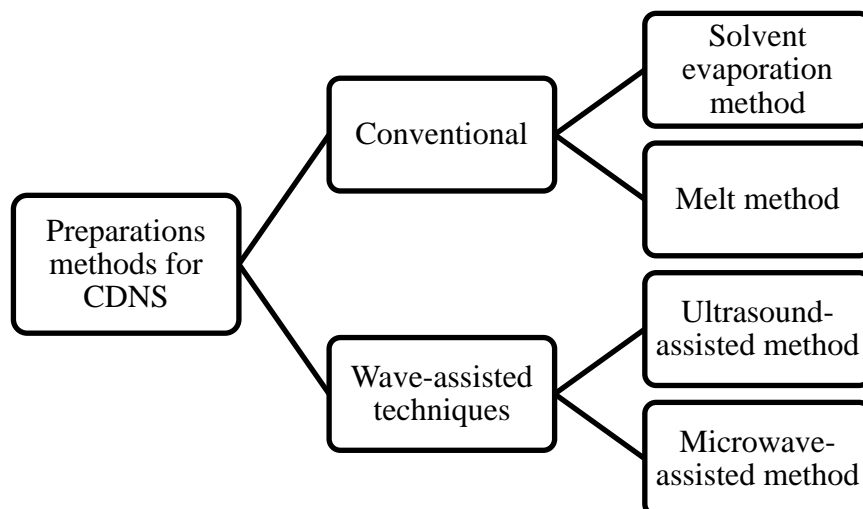
Figure 2.4: Preparation method for nanosponges

2.2.8.1. Solvent evaporation method

This method involves mixing the polymer (cyclodextrin) with polar aprotic solvents such as dimethylformamide and dimethyl sulfoxide and adding a sufficient quantity of cross-linker, preferably a carbonyl-based linker. The majority of the investigation studies reveal quantitative concentrations of polymer/ crosslinker in molar ratios ranging from 1:2 to 1:10 [72]. In this technique, the reaction mixture was kept for up to 48 hours at a temperature ranging from 10 °C to the reflux temperature of the solvent. Polymeric mass is obtained in a vessel after completion of the reaction, allowing the composite to cool at room temperature before pouring it into a large quantity of water, acetone or ethanol. Subsequently, the mixture containing the NS is filtered under vacuum, and, if necessary, further purified using Soxhlet extraction. [41], [83].

2.2.8.2. Fusion/Melt method

The fusion procedure is principally a "green" technique, as there is hardly any use of harsh organic solvents. In this method, crosslinker (carbonyl type) and polymer (cyclodextrin) are melted together at a higher temperature [83]. Each component was well blended together. The reaction is conducted at 100°C for 5 hrs with continuous stirring in a flask and then the mixture is cooled. The NS are recurrently washed with an appropriate solvent and collected. Washing of NSs is compulsory to remove the unreacted polymer, by-products and reagents. Finally after drying, breaks the mass into NS form [108].

2.2.8.3. Ultrasound-assisted synthesis

When compared to previously synthesized material, the nanosponges created using this process stand out for a number of reasons, including their substantially more spherical particle shape, their homogeneity of particle size, and their diameters being less than 5 microns. Trotta F and his team are the innovators behind this technique, as well as the ones that patented it [35]. They have suggested many procedures for nanosponge synthesis using ultrasonication. These procedures can be differentiated based on polymer/linker ratio, use of solvents or without solvent, type of sonicator (bath or probe type), and techniques for removing phenol and unreacted linker and sonication time.

Ultrasonication has been investigated as a method for fine-tuning the properties of nanosponge crystallinity**.** In a reaction flask, anhydrous cyclodextrin is reacted with DPC at 90°C for five hours using ultrasound sonication [83]. The reaction mixture is concentrated in a small volume in the rotavapor after being allowed to cool. It is necessary to wash off unreacted reagents with water and then perform a extended Soxhlet extraction with ethanol. Finally, the product is vacuum-dried and kept at 25 °C. Depending on the period of ultrasonication, work-up is undertaken to utilize the aforesaid processes to generate either crystalline or paracrystalline NS [107].

2.2.8.4. Microwave-assisted synthesis

Anandam and colleagues investigated this method of producing crystalline NS for the first time [104]. Microwave reactions are generally carried out in a scientific microwave system at 2450 MHz, with a fiber optic temperature probe, infrared camera and magnetically stirring system. This integrated system is very useful for maintaining and observing the reaction conditions prerequisite for nanosponge synthesis. The extensively accepted procedure includes a blend of polymer and crosslinker in a 250 mL flask with a suitable solvent and proceeds to microwave irradiation. After carrying the reaction for a specific period, the distillation process is used to remove the solvent. Once the solvent has been completely removed from the final product, water is used to wash it, and then ethanol is used to purify it by Soxhlet extraction for approximately 4 hours. The final product is dried overnight at 60 °C in an oven and subsequently powdered in a mortar. In comparison to other methods, the microwave irradiation method consumes less reaction time for NS synthesis and provides a high yield with particles having uniform size distribution and high crystallinity [109].

2.2.8.5. Need of novel synthetic approach

Despite being an encouraging carrier system for many active pharmaceutical molecules and rapidly growing technological applications of CDNS, a lot of questions regarding their synthetic approaches and their influence on the physicochemical properties of nanosponges are still existent. Many pioneer reviews from the nanosponge field have already considered the method of preparation as a crucial factor for the success of these nanosponges for their intended purpose [110]. Numerous synthetic processes have been scrutinized to fabricate nanosponge crystals having harmonized nano-size and morphology. Initially reported methods for the synthesis of CDNS were based on conventional heating techniques such as the fusion method and solvent evaporation method. These techniques had been the popular and the most used approach historically. Conventional methods have also been reported to produce non-uniform reactions triggered by thermal gradients in bulk solutions and have difficulties in preparation steps. Mass scaling was very difficult in these conventional methods, due to large solvent requirements and heat instability during the reaction. Longer duration and low yield during synthesis were other major concerns regarding conventional methods [104]. It was felt that most studies and research on the nanosponges have depended on the time-consuming conventional methods, and the product obtained exhibits less crystallinity, which ultimately leads to lessened capsulation of the molecule under study.

Thus, it was paramount to implement newer techniques like microwave and ultrasonic-assisted synthesis of CDNS and study the ramifications of these novel synthetic strategies on the physical, morphological, and performance characteristics of nanosponges. This revolutionary idea could help a lot in the evolution of unfussy, financially viable, fast and expansible methods for the bulk fabrication of monodisperse, steady, and dimension /structure-controlled NS. Recently a lot of researchers have shifted their focus towards these wave-assisted methods for the assembly of crystalline nanosponges, having ameliorated properties with better yield and loading capacity in comparison to nanosponges obtained by conventional methods.

2.2.9. Loading of drugs into nanosponges

The 3D structure of nanosponges with many interaction sites and adjustable polarity allows several guest molecules with varied structures and lipophilic characteristics to interact. This

distinct attribute of CDNS is responsible for high solubility and protecting the ability of NSs toward poorly soluble drugs. There are two reported methods (solvent evaporation and freeze drying) for loading drugs into nanocavities of synthesized nanosponges [38,71].

Suspended in a drug solution, the nanosponges are sonicated to avoid agglomeration. For this suspension of nanosponges to undergo complexation, constant stirring will be done for a set period. Drugs that aren't complexed, are separated from suspensions using the centrifugation method. Following this procedure, solid crystals of nanosponges are produced by either evaporating the solvent or drying the solution using freeze-drying techniques. Trotta and his team used a similar approach to load the drug Flurbiprofen into CDNS with an efficiency of 10 mg/100 mg, using 20 mg of Flurbiprofen and 100 mg of nanosponges in 3 mL of water. The loading efficiency of drugs with the nanosponges is largely dependent on the crystal structure of the nanosponge. Analytical techniques like differential scanning calorimetry (DSC) and thermogravimetry disclosed that both forms (crystalline and para-crystalline) have the potential to encapsulate the drugs satisfactorily [107]. Based on experimental studies it has been observed that crystalline nanosponges have better drug loading capacity as compared to para crystalline. Moreover, if nanosponges are inadequately crystalline, during loading process drug will just form a mechanical mixture rather than an insertion complex. The NS formed by the non-conventional heating method, always have high loading capacity due to their crystalline nature. However, the NS prepared by the conventional approach showed a lower level of drug loading than those formed by the non-conventional method [10].
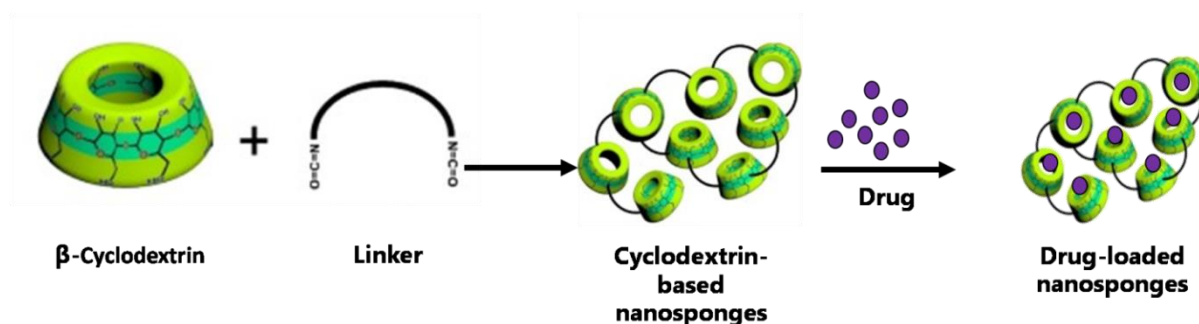
Figure 2.5: Loading of the drug into nanosponge

2.2.10. Drug release mechanism for nanosponges

Since the 3D structure of the nanosponge is porous, when drug-loaded NS is added to the vehicle, the drug particles will show unrestricted inward and outward traffic vis-à-vis its vehicle. This in and out movement of drug will continue until the medium is overloaded with the respective drug and the equilibrium is achieved. When drug-loaded NS formulation is given topically or by mouth, the encapsulated drug gets discharged from the formulation into the medium and finally taken up the skin or gastrointestinal environment. This depletion of drugs from the vehicle will promote sink condition due to disturbance of equilibrium. Now more drug will come out from the nanosponge formulation to maintain the equilibrium with the vehicle. This process will keep going till the body has expended all of the drug. The selection of vehicles is very important for the aforementioned mechanism. We cannot expect to sustain the release of drugs from NS with a vehicle having greater solubility for drug moiety. Under these conditions, the drug molecule will drift as if it were free-floating in the vehicle rather than captured. For that reason, a medium that can disperse the drug gradually from NS formulation should be selected [111,112].
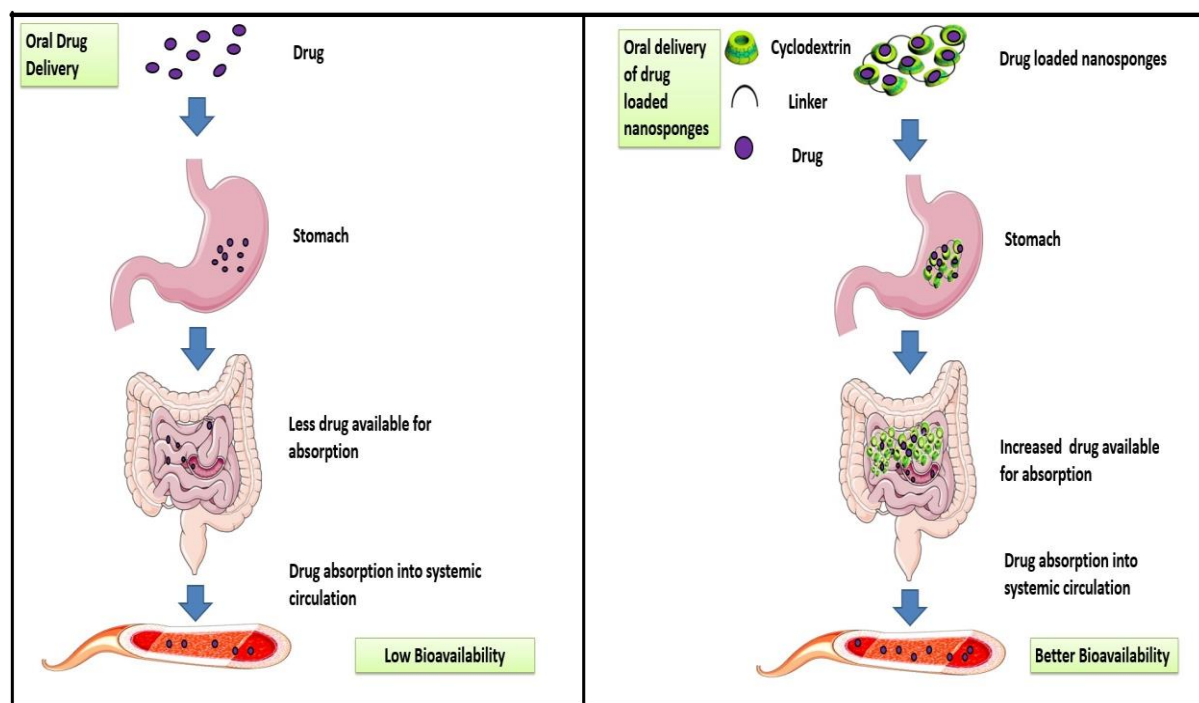
Figure 2.6: Mechanism of drug release through nanosponges

2.2.11. Characterization of nanosponges

With the progressions in the purposes of NS, a number of researchers have deliberated and appraised wide-ranging characterization practices such as transmission electron microscopy (TEM), scanning electron microscopy (SEM), differential scanning calorimetry (DSC), and X-ray diffractometry (XRD) to reveal that nanosponges are vastly-diverged, crystalline or paracrystalline, spongy nanostructured compounds that form 3D meshwork complexes. The parameters like solubilization efficiency, loading efficiency, microscopy studies, thermal degradation and inclusion complex formation are used to characterize nanosponges to comprehend the route of their synthesis, and assembly and to study their interactions with loaded pharmaceutical actives.

2.2.11.1. Particle size and zeta potential

The scrutiny of particle size is an important constraint for nanosponge optimization since it impacts drug discharge and solubilization. Smaller particles dissolve more quickly because they have more surface area per unit volume. This means that they also absorb more quickly. For poorly soluble drugs, the size of the particles can make a big difference in their bioavailability. The zeta potential is a surface charge measurement that predicts colloidal stability in nanosponges. The higher the value of a colloidal dispersion's zeta potential, the more stable it is. Zeta potential values of roughly ± twenty five mV, are satisfactorily lofty to give stable nano-suspensions that do not endure clumping throughout their shelf-life [41], [113].

2.2.11.2. Microscopy studies

Both types of microscopic techniques TEM and SEM can be used to scrutinize the morphological properties such as the shape and size of the nanosponges with or without drug candidates. It is possible to identify the growth of inclusion complexes by observing variations in the crystal lattice of starting resources and products underneath an electron microscope. Many reports also suggest that these techniques can show the presence of a consistent spherical form and size in developed NS. The findings of Ansari and his colleagues also revealed that the shape and size of the nanosponges produced persisted unchanged even once the medication was encapsulated into them [65].

2.2.11.3. Polydispersity index (PDI)

The PDI measures variance in the particle size dispersal, with a greater PDI value indicating polydisperse particle size scattering and a lower PDI indicating monodispersity. Here in **Table 2.4,** we have shown the relationship between dispersion forms and their obtained PDI values [114].

Table 2.4: Polydispersity index

Type of Dispersion	Expected Polydispersity Index
Monodisperse standard	0-0.05
Nearly monodisperse	0.05-0.08
Mid-range polydispersity	0.08-0.7
Very polydisperse	> 0.7

2.2.11.4. Drug loading and entrapment efficiency

Nanoparticles like nanosponges have two important characteristics: how much drug they hold and how well they hold it. The mass ratio of drugs trapped in nanosponges is shown by the drug-loading content, and the efficiency of drug entrapment is shown by the amount of drugs used in the feed during the nanosponge-making process. The carrier material's structure, physical properties, and chemical properties can influence how much drug can be loaded into it. The drug-entrapment efficiency is based on the drug-loading mechanism, the amount of drug in the feed, and other experimental variables. Higher drug loading content is harder to achieve than drug loading efficiency. Most of the time, the drug-loading process does not work well because of physical and electrostatic adsorption. However, it often works well because of crystallization and covalent and coordinating bonding. Most of the time, processes with high drug-entrapment efficiency are used to make nanosponges with a lot of drugs in them. Despite the excellent drug-entrapment efficiency of nanomedicines, high drug-loading content is difficult if the carrier material's space capacity is low. A gain in high drug-loading content may need high drug efficiency, although this is not necessarily the case all the time. This conclusion is drawn from the majority of the research hypothesis that was investigated. Based on the outcomes of the drug loading competence test, nano-sponges could be wrought as potential haulers to carry drugs [115].

The excess drug is mixed with water dispersed cyclodextrin nanosponges media followed by sonication for 15 mins and further stirred for 24 hrs then centrifuged and the NS aliquot is lyophilized. The acquired lyophilized product can be spent to calculate the extent of the drug existing in the system. For the entrapment competence investigate, the NS that have been loaded with the drug are scattered in a liquid medium in which the drug is dissolvable. The complex is thenceforth broken up by sonic vibrations, which makes it possible for the medicine to escape the nanosponges and dissolve in the solvent. To calculate the amount of medicine that is contained within the nanosponge, an appropriate analytical method, such as UV-Visible spectrophotometry [65] or High-Performance Liquid Chromatography [82], can be utilized. The following formulas can be used to compute the drug loading and entrapment efficiency of nanosponge formulation [49]:

$$Drug\ loading\ (\%) = \frac{Entrapped\ drug}{Total\ weight\ of\ CDNS}\ X\ 100\ \dots\dots\dots\dots\dots\dots Eq\ (2.1)$$

$$Entrapment\ efficiency\ (\%) = \frac{Encapsulated\ drug}{Total\ drug\ added}\ X\ 100\ \dots\dots\dots Eq\ (2.2)$$

2.2.11.5. Fourier transform-infrared spectroscopy (FTIR)

It aids as a foremost approach to ascertain the occurrence of functional units. Following the creation of nanosponges, the formation of bonds between utilized beta-cyclodextrin and linker (such as DPC) can be determined by evaluating the FTIR spectra to identify whether or not functional group peaks are present. To acquire a deeper knowledge of the interactions linking the different components, FTIR spectra are generated in the wave number span of 4000 to 650 cm^{-1} for the carrier nanosponges, pure drugs, and drug-loaded nanosponges. The completion of the cross-linking reaction is indicated by the lack of non-hydrogen-bonded O-H stretching at a frequency of 3450 cm^{-1}, which is supplied by the primary alcohol group of CDs. Similarly, FTIR bands of NS reveal a characteristic crest at around 1750 cm^{-1}. This peak is imparted by the carbonate group of the carbonyl-based cross-linker that was employed [83]. Other peaks of CDNS can be spotted in the range of 1460–1600 cm^{-1} and 1270–1290 cm^{-1}. On comparisons of the FTIR spectra of the drug and its nanosponge complex and the findings showed that there were considerable disparities in the fingerprint as

well as in the functional group region, which indicated drug loading in nanosponges. The FTIR spectra unveiled that there was a molecular collaboration amid the drug and the nanosponge, which resulted in the broadening or shifting of the drug peak [61, 65, 116].

2.2.11.6. Thermal analysis

Thermal analysis plays a judicious role in determining the nature, interaction pattern, and crystallinity of NS. Thermogravimetric Analysis (TGA), Differential Scanning Calorimetry (DSC), and Differential Thermal Analysis (DTA) are all crucial thermoanalytical modes for determining melting temperatures (T_m), crystallization temperatures (T_c), degree of crystallinity (X_c), thermal and thermoxidative steadiness of drugs, nanosponges and drug-loaded nanosponges [117]. The DTA and DSC thermograms can both be analyzed to search for peak expansion, budging, and the advent of unfamiliar peaks, in addition to the disappearance of some peaks. In the DSC thermogram, the nonappearance of the liquefying peak of the drug indicates that the drug is molecularly disseminated inside the polymer. The fluctuation in weight loss that takes place during the thermal examination of nanosponges may also be used as a sign that inclusion complexes have formed [10,81].

2.2.11.7. Powder X-ray diffraction (PXRD)

Chemical breakdown and cosolidation are primarily determined as a function of dispersion angle using the PXRD technique. It is typically applied to examine the inclusion complexation of solely solid-state drugs. When the drug forms a complex with the CDNS, the diffraction pattern changes and the drug's crystalline nature also changes [82,118]. Complex formation is characterized by peak sharpness, the appearance/disappearance of new peaks, and the shifting of a single peak. CDNS carrier-drug molecule interactions and accurate geometrical correlations can be determined using the PXRD technology [119].

2.2.11.8. NMR spectroscopy

NMR can also be used to analyze the molecular structure, determine the molecular kinesis of CD in NS structures, and analyze the interfaces in drug-polymer complexes. In NMR investigations, changes in chemical shift values reveal proton swap between reacting groups, resulting in the creation of NS. The ^{13}C NMR, ^{1}H NMR, 2-D NMR (ROESY and COSY),

and high-resolution magic angle spinning (HR-MAS) NMR have turn out to be essential methods for studying the structure of cyclodextrin-based cross-linked nanosponges [120], [121]. It was also revealed that HR-MAS NMR spectra can be utilized to describe insoluble cross-linked cyclodextrin materials with limited mobility and to detect polymeric structures for the first time [122].

2.2.11.9. Phase solubility

The phase solubility method is employed to gauge the impact of nanosponges on drug solubility [123]. To ascertain phase solubility coefficients, the surplus drug is added to appropriate mediums to form saturated mixtures. Various concentrations of nanosponges, such as 1:1, 1:2, 1:3, etc., are used to treat drug-saturated solutions. As NS concentration increases, a larger percentage of the drug interacts with them. A plot of NS concentration against drug concentration can be generated using the Higuchi and Connors method and the type of plot is determined [124]. The obtained stability constant values reveal light on aspects of the drug-nanosponge interaction. The interaction of weakly water-soluble medicines with nanosponges can increase their solubility and consequently their rate of dissolution. Similar research was accomplished by Swaminathan and his colleagues on itraconazole-loaded cyclodextrin nanosponges and reported that the solubility of itraconazole was boosted more than 25-times in presence of cyclodextrin nanosponge as a binary system [52].

2.2.11.10. Invitro release studies

Dialysis is a method of separating substances by the use of a membrane. Using a dialysis membrane approach, the drug liberation from the appropriately designed NS-loaded formulation is analyzed. Dialysis involves separating two solutions (the reception solutions and the feed) using a semipermeable membrane. Due to the concentration gradient, small molecules like the drug can cross the membrane and enter the dialysate solution, while larger molecules (carrier nanosponges) are blocked. Consequently, dialysis can be seen as a extremely effective technique for seceding drug molecules from loaded nanosponges. Molecules pass through a dialysis membrane at a pace that is inversely proportional to its thickness and is determined by the porosity and contours of the membrane. At predefined intervals, aliquots are withdrawn from the receptor compartment and refilled with distilled

water, which is subsequently tested using a UV-Visible spectrophotometer, HPLC, or GC-MS method [113]. Many studies have found that when quercetin, isoniazid, naproxen, and ibuprofen are complexed and incorporated into nanosponges, they release at a faster rate than their simplest counterparts [104, 125, 126].

2.2.12. Incorporation of nanosponges in various dosage forms

By nature, nanosponges are solid, but they can be modified to be administered orally, parenterally, topically, or in an inhalable form. CDNS can be administered through a selection of routes, and is not limited to the more popular oral, pulmonary, intravenous, and topical [98, 127]. The physicochemical properties of the medicine, the targeted site in the body, and the physiology of the patient's condition can all influence the amount of drug used. Because the oral approach is the most popular among the others. The majority of researchers engaged in developing improved features of the oral route and investigating therapeutic bioavailability such as paclitaxel, tamoxifen, atorvastatin, griseofulvin, artemether and lumefantrine through the oral way [49, 50,102, 32]. CDNS has recently been tested with a variety of dosage forms, and this novel carrier has shown tremendous promise in its delivery mechanism. Most of the medicines investigated fall to BCS class II. Some drugs, such as doxorubicin and acyclovir, with high solubility but poor intestinal penetrability (BCS Class III), have been identified as potential candidates for investigating the consequences of this fascinating transporter on their diffusion across several biological obstacles, including the intestine. Many published reports revealed that CDNS not only improve the solubility of medications but also has a significant impact on their penetration when compared to conventional medication. Although it is unknown how they alter permeation, some research suggests they may inhibit the P-gp efflux carrier for P-gp substrate molecules in the gut [128, 129].

2.2.13. Pharmaceutical applications of nanosponges

Over the last 20 years, NS has mostly been employed in the pharmaceutical and biomedical industry, but various groups have explored non-pharmaceutical applications such as environmental remediation, agricultural applications, sensors, catalysis applications and flame retardants etc. [83,130,131].

In pharmaceutical formulations, NSs produced from cyclodextrins are thought to be innovative drug carriers. Encapsulating actives into adequate CDNS can overpower insolvability, perviousness, stability, sensitivity, and other challenges, permitting innocuous and effective drug transport [57]. Nanosponges can increase the rate of dissolution, solubility, and stability of BCS class II and IV pharmaceuticals. The entrapment of flavours by adsorption is influenced by a nanoporous structure of nanosponges, masking unpleasant aromas. According to studies, controlled-release β-CD nanosponges can also effectively transport medicine to target sites. The application of carbonate-based nanosponges as a carrier for anticancer medications like paclitaxel and camptothecin has given tremendously promising results. [37]. Because NSs are involved in so many segments of the pharmaceutical industry, it is one of the most exciting areas to research. Here, we have also summarized how NSs are being used in the pharmaceutical and biomedical fields.

2.2.13.1. Sustained drug delivery

The sustained release formulation is meant to optimize the dosage regimen by delivering the drug continuously throughout the dosing interval, reducing dosing rate and improving total patient outcomes. Using the right ratio of polymers and crosslinking agents, the drug release kinetics from the NS carrier system can be changed for a prolonged period. Due to the variable pharmacokinetics of the antiviral drug acyclovir, currently available formulations are not able to end in appropriate and prolonged strengths of this drug at target sites. The in vitro release summaries of acyclovir from its NS-loaded formulation indicated a lasting release of the drug indicative of the entrapment of acyclovir inside the nano assemblies. There was no initial burst effect in this nanosponge-based formulation, suggesting that the no drug was feebly bound to the surface [61].

2.2.13.2. Solubility enhancement

The occurrence of cross-linking and CD voids in nanosponge arrangement encourages collaboration with drug actives. These properties allow a variety of compounds to be incorporated and solubilized in the created cavities. Solubility or rate of dissolution of inadequately water-soluble pharmaceuticals can be improved by the inclusion complexation or matrix loading of these drugs within CD-based nanosponge resulting in reduced drug's

crystallinity. The resulting complex conceals the majority of the CD's hydrophobic activity inside the cavity, while the hydrophilic primary -OH factions present on the exterior facade remain unmasked to the environmental milieu, resulting in a water-soluble complex [105]. A BCS Class II drug, itraconazole has a dissolution rate restricted bioavailability. Phase solubility studies showed that nanosponges increased the drug's solubility by more than 27-fold, and when co-polyvidonum was included as a reinforcing constituent of the NS-loaded formulation, this increased by more than 55-fold [52].

2.2.13.3. Drug carriers

Cyclodextrin nanosponges are biodegradable carriers that are non-mutagenic and non-irritating. They are versatile carriers for delivering a variety of drugs having different molecular weights. The biggest challenges they face while loading large drug molecules can be overcome by adjusting the cross-linker ratio [109]. This delivery strategy enhances the solubility and stability of the capsulated pharmaceutical actives, as well as its absorption and bioavailability, reducing the possibility of adverse manifestations and, eventually, the over-all dose of the active moiety [24, 133]. This carrier system inhibits the recrystallization of hydrophobic pharmaceuticals, is stable after lyophilization, and is simple to redisperse in water. This carrier can keep the loaded drug in molecular form without surfactants, and its size and shape are the same as the non-complexed variant [26]. CDNS is recommended as an innovative and versatile carrier system for pharmaceutical and medical research. The following sections cover the delivery of various types of drugs using cyclodextrin-based nanocarriers.

2.2.13.3.1. Delivery of anticancer drugs

Cyclodextrin-based nanosponge could be a carrier system for antitumor medicines like paclitaxel, camptothecin, and tamoxifen, since their solubility in water is very poor, posing a bioavailability difficulty. Paclitaxel's absolute bioavailability increased after it was loaded into NS, and it was discovered to be 2.5-times higher than stark medication [49].

With cyclodextrin-based nanocarrier, these drugs can also pull off regulated target-aimed delivery at the tumor site and overcome the inadequacy of therapies and the impediments concomitant with traditional antineoplastic formulations. Cyclodextrin-based NS are very

effective for targeting drug delivery, as they stay in the bloodstream until they reach their target site, where they adhere to the exterior and discharge the drug. Numerous nanosponges containing anticancer drugs have been produced and evaluated on a range of cell lines to determine their antiproliferative efficacy. The effect of nanosponge complexes was greater than that of the drug alone. Matencio and his team designed CDNSs for oxyresveratrol (OXY) administration. On PC-3 (prostate) and HT-29 and HCT-116 (colon) cancer cell lines, the new formulation demonstrated considerable dose-dependent suppression of cell survival compared to the free drug [134].

2.2.13.3.2 Delivery of antifungal drugs

Econazole nitrate is a topical antifungal that can be used to treat surface candidiasis, dermatophytosis, versicolor, and other dermal infections. It comes in cream, ointment, lotion, and solution forms. Due to its insignificant absorption through the skin, the drug is loaded into nanosponge-based hydrogel for effective and sustained release of econazole nitrate [51, 135].

2.2.13.3.3 Delivery of antiviral drugs

Nanosponges are a good carrier for delivering antiviral medicines or small interfering RNA (siRNA) to the nasal epithelia and lungs to aim at viruses such as influenza, respiratory syncytial, rhinovirus, HIV (human immunodeficiency virus) and HBV (hepatitis B virus). Acyclovir drug showed good loading capacity when carboxylated nanosponge is used as a carrier system. Furthermore, the in vitro profile revealed a prolonged release model as well as excellent antiviral activity against HSV in cell culture compared to the free drug [136, 137]. The use of nanostructured cyclodextrin nanosponge to encapsulate silencing RNAs provides an alternative stratagem for anti-viral treatments while also protecting susceptible molecules such as proteins/peptides. Nanosponges made of CD mimic and contend with cell-exterior receptors used by viruses for cell attachment to give an antiviral effect [138].

2.2.13.4. Carrier for biocatalysts

The disadvantages of industrial processes, such as yield in short supply, higher resources expenditure, and significant volumes of water in downstream processes, can be avoided by

utilizing enzymes as biocatalysts. The enzymes have the benefit of reacting under mild conditions, are extremely selective, and have little impact on the environment, reducing pollution formation. The CDNS is a top-quality carrier for encapsulating enzymes, proteins, and antibodies than other nanoparticulate systems because it retains their activity, effectiveness, and functionality throughout a extensive range of temperatures up to 300 °C and pH ranging from 1 to 11 [21].

2.2.13.5. Carrier for the delivery of gases

Gases are used extensively in the practice of medicine, whether for diagnostic or curative purposes. In clinical practice, it might be challenging to give oxygen in the correct form and amount. Cavalli et al. created an oxygen delivery system based on nanosponges for topical application that can store and release oxygen slowly over time [139]. These NS can produce oxygen independently of ultrasound. On the other hand, an in vitro release investigation discovered that ultrasound improved oxygen release and penetration. This research found that NS can be employed efficiently as a transporter and pool of O_2 for dermal application.

2.2.13.6. Carrier for proteins and peptide drugs

Pharmaceuticals, notably macromolecular-like proteins, require long-term stability to be developed successfully. When protein molecules are lyophilized, they may denature reversibly or permanently, resulting in a very different conformation than the native protein molecule. Maintaining the natural structure of proteins in the course of the formulation procedure and long-term storage presents a significant challenge for protein formulation development [140]. As a result of crosslinking CDs with poly(amidoamine) molecules, Swaminathan et al. obtained novel swellable CDNS. Poly(amidoamine) nanosponges based on CD had a high protein complexation capacity as well as high stability even at 300 °C [81].

2.2.13.7. Protection against degradation

Natural antioxidant gamma-oryzanol has received a lot of attention recently for its use as a stabilizer in the food and pharmaceutical industry, as well as a sunscreen agent. Because of

its high instability and photodegradation, its use is constrained. Gamma-oryzanol encapsulated in nanosponges as an O/W emulsion or gel formulation demonstrated good photodegradation protection [105].

2.2.13.8. Diagnostic tools

Supramolecular chemistry is the study of the interactions between two or more chemical species that are bound together by intermolecular forces and exhibit both self-assembly and molecular recognition. CD is a popularly used supramolecular assembling unit in the fabrication of a wide range of substances for biological purposes [141]. A recent study has resulted in the development of a supramolecular nanoparticulate cyclodextrin/adamantine cross-linked polymer, which has been spliced with polyamidoamine for use in molecular diagnostics and therapies. Supramolecular nano assemblies can be configured to have on-demand usefulness for illness avoidance, identification, and therapy [142].

CDNS with different levels of cross-linkers could be used to solve the concerns of prolonged accumulation caused by synthetic polymers. By attaching gold molecules to the more hydroxyl groups that are accessible for cross-linking, it is achievable to produce thermos-susceptible nanosponges. Cyclodextrin nanosponges are ideal as diagnostic tools due to their superior biocompatibility, protracted movement in the circulation, comprehensive cargo scaling from minute molecules to macro biomolecules, unmatched size traits for tissue perviousness, exceptional formulation aptitude, and ease of modifying for active targeting [143].

2.2.13.9. Prostheses and implants

Prosthetic devices and grafts have turn out to be the system of preference in heart conditions, diabetes, and malignancies. They are likewise used for repairing fractured bones, and ligaments, and for delivering visual sense to the visually challenged by means of bionic eyes. CD-based polymers have been used in these systems since a long time. To repair or sidestep impaired arteries, polyester vascular inserts are employed. Those can be adorned with CDNS to accomplish the regulated release of antibiotics and other therapeutics to limit the peril of infectivity before and after invasive maneuvers [144]. CDNS has also been explored for usage in dentistry. To restore teeth cosmetically, cyclodextrin nanosponges offer a superior bonding material, reducing the development of discolouration and other interfacial flaws [145].

2.3 Marketed preparations
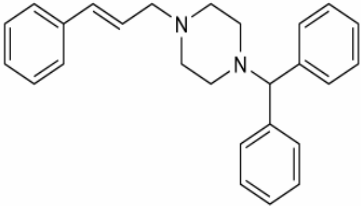
The assorted marketed preparations of β-cyclodextrin-based NS-loaded formulations are itemized in **Table 2.5** [146-148].

Table 2.5: Nanosponge-based marketed products

Trade name	Composition	Dosage form	Indication	Market
Nitropen	Nitroglycerin and β-cyclodextrin	Sublingual	Treat/prevent chest pain or pressure	Japan
Meiact	Cephalosporin and β-cyclodextrin	Oral	Antibiotic	Japan
Glymesason	Dexamethasone and β-cyclodextrin	Topical	Anti-inflammatory, treat eczema/dermatitis	Japan
Mena-gargle	Iodine and β-cyclodextrin	Topical	Throat infection	Japan
Prostarmon E	Dinoprostone and β-cyclodextrin	Tablet (Sublingual)	Oxytocic	Japan
Brexin	Piroxicam and β-cyclodextrin	Capsule (Oral)	Analgesic, antipyretic, anti-inflammatory	Europe
Clinoril	Sulindac and β-cyclodextrin	Oral	Anti-inflammatory	Europe
Omebeta	Omeprazole and β-cyclodextrin	Oral	Intestinal/esophagus ulcers, reflux disease and heartburn	Europe
Surgamyl	Tiaprofenic acid and β-cyclodextrin	Oral	Analgesic, antipyretic, anti-inflammatory	Europe
Nicorette	Nicotine and β-cyclodextrin	Sublingual	Aid to smoking cessation	Europe
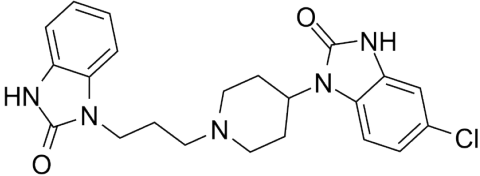
2.4 Drug profiles

2.4.1 Cinnarizine

Characteristic	Description
Chemical Structure	
Molecular formula	$C_{26}H_{28}N_2$
CAS No.	298-57-7
IUPAC name	1-(Diphenylmethyl)-4-(3–phenyl– 2–propenyl) piperazine
Molecular Weight	368.5 g/mol
Appearance	White crystalline powder
Melting point	118 ± 2 °C
Solubility	Insoluble in water and slightly soluble in alcohol and methanol, freely soluble in methylene chloride, and soluble in acetone.
Aqueous solubility and BCS class	0.95μg/mL and BCS Class II
Bioavailability	10-12%
Half-life	3 to 6 hrs
Lethal dose (LD_{50})	>6500 mg/kg (Oral, rat)
Drug category	Anti-Histaminic and Ca^{2+} channel blocker
Pharmacological indication	It is valuable for treating vestibular symptoms of other origins as well, conditions such as Vertigo, Meniere's disease, nausea and vomiting.
Metabolism	Hepatic
Mechanism of action	The effect of cinnarizine is to inhibit the contraction of smooth muscle cells in the vascular system by inhibiting L-type and T-type voltage-gated Ca^{+2} conduits. It may be effective in alleviating motion sickness-induced vomiting due to its affinity for dopamine D_2 receptors, histamine H_1 receptors, and muscarinic acetylcholine receptors. It

	works by interloping with signal conduction between the vestibular apparatus located in the inner ear and the hypothalamus' vomiting centre.
Dosage prescribed	For oral dosage form(tablets): -Treatment of vestibular symptoms of peripheral and central origin: Dose: For adults and children above 12 years 30 mg three times a day. For children of age ranging from 5 to 12 years half dose is suggested, 15 mg three times daily. -Motion Sickness: Dose: for prophylaxis of motion sickness, 30 mg should be swallowed 2 hours afore journey and then 15 mg each 8 hours during the voyage. Children from 5 to 12 years should be given half the adult dose. -Peripheral arterial diseases: Dose: Starting dose is one 75 mg capsule three times daily. The maintenance dose is one 75 mg capsule 2 to 3 times every day subjected to therapeutic comeback.

2.4.2 Domperidone

Characteristics	Description
Chemical Structure	
Molecular Weight	425.9 g/mol
CAS No.	57808-66-9
IUPAC name	5-Chloro-1-{1-[3-(2-hydroxy-1H-benzimidazol-1-yl) propyl]-4-piperidinyl}-1H-benzimidazol-2-ol
Appearance	A white or pale-yellow powder
Melting point	$242 \pm 2^{\circ}C$
Solubility	Domperidone is insoluble in water and soluble in dimethyl sulfoxide (DMSO), dimethyl formamide (DMF), ethanol and methanol.
Aqueous solubility and BCS class	5.8 µg/mL, BCS class II
Bioavailability	13-17%
Half-life ($t_{1/2}$)	7 hrs
Lethal dose (LD_{50})	5243 mg/kg (Oral, rat)
Drug category	A specific blocker of dopamine receptors and used as an antiemetic, gastric prokinetic agent.
Pharmacological indication	Symptoms of dyspepsia, heartburn, epigastric pain, nausea, and vomiting can be managed with this drug.
Metabolism	Hepatic
Mechanism of action	The effects of Domperidone include delayed gastrointestinal emptying and peristaltic stimulation. Dopamine receptors on peripheral nerves are blocked by domperidone and this contributes to its gastroprokinetic properties. By intensifying esophageal and gastric peristalsis and by lessening esophageal

	sphincter stress, DOM assists gastric emptying and subsides the small bowel passage time. **Antiemetic**: Domperidone has antiemetic properties because it blocks dopamine receptors at the gastric and chemoreceptor trigger zones. The drug exhibits a strong affinity for the D2 and D3 dopamine receptors that are found just outside the blood-brain barrier in the chemoreceptor trigger zone, which regulates nausea and vomiting.
Dosage	For oral dosage form (tablets): -Treatment of gastrointestinal motility ailments: Adults: 10 mg, 3 to 4 times daily. A few patients may have need of elevated doses of up to 20 mg, 3 to 4 times every day. -Nausea and vomiting: Adults: 20 mg, 3 to 4 times on a daily basis.

Chapter 3
Rationale of the Study

3. RATIONALE OF THE STUDY

3.1. Hypothesis

Drugs having the problem of low aqueous solubility ultimately landed into poor bioavailability. Hence to maintain maximum permissible concentration in plasma for therapeutic activity a larger dose of these drugs is required, which may lead to systemic toxicity and adverse effects. The problem gets worse when these inadequately aqueous soluble drugs are used often to treat certain disorders. Throughout time, nanotechnology has attracted further broad perspective, and it is now capable of addressing difficulties with solubilities, stabilites, and sustained release profile.

Nanosponges are nanoporous colloidal systems which can be used as versatile carriers for the delivery of weekly soluble drugs. Among different classes of nanosponges 'cyclodextrin-based nanosponges' have a special place in the pharmaceutical field. As non-toxic, biodegradable cyclodextrin is being used in the field of pharmaceuticals for a long time and has no regulatory issue. So, this makes the path of novel nanocarriers like cyclodextrin-based nanosponges easier as compared to other nanocarriers. In order to form a three-dimensional mesh-like structure, cyclodextrins and linkers can be cross-linked to generate nanosponges. Like cyclodextrins, they can be brought into play to solubilize inadequately water-soluble drugs and improve a drug's bioavailability. But their unique features like the possibility of fabrication of particles within a nano range, tailored release profile by simply changing the ratio of cyclodextrin and crosslinker, and capability to encapsulate lipophilic and hydrophilic drugs both in their crystalline structure by inclusion and non-inclusion phenomenon make them superior to native cyclodextrins. In contrast to most alternative carriers, this unique carrying mechanism can retain the loaded drug in its molecular form, and the nanocarrier itself is biodegradable.

Hence, in the present study, we hypothesized that delivering the poorly soluble drugs through the cyclodextrin-based nanosponge carrier could be a promising approach to enhance solubility and achieve the desired concentration of these drugs in the specific site. Here, we have selected two model drugs Cinnarizine and Domperidone belonging to BCS class II, exhibit poor solubility and thereby dissolution rate-limited bioavailability. These model

drugs have short half-lives and use in the treatment of the same physiological conditions. In the present study, these two drugs will be loaded simultaneously into a nanosponge carrier in a single unit oral dosage form to get enhanced bioavailability, controlled release and synergistic effect of combination therapy.

Despite being a favorable delivery approach for numerous active molecules and rapidly growing technological applications of CDNS, a lot of questions regarding their synthetic approaches and their influence on the physicochemical properties of nanosponges are still existent. Many pioneer reviews from the nanosponge field have already considered the method of preparation as a crucial factor for the success of these nanosponges for their intended purpose [110]. Several synthetic processes have been scrutinized to yield nanosponge crystals having homogeneous nano-size and morphology. Initially reported methods for the synthesis of CDNS were based on conventional heating techniques such as the fusion method and solvent evaporation method respectively. These techniques had been the popular and the mostly used approach historically. Usually, the reaction between the polymer and crosslinker is solvent-aided or solvent less and carried out at a temperature between 90 to 110 °C [149]. In the solvent evaporation method; the process involves the usage of aprotic solvents, in which both the components are soluble. In this reaction, a reticulate is generated, which engulfs several organic molecules. In addition, it has been reported that severe heat gradients in the bulk solution cause conventional methods to produce non-uniform reactions, which in turn makes the preparative processes more challenging. Bulk scaling was very difficult in these conventional methods due to large solvent requirement and heat instability during the reaction. Longer duration and low yield during synthesis were other major concerns regarding conventional methods [150]. It was felt that most studies and research on the nanosponges have depended on the time-consuming conventional methods, and the product obtained exhibits less crystallinity. It ultimately leads to less encapsulation of the molecule under study.

Thus, it was paramount to implement newer techniques like microwave, ultrasonic-assisted synthesis of CDNS and ramifications study of these novel synthetic strategies on the physical, morphological, and performance characteristics of nanosponges. This revolutionary idea could help a lot in the evolution of uncomplicated, financially viable, fast and scalable methods for the bulk manufacture of monodisperse, steady, and dimension/morphology-

controlled nanosponges. The work would entail the development of the synthetic pathway along with its optimization to identify the relevant product and process parameters that could have a bearing on the quality and behavior of the final product. This would help other researchers working in the area of solubility, stability and bioavailability enhancement to apply these techniques to find solutions to drugs suffering from these limitations. Thus, the current study is aimed to develop a novel CDNS-based nanocarrier for the delivery of a combination of drugs, with a focus on developing the carrier using novel and greener approaches.

Chapter 4
Aim and Objectives

4. AIM AND OBJECTIVES

4.1. Aim of the work

Formulation, characterization and evaluation of nanosponge-based drug delivery system for poorly soluble drugs

4.2. Objectives of the study

The aforementioned aim would be achieved by fulfilling the following objectives:

1. Identification of drugs fulfilling the criteria set for the said work and carrying out extensive preformulation studies.

2. Preparation of nanosponges by suitable methods by employing the principles of Quality by Design and loading the drugs into them.

3. To optimize the developed formulation and carry out in vitro analysis of the optimized formulation.

4. In vivo testing of pharmacokinetics parameters and comparing them with the parent molecule.

5. Accelerated stability studies as per the guidelines laid down under ICH Q1A(R2).

Chapter 5

Experimental Work
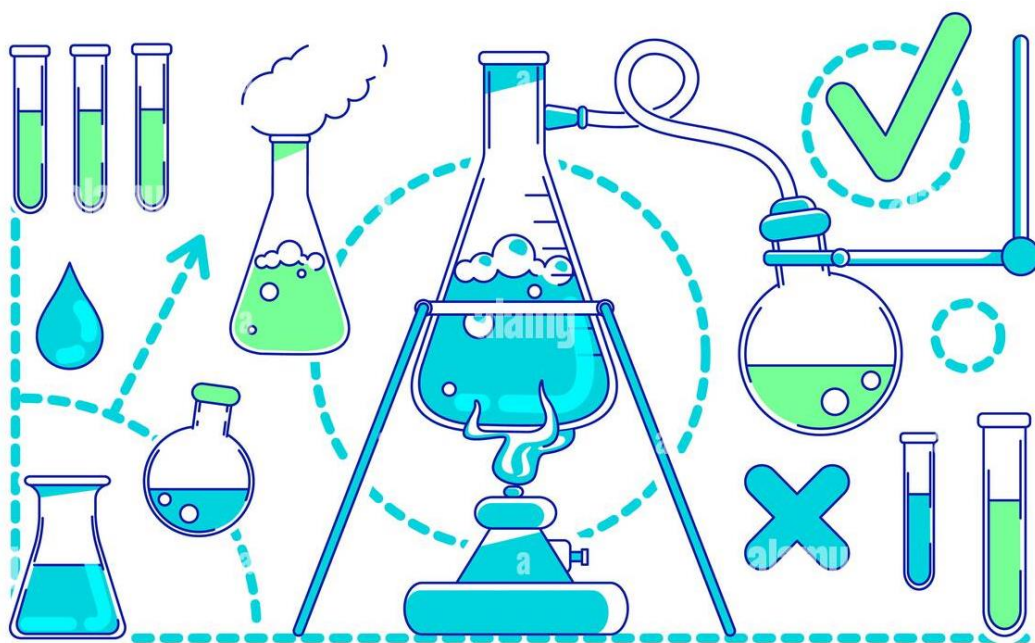
5. EXPERIMENTAL WORK

5.1. Materials and instruments

5.1.1. Chemicals

Here, **Table 5.1** provides an overview of the various chemicals employed in the present research.

Table 5.1. Representing detailed list of chemicals used in the study

Materials	Manufacturers	CAS number
Cinnarizine	Hikal Ltd., India	298-57-7
Domperidone	Ankur Drugs & Pharma Ltd, Baddi, India	57808-66-9
Acetonitrile HPLC Grade	E. Merck Ltd., India	75-05-8
Carbonyldiimidazole	Sigma Aldrich, USA	530-62-1
Dichloromethane	Loba chemie Pvt. Ltd., Mumbai, India	75-09-2
Dimethylformamide	Loba chemie Pvt. Ltd., Mumbai, India	68-12-2
Diphenyl carbonate	Sigma Aldrich, USA	102-09-0
Ethanol	E. Merck Ltd., India	64-17-5
Ferric chloride ($FeCl_3$)	Loba chemie Pvt. Ltd., Mumbai, India	7705-08-0
Hydrochloric acid (HCl)	Loba chemie Pvt. Ltd., Mumbai, India	7647-01-0
Hydroxypropyl-β-cyclodextrin	Roquette India Pvt Ltd, Mumbai, India	128446-35-5
Methanol	Loba chemie Pvt. Ltd., Mumbai, India	67-56-1
Methanol HPLC Grade	E. Merck Ltd., India	67-56-1
Methyl-β-cyclodextrin	Roquette India Pvt Ltd, Mumbai, India	128446-36-6
Orthophosphoric acid	Loba chemie Pvt. Ltd., Mumbai, India	7664-38-2
Potassium dihydrogen orthophosphate	Loba chemie Pvt. Ltd., Mumbai, India	7778-77-0
Sodium hydroxide	Loba chemie Pvt. Ltd., Mumbai, India	1310-73-2
β-cyclodextrin	Roquette India Pvt Ltd, Mumbai, India	7585-39-9

5.1.2. Equipment and Machines

Table 5.2 provides a summary of the numerous tools and machinery employed in the present study.

Table 5.2. Showing list of equipments and their manufactures used in the present study

Equipment and Machines	Model and manufacturer
Bath sonicator	PCI services, Mumbai.
Centrifuge	Remi Equipments, Mumbai, India
Differential scanning calorimeter	DSC 7020, Hitachi, Japan
Disintegration rate test apparatus	DT 1000, Lab India, India.
Dissolution rate test apparatus	DS 800 (Manual) Lab India, India.
Electronic Weighing balance	Wensar Weighing Scales Limited, Chennai, India.
FTIR-ATR spectrophotometer	Infra 3000, Analytical Technologies Limited, India
High performance liquid chromatography	LC-20AD Shimadzu Co. Ltd., Japan.
Hot air oven	Navyug India, Ambala, India
Lyophilizer	BTI-10 FDMN, Biotechnologies Inc., India.
Magnetic stirrer	Remi Equipments, Mumbai, India
Mechanical shaker	Neolab, Mumbai, India
Micropipette	Perfitt, India.
Multi punch tablet compression machine	Cadmach Machinery Ltd., Ahmadabad, India.
Particle size analyzer	Malvern Zetasizer, USA
pH meter	Phan, Lab India, Mumbai, India
Probe Sonicator	Leelasonic- 500UPP, Mumbai, India.
Scanning electron microscope	JSM-7610F Plus, JEOL, Japan
Scientific microwave	700 watts / 2450 MHz Raga Tech, Pune, India.
Stability chamber	Remi Equipments, Mumbai, India
Syringe filter (0.22μm), (0.45μm)	Millipore, Germany.
UV spectrophotometer	UV-1800, Shimadzu, Japan.
Vacuum filtration pump	Millipore, India.
XRD analyzer	D8 Advance, Bruker, USA

5.2. **Methodology**

5.2.1. Analytical method development

The HPLC system was equipped with an eluent transport pump (LC-20AT; Shimadzu, Japan), a 20μL loop (Rheodyne), a UV/Visible detector (SPD-20A; Shimadzu, Japan) and LC Solution software. In order to quantify and separate cinnarizine (CIN) and domperidone (DOM) in a CIN-DOM mixture, a C-18 reverse-phase column (Water SunFire C18, length of 25 cm, internal diameter of 0.46 mm, and the size of silica particles: 5 μm) was utilised. One millilitre per minute flow rate was maintained and detected at 270 nanometers wavelength. Standard solutions (10μg/mL) were prepared and evaluated in the mobile phase [151].

5.2.2. Analytical method validation

5.2.2.1 Develop quality control standards

Three levels of quality control criteria for the calibration curves were established: 80%, 100%, and 120% of the mean concentration (6μg/mL for both CIN and DOM). Lower quality control (LQC, as 4.8 μg/mL), medium quality control (MQC, as a 6μg/mL), and higher quality control (HQC, as a 7.2 μg/mL) standards were assigned to these levels. All three concentrations were obtained in methanol. The developed analytical method was validated according to the Q2 (R1) guiding principle of the International Council for Harmonization (ICH). The performance of the system was evaluated by assessing its suitability parameters. Six replicate injections of standard solutions (6μg/mL) of CIN and DOM were run into HPLC to assess the system's suitability. In addition, measurements were performed for the height equivalent to a theoretical plate (HETP), theoretical plate, theoretical plate/meter, tailing factor, and peak purity index [152].

5.2.2.1.1. Linearity and range

Calibration chart was constructed by drawing the average crown area of six imitates against the standard solution (2-12 μg/mL) of DOM and CIN, followed by reading and understanding the regression equation.

5.2.2.1.2 Accuracy

To determine the accurateness of the method, the CIN and DOM recovery were determined from mobile phase (CH₃OH: Acetonitrile) quality control standard solutions. All three of quality control solutions were instilled into the HPLC six times, and the mean response was documented. Percent recovery was estimated by dividing real drug recovery with theoretical concentration and multiplying by a hundred, as given in equation 5.1. The mean of the responses was then determined, and the relative standard deviation as a percentage was calculated.

$$\text{Percent recovery} = \frac{\text{Actual concentration recovered}}{\text{Theoretical concentration}} \text{ X } 100 \ldots\ldots\ldots\ldots\ldots \text{ Eq (5.1)}$$

5.2.2.1.3 Precision

The procedure's repeatability as well as intermediate precision were considered while assessing its precision. A total of six quality control samples were injected under the alike experimental conditions on the similar day. During intermediate precision estimation, all three control samples were determined 6 times on 3 different days (inter-day) and by 3 individual experts (interanalyst) under similar experimental conditions. The percentage RSD was determined based on the mean of responses. If the obtained percent RSD was less than 2%, the approach was considered precise.

5.2.2.1.4. Robustness

Robustness testing is commonly used to assess the impact of minor modifications on the precision of a developed approach. The mobile phase's flow rate (0.8, 1 and 1.2 mL/min), wavelength (265 nm, 270 nm, and 275 nm) and mobile phase (methanol:acetonitriles:70:30) mixture ratio (65:35, 70:30, and 75:25 v/v) were all varied. Quality control sample of medium concentration (6 μg/mL) was injected repetitively for six times. The influence on peak area and retention time were noted by injecting six replicates of medium concentration (6 μg/mL). Then, percentage relative standard deviations were calculated.

5.2.2.1.5. Estimation of LOD and LOQ

LOD and LOQ were premeditated using the slope of the calibration graph(s) and the standard deviation of the response (σ). The standard deviation was computed using the standard

deviation of the Y intercepts of the regression line. Equations 5.2 and 5.3 for LOD and LOQ are presented below:

$$LOD = \frac{3.3\sigma}{S}$$ ……………………………Eq (5.2)

$$LOQ = \frac{10\sigma}{S}$$ ……………………………Eq (5.3)

Here, S represents the slope of the calibration curve and σ is the standard deviation of the response.

5.2.2.1.6. System suitability

The HPLC system's theoretical plate number, tailing factor, resolution among CIN and DOM drug's peaks as well as HETP were all assessed. Six replicates of mid concentration (6 μg/mL), CIN and DOM were injected into the mobile phase (methanol:acetonitriles:70:30) for this examination [153].

5.2.3. Constructions of calibration curves

5.2.3.1. UV-Visible spectrophotometric method

5.2.3.1.1. Determination of absorption maxima (λ$_{max}$) of Cinnarizine and Domperidone

Standard solutions (10μg/ml) of CIN and DOM were prepared in distilled water, methanol and 0.1 N HCl. The prepared solutions were scanned on a UV-visible spectrophotometer for the determination of absorption maxima (λ$_{max}$).

5.2.3.1.2. Preparation of calibration curve in distilled water

Methanol was used to dissolve 50 mg of CIN and DOM, and the volume was adjusted to 50 ml. 1 ml of the 1000 ppm solution was diluted with methanol up to 10 ml to develop a solution with a concentration of 100 ppm. Dilutions in the range of 0-20 ppm were achieved by diluting this solution with pure distilled water. To create calibration curves, the absorbance values at 254 nm and 287 nm were measured against the blank. These calibration curves are used for the measurement of solubility.

5.2.3.1.3. Calibration curve in 0.1 N HCl

In 50 ml volumetric flasks, 50 mg of each drug was added and the volume was made up to 50 ml with methanol. To obtain a solution of 100 ppm, the 1 ml of this solution (1000 ppm) was further diluted to 10 ml using methanol. These solutions were further diluted accordingly with 0.1 N HCl to get different concentrations in the range of 0-20 ppm. The absorbance values were measured at 254 nm and 287nm against the blank and the calibration curve were constructed. These calibration curves were used for carrying out dissolution studies.

5.2.3.1.4. Calibration curve in methanol

In 50 ml volumetric flasks, 50 mg of each drug was added and dissolved with 50 ml of methanol. Further, 1 ml of above obtained solution was diluted with methanol to get a 100 ppm solution. These solutions were further diluted with methanol to achieve concentrations ranging from 0 to 20 ppm. The absorbance values at 254 nm and 287 nm were measured against a blank, and a calibration curve was produced. These calibration curves were used for drug content measurement.

5.2.4. Solubility analysis of CIN and DOM

5.2.4.1. Aqueous solubility

The shake-flask technique was employed to assess the solubility of plain CIN and DOM drug in water at room temperature. To create a saturated solution, an excess of each pure drug (CIN and DOM) was incorporated to 10 mL of distilled water. The liquid mixture was shaken for 48 hours at $37 \pm 0.2°C$ in a shaking water bath at 50 rpm on a mechanical shaker. The mixture was then incubated at room temperature for 24 hours to achieve an equilibrium between dissolved and undissolved pharmaceuticals, and the excess pharmaceutical was eliminated via filtration utilizing Whatman No.1 filter paper. The resultant solution was appropriately diluted with distilled water and the dissolved quantity of the medication was assessed spectrophotometrically at 254 nm and 287nm.

5.2.4.2. pH-dependent solubility

Different buffers of pH 1.2, 2, 4, 6, 8, and 10 were prepared according to the procedure in Indian pharmacopoeia (IP). The drugs (CIN and DOM) were added in excess of 10 ml of

each buffer solution in separate six vials that were sonicated for 20 minutes and mechanically shaken for 6 hours. The solutions were filtered and diluted appropriately. The samples were analyzed spectrophotometrically for drug content at 254 nm and 287 nm.

5.2.5. Synthesis of cyclodextrin-based nanosponges

5.2.5.1. Selections of the polymer

To determine the degree of complexation between the drugs and various cyclodextrins, phase solubility studies were conducted using the method proposed by Higuchi and Connors [154]. Excess of the drugs (50 mg each) was put into 10 ml of distilled water containing various concentrations of β-cyclodextrin (β-CD) (0-10 mM), hydroxypropyl-β-cyclodextrin (HPβ-CD) (0-10 mM), and methyl-β-cyclodextrin (Mβ-CD) (0-10 mM), in a series of transparent vials. The resulting suspensions were agitated for 48 hrs at ambient temperature on a vibratory shaker. The dispersions were filtered through a Whatman filter paper (No.40) after they had been equilibrated. The filtered samples were diluted appropriately and the CIN and DOM concentrations were determined using UV analysis in comparison to a blank. The same concentrations of β-CD, HPβ-CD, and Mβ-CD did not show any significant absorbance at 254 nm and 287 nm. Experiments were conducted in triplicate. The phase solubility diagrams were established by charting a graph of the concentration of each drug against the respective concentrations of cyclodextrins. The binding constants were calculated from their incline and intercept values using the equation 5.4,

$$K_{1:1} = \frac{Slope}{S_0(1-slope)} \ldots\ldots\ldots\ldots\ldots\ldots\ldots\text{Eq (5.4)}$$

Where S_0 signifies the drug's intrinsic solubility (drug solubility in aqueous solutions in the absence of CD) and slope denotes the inclination of the linear drug-CD solubility curve (i.e., A_L-type).

5.2.5.2. Selection of Cross-linkers:

Using a range of cross-linkers, including carbonyl, diisocyanate, anhydride, and epichlorohydrin, cyclodextrins are changed into highly porous structures to make

cyclodextrin nanosponge, a versatile drug carrier. Cross-linkers connect the cyclodextrin molecules, creating nanochannels and a nanoporous structure. Synthesis of NSs using two carbonyl-based linkers, diphenyl carbonate and carbonyldiimidazole was undertaken. The criteria for prioritizing carbonyl crosslinkers were the quality of the end product and the simplicity of the synthetic process.

5.2.6. Wave-assisted synthesis of nanosponges

Both typical non-conventional heating methods, such as microwave (MW) and ultrasonic (US) wave-assisted methods, as well as well-known traditional heating methods, such as solvent evaporation method and melt method, can be used to manufacture nanosponges. Here, wave-assisted unconventional techniques were applied to obtain a higher yield of nanosponges in a shorter time. The various process variables related to microwave and ultrasonication procedures, affecting the size and yield of nanosponges were optimized using the Design of Experiments (DoE).

5.2.6.1. Microwave-assisted synthesis of CDNS (MW-NS)

5.2.6.1.1. Initial trials

Microwave reactions were performed in a scientific microwave system (Raga Tech) 2450 MHz, with a fibre optic temperature probe, equipped with an infrared camera, and a magnetically stirring system. This integrated system was very useful for maintaining and observing the reaction conditions prerequisite for nanosponge synthesis. The procedure involved blending the polymer (β-CD) and crosslinker (DPC) in different molar ratios (double, quadruple, and sextuple) in a 250 mL flask with 100 ml suitable solvent dimethylformamide (DMF) and proceeded to microwave irradiation. After carrying the reaction for a specific period, a distillation process was used to remove the solvent. To purify the product after complete solvent removal, the final product was cleansed with water and then extracted using Soxhlet with ethanol for around 4 hr. The final product named Microwave nanosponges (MW-NS) was dried overnight at 60°C in an oven and subsequently powdered in a mortar [150].

5.2.6.1.2. Optimization of nanosponges synthesis by microwave-assisted method

Based on the previous experiments, 3-factor, 3-level Box-Behnken experimental strategy was mapped out to explore the effect of the microwave power level (A), reaction time (B), and stirring speed (C) at 3 levels which were found to influence the extent of polymerization by quantifying the practical yield and particle size. In **Tables 5.3** and **5.4**, independent and dependent variables are listed [155].

Table 5.3: List of independent variables selected to optimize the preparation of MW-NS

Name of the independent variable	Code	Unit	Levels		
			Low	Medium	High
Microwave power level	A	Watt	350	455	560
Reaction time	B	Min	40	60	80
Stirring speed	C	rpm	500	1000	1500

Table 5.4: List of dependent variables selected to optimize the preparation of MW-NS

Name of the dependent variable	Unit	Goal
Yield	%	Maximize
Particle size	nm	Minimize

In accordance with the design, the experiments were conducted and the responses were obtained. Stat-Ease Design Expert® software V13.0 was used to analyze the response surfaces of the variables within the investigational sphere by performing Analysis of Variance (ANOVA).

5.2.6.2. Ultrasound-assisted synthesis of CDNS (US-NS)

5.2.6.2.1. Initial trials

In a 100 mL beaker, anhydrous β-CD and diphenyl carbonate were mixed in the aforementioned molar ratios in DMF. To facilitate the melting of diphenyl carbonate, the beaker was placed in an oil-based bain-marie and heated to 90 to 100°C. The linker has a melting point of 89°C, thus an operating temperature above its melting point was chosen to ensure complete and rapid cross-linking of the cyclodextrins to form nanosponges. The

mixture was sonicated for 2 hrs using an ultrasound probe (Leelasonic- 500UPP) capable of supplying a maximum power of 500 W at 20kHz. The ultrasound operated under 6 sec pulse/5 sec rest cycles. As the process progressed, crystals of phenol formed at the flask's neck. During cross-linking, the carbonyl functional group of DPC results in phenol being liberated. A cooling process was followed by the removal of the phenol crystals from the reaction mixture. After the completion of the reaction, distillation was used to remove residual solvent and the mixture was dried completely in the rotavapor. The resultant artifact was cleansed with water and then decontaminated by Soxhlet extraction through ethyl alcohol for four hours to remove unreacted DPC and phenol. The washing water was tested for phenol after every wash by adding 2 drops of acidified ferric chloride solution 1% w/v. After drying overnight at 60 °C in an oven, the obtained US-NS were powdered in a mortar [156].

5.2.6.2.2. Optimization of nanosponges synthesis by the ultrasound-assisted method

The ultrasound-assisted synthesis process of nanosponges was also optimized using the Box-Behnken approach of response surface methodology. It was engaged to investigate the effect of total sonication time (A), power intensity (B), and the duration of pulse on the percent yield (Y1) and particle size (Y2). The list of independent and dependent variables is depicted in **Tables 5.5 and 5.6** respectively.

Table 5.5: List of independent variables selected to optimize the preparation of US-NS

Name of the independent variable	Code	Unit	Levels		
			Low	**Medium**	**High**
Sonication time	A	Hr	1	2	3
Power intensity	B	Watt	250	375	500
Duration of pulse	C	Sec	6	8	10

Table 5.6: List of dependent variables selected to optimize the preparation of US-NS

Name of the dependent variable	Unit	Goal
Yield	%	Maximize
Particle size	nm	Minimize

5.2.7. Fourier transformed infrared-attenuated total reflectance spectroscopy (FTIR-ATR) of the blank nanosponges

FTIR-ATR spectra were measured using FTIR-3000B (Analytical technologies ltd., India) in the frequency range 4000-600 cm^{-1} for unloaded nanosponges prepared by wave-assisted methods. To avoid dirty contributions, each spectrum was captured with a sensitivity of 4 cm^{-1} in a dry atmosphere and averaged over 100 repetitions, resulting in a good signal-to-noise ratio and reproducibility. It was not mathematically corrected (e.g., smoothed).

5.2.8. Loading of the drug into nanosponges

The optimized formulations of nanosponges prepared by both methods and drug powders (CIN, DOM, and their combination) were used in the 1:1 w/w ratio to yield six drug-loaded formulations F1-F6, as illustrated in **Table 5.7**. The 70 mg of optimized nanosponges were suspended in distilled water (30 ml) and homogenized for 10 mins. Then, a 70 mg quantity of the drug/ combination of drugs was dispersed in this homogenized mixture and was sonicated for 10 minutes. This preparation was mixed for 24 hours employing a magnetic stirrer. The aqueous suspension so obtained was centrifugated for 10 minutes at 2,000 rpm to isolate the non-complexed drug as a clump. The supernatant was then lyophilized by employing a lyophilizer (Bio gene, India) to get CIN loaded, DOM loaded and combination loaded nanosponges. Drug-loaded lyophilized NS was stored at room temperature in a desiccator until use.

Table 5.7: Different formulations of drug-loaded nanosponges

Formulation Code	Description
F1	CIN loaded US-NS
F2	DOM loaded US-NS
F3	Combination loaded US-NS
F4	CIN loaded MW-NS
F5	DOM loaded MW-NS
F6	Combination loaded MW-NS

5.2.9. Characterization of drug-loaded nanosponges

5.2.9.1. Particle size, PDI and zeta potential

Using a Malvern® Zetasizer Nano Zs 90 (Malvern® Instruments Limited, Worcestershire, UK), the average size, polydispersity index (PDI), and zeta potential were measured for all drug-loaded nanosponges. Each test sample was diluted 200-times with deionized water and measurements were taken three times at a fixed scattering angle of 90° and a temperature of 25°C respectively.

5.2.9.2. Drug loading and entrapment efficiency

The 50 mg NS was washed properly with methanol to remove any free drug. They were then dried, further, triturate with methanol and sonicated for 15 mins to release the encapsulated drug. It was then filtered and the solutions were analyzed spectrophotometrically at 254 nm and 287 nm, as well as by HPLC at 270 nm. Calculation of drug loading capacity (%) and drug encapsulation efficiency (%) was performed using the following equations (Equations 5.5 and 5.6).

$$\text{Loading capacity (\%)} = \frac{\text{Amount of drug in the nanosponges}}{\text{Amount of nanosponges from which drug is extracted}} \, X \, 100 \, \dots \, \text{Eq (5.5)}$$

$$\text{Entrapment Efficiency (\%)} = \frac{\text{Amount of drug in the nanosponges}}{\text{The initial amount of drug added in the process}} X \, 100 \, \dots \text{Eq (6.6)}$$

5.2.9.3. Fourier transformed infrared-attenuated total reflectance spectroscopy (FTIR-ATR)

FTIR-ATR spectra were measured via FTIR-3000B (Analytical technologies ltd., India) in the frequency range 4000-600 cm^{-1} for unloaded nanosponges prepared by wave-assisted methods. To avoid dirty contributions, each spectrum was recorded with a sensitivity of 4 cm^{-1} in a dry atmosphere and averaged over 100 repetitions, resulting in a good signal-to-noise ratio and reproducibility. It was not mathematically corrected (e.g., smoothed).

5.2.9.4. Differential scanning calorimetry (DSC)

DSC analysis was conducted by employing a DSC 7020 calorimeter (Hitachi, Japan). Calibrations were performed on the instrument based upon indium melting point and heat of fusion. Temperatures between 35 and 300 °C were attained by heating at a rate of 10 °C/min. Aluminium sample pans were sourced; an empty sample pan served as a benchmark. In triplicate, 5 mg samples were analyzed under nitrogen purge. This was done to discover whether drugs were included within the NS.

5.2.9.5. X-ray powder diffraction (XRPD)

We used a Bruker diffractometer (D8 Advance, Coventry, UK) to conduct a comprehensive XRPD investigation to investigate the differential crystallinity behavioural patterns of plain NS and loaded NS. The chosen specimens were photographed over a 2θ range across 5-90° angle at a 40 kV voltage and 40 mA current utilizing copper wire as a source of radiation.

5.2.9.6. Morphological evaluation

Field Emission SEM (JSM-7610F Plus, JEOL) was used to determine the surface morphology of the particles Using a double-sided carbon adhesive tape, the nanosponges were frivolously scattered on the tape. Those were then impacted on gold-coated aluminium stubs of 300 Å to reduce the charging effects and photomicrographs were taken at an accelerating voltage of 20 kV.

5.2.9.7. In vitro drug release studies

The release studies were performed for drug-loaded NSs prepared by wave-assisted methods as well as for plain drugs and the physical mixture of the combination of drugs with β-cyclodextrin using USP dissolution tester apparatus II (Paddle type, Labindia). The rotation of the paddles was 50 rpm, and the temperature was maintained at 37°C ± 0.5°C. Amounts of drug-loaded NS equivalent to 20 mg of cinnarizine and 15 mg of domperidone as well as 20 mg and 15 mg pure cinnarizine and domperidone with and without β-cyclodextrin were weighed and filled in dialysis bags. The dialysis bags were tied to a paddle and dipped in the release medium. The initial release experiments were performed in 900 mL of 0.1 N HCl (pH 1.2) for two hours, following which the sample containing the dialysis bag was transferred to a hemispherical dissolution container holding 900 mL of pH 6.8 phosphate buffer for a

further twenty two hours. Then, 5 ml samples were withdrawn after 2, 4, 6, 8, 10, 12 and 24 hrs periods and replenished with an equal volume of new media. Spectrophotometric analysis was carried out on the filtered samples at 254 nm and 287 nm wavelengths. We conducted the release studies in triplicate and plotted the average values as cumulative percent drug released over time. In addition, the difference factor (f1) and similarity factor (f2) were used to compare release profiles between drug-loaded NS and plain drug combinations. Based on the in vitro release data, kinetic models were fitted to the data.

5.2.10. Formulation of orally disintegrating tablet

Using the direct compression approach, nanosponges were compressed into oral dispersible tablets (ODTs). Therefore, trials were conducted to screen the diluents and superdisintegrants to develop the ODTs. All excipients were first sieved through mesh #100. Drug-loaded nanosponges equivalent to 20 mg CIN and 15 mg DOM, as well as other ingredients like diluent, superdisintegrants, sweetener and glidant, were mixed and followed by the addition of lubricant and flavour. The powder was compressed on a single punch machine using a flat bevelled 8 mm punch (Cadmach, India). To assess the suitability of superdisintegrants and diluents, various formulations were prepared as shown in **Tables 5.8** and **5.9**. All the compressed ODT batches (A1-A9 and B1-B9) were subjected to post-compression evaluation for hardness and in vitro disintegration time.

Table 5.8: Trial batches for the ODT of optimized drug-loaded MW-NS

Ingredient	Quantity per tablet (mg)								
	A 1	**A 2**	**A 3**	**A 4**	**A 5**	**A 6**	**A 7**	**A 8**	**A 9**
MW-NS	88	88	88	88	88	88	88	88	88
Galen IQ 720	105	105	105	--	--	--	--	--	--
Avicel PH-102	--	--	--	105	105	105	--	--	--
Dicalcium phosphate	--	--	--	--	--	--	105	105	105
Ac-di-sol	2	--	--	2	--	--	2	--	--

Ingredient	Quantity per tablet (mg)								
	A 1	A 2	A 3	A 4	A 5	A 6	A 7	A 8	A 9
Primojel	--	2	--	--	2	--	--	2	--
Crospovidone	--	--	2	--	--	2	--	--	2
Aerosil	1	1	1	1	1	1	1	1	1
Sodium saccharine	2	2	2	2	2	2	2	2	2
Mint powder	2	2	2	2	2	2	2	2	2
Total Quantity (mg)	200	200	200	200	200	200	200	200	200

Table 5.9: Trial batches for the ODT of optimized drug-loaded US-NS

Ingredient	Quantity per tablet (mg)								
	B 1	B 2	B 3	B 4	B 5	B 6	B 7	B 8	B 9
US-NS	105	105	105	105	105	105	105	105	105
Galen IQ 720	88	88	88	--	--	--	--	--	--
Avicel PH-102	--	--	--	88	88	88	--	--	--
Dicalcium phosphate	--	--	--	--	--	--	88	88	88
Ac-di-sol	2	--	--	2	--	--	2	--	--
Primojel	--	2	--	--	2	--	--	2	--
Crospovidone	--	--	2	--	--	2	--	--	2
Aerosil	1	1	1	1	1	1	1	1	1

Ingredient	Quantity per tablet (mg)								
	B 1	**B 2**	**B 3**	**B 4**	**B 5**	**B 6**	**B 7**	**B 8**	**B 9**
Sodium saccharine	2	2	2	2	2	2	2	2	2
Mint powder	2	2	2	2	2	2	2	2	2
Total Quantity (mg)	200	200	200	200	200	200	200	200	200

5.2.11. Characterization of prepared ODTs containing CIN and DOM

The batches showing the best balance between hardness and in vitro disintegration time would be evaluated for further evaluation. These include pre-compression flow characterization of the blend and post-compression tests like assessing the hardness, thickness and diameter, drug content, uniformity of weight, in vitro disintegration time and in vitro drug dissolution and its kinetics.

5.2.11.1. Flow and compaction properties

Blend equal to 5 gm was allowed to flow into a calibrated cylinder and the volume inhabited by the powder (V_0) was logged and used to calculate the bulk density (D_0), the blend-filled cylinder was then dropped from the height of 6 inches for a total of 1250 taps, the reduced volume was noted (V_F) and used to calculate the tapped density (D_F). The flowability of the powder was assessed by computing the % compressibility and Hausner ratio using the formula $100*(D_0 - D_F)/D_0$ and D_0/D_F respectively. The flow property of the blends was confirmed by measuring the angle of repose of the powder by allowing the powder to flow through a funnel set up at a height of 2 cm and the diameter of the powder-formed cone's base was measured. This was used to compute the value of the angle of repose (AOR) using the formula given in equation 5.7 [157]. All experiments were performed in triplicate.

$$AOR\ (\theta) = tan^{-1} h/r \ldots\ldots\ldots\ldots\ldots Eq\ (5.7)$$

Where h is the height of the cone and r is the radius of the base of the cone.

5.2.11.2. Hardness
Ten tablets from each batch were tested for crushing strength (kg/cm^2) using a Monsanto hardness tester.

5.2.11.3. Uniformity of thickness and diameter
To determine the uniformity of the diameter and thickness, 10 tablets were selected and diameter, as well as thickness, was measured using a vernier calliper. The average diameter and thickness of the tablet were determined. If no individual diameter or thickness value deviated by more than 5% from the average, then the test requirements were considered met.

5.2.11.4. Uniformity of weight
A random sample of 20 tablets was selected and weighed, and then their average weight was calculated. There should not be more than two individuals whose weights differ from the average by more than 7.5 percent, and none should differ by more than twice that percentage.

5.2.11.5. Drug content
RP-HPLC method described under section 5.2 was used to carry out the assay.

5.2.11.6. In vitro disintegration time
Six tablets were tested for disintegration using an in-house modified method. The tablet was placed in basket #10 and agitated at a speed of 40 shakes per minute in 25 mL of artificial saliva (**Table 5.10**) at 37°C using a mechanical shaker.

Table 5.10: Composition of artificial saliva

Ingredient	Quantity in percentage
Sodium Sulphate	0.03
Urea	0.02
Ammonium Chloride	0.04
Potassium Chloride	0.03
Lactic acid	0.3
Sodium chloride	4.5
Purified water	Up to 100 ml
pH	6.5 to 7 with 5 M NaOH

5.2.11.7. *In vitro drug release*

The dialysis technique was used to assess the release of drug from loaded NS. The early release studies were carried out in 900 mL of 0.1 N HCl (pH 1.2) as dissoltion media for two hours, after that the same sample present in dialysis bag was shifted to a hemispherical dissolution vessel holding 900 mL of phosphate buffer dissolution media having pH 6.8 for ten hours. After 2, 4, 6, 8, 10, 12 and 24 hr intervals, five ml samples were withdrawn and swapped with equivalent volumes of fresh dissolution media. Filtered samples were spectrophotometrically investigated for drug existence at 254 nm and 287 nm wavelengths. Release studies were conducted in triplicate.

The batch showing the best results was scaled up and subjected to accelerated stability testing and in vivo evaluations.

5.2.11.8. *Release kinetics of the nanosponge formulations*

The release of the drugs from their nanosponge formulations was analyzed using a variety of kinetic models [158]. Based on the regression coefficient (R^2), the most appropriate model for defining the release mechanism was selected. Statistical and mathematical analysis of dissolution properties was the primary advantage of this method. The available types of kinetic simulations include:

a) Zero-order kinetic model

b) First-order kinetic model

c) Korsmeyer-Peppas model

d) Hixson-Crowell model

e) Higuchi model

a) Zero order kinetic model

Zero-order drug release occurs when drug release is independent of its concentration. This technique is used to achieve a pharmacologically prolonged effect. Equation 8 expresses zero-order kinetic behavior. There are several types of modified release pharmaceutical dose forms, including transdermal systems, matrix tablets with low soluble drugs, osmotic systems, and others, that can all be described using this relationship.

$$C = K_o t \dots\dots\dots\dots\dots.\text{Eq (5.8)}$$

Where, K_0 = zero order rate constant; t = time

The graphical representation is between concentration and time.

b) First order kinetic model

This kinetic model describes drug absorption and/or elimination. Equation 5.9 can be used to express it.

$$Log C = Log C_o - \frac{K_1 t}{2.303}\dots\dots\dots.\text{Eq (5.9)}$$

The graph of the logarithm of drug release vs time curve will be linear. Dissolution profiles such as this are typical for water-soluble drugs in porous matrixes, where the drug release is proportional to the amount of drug remaining in the matrix.

c) Korsmeyer-Peppas model

This simple method was developed by Korsmeyer in 1973 and it relates the drug release to the time elapsed (equation 5.10).

$$\frac{M_t}{M_\infty} = K t^n\dots\dots\dots\dots\dots. \text{Eq (5.10)}$$

Where K = drug release constant

t = release time

M_t/M_∞ = fraction of drug release

n = diffusion constant

d) Hixson-Crowell model

This model describes drug release as a function of particle surface area or particle diameter (equation 5.11). An analysis of the % of drug remaining in the matrix versus time was performed on the results of in vitro drug release experiments to determine the release kinetics.

$$W_0^{1/3} - W_t^{1/3} = \kappa t \ldots\ldots\ldots\ldots\ldots\ldots\ldots\text{Eq (5.11)}$$

Where W_0 = Initial amount of drug in the formulation

W_t = Amount of drug left after time t

κ = Surface-volume relation constant

t = time in hr

e) Higuchi model

To determine drug release from inert matrices, the Higuchi model is used. Based on Fick's law, the model describes diffusion as a drug release process. As a result of this relationship, drug dissolution can be explained for a variety of modified-release pharmaceutical dosage forms, such as some transdermal systems and matrix tablets.

$$ft = K_H t^{1/2} \ldots\ldots\ldots\ldots\ldots\ldots\ldots \text{Eq (5.12)}$$

Where, ft = Amount of drug released in time t.

KH = Higuchi dissociation constant.

5.2.12. Stability studies

As suggested by the ICH Q1A(R2) guidelines (ICH, 2018), the optimized ODTs were tested for six months to see how stable they were in two different conditions. Based on these rules, India is in zones III and IV, so accordingly, temperatures and levels of humidity were chosen. The tablets were stored in stability chambers maintained at 40ºC/75% RH and 30ºC/65% RH and evaluated for their appearance, in vitro disintegration time, in vitro drug release and content of active ingredient with freshly prepared ODTs at 30, 90 and 180 days of storage period. All the tablets were packed in ALU- PVC-PVC-ALU type strip package.

5.2.13. Bioanalytical method development and validation using HPLC

A straightforward, exact, and robust bioanalytical approach was required to perform the pharmacokinetic study of CIN and DOM-loaded nanosponges in a suitable animal model, which was developed using RP-HPLC.

5.2.13.1. Method development of CIN and DOM using mobile phase and rat plasma

A bioanalytical method was developed with the help of ICH M10 guidelines to quantify drugs found in the plasma of rats. In the process of developing the bioanalytical method, similar chromatographic conditions to those specified in the analytical method were applied. We have performed separation of CIN and DOM using a reverse phase column (C-18) and a mobile phase combination of methanol and acetonitrile in a 70:30 v/v ratio. Run duration was limited to 10 minutes. The eluent was pumped with a speed of 1 mL/min and the samples were detected at 270 nm [159].

5.2.13.1.1. Blood collection and plasma extraction

The rats were immobilized while a tiny scratch on his neck caused his eye to bulge out of its socket. Blood was taken in vials having ethylene diamine tetraacetic acid (EDTA) crystals inside after rats were retro-orbitally punctured with a capillary tube. The blood-containing EDTA tubes were centrifugated at 5000 rpm for 15 minutes. The transparent supernatant was pipetted off and housed in a deep freezer at -20 °C for subsequent analysis [153].

5.2.13.1.2. Preparation of blank plasma

1 mL of plasma was combined with 2 mL of a mixture of methanol and acetonitrile and agitated for 5 minutes to isolate the plasma proteins. The supernatant was taken out and spun in a refrigerated centrifuge for 15 minutes at 5000 rpm. A 100 mL volumetric flask with supernatant was filled and adjusted to a volume of 100 mL.

5.2.13.1.3. Preparation of standard stock solution of CIN and DOM in the mobile phase

CIN and DOM (100 mg each) were precisely measured and dispensed to different 100 mL graduated flasks comprising 20 mL of the mobile phase in it. The solutions were sonicated for 5 minutes before being diluted to 100 mL with the mobile phase to achieve a 1000 μg/mL concentration of CIN (labelled as Solution A) and DOM (labelled as Solution A1). Further, a 10 mL aliquot from each flask was then taken then diluted with 100 mL of mobile phase to obtain 100 μg/mL solutions of CIN (labelled as Solution B) and DOM (labelled as Solution B_1). In addition, a 10 mL aliquot from each solution B and B_1, were transmitted to standard

volumetric flasks of 100 mL capacity and the volume was make up using mobile phase to get a 10 μg/mL concentration of CIN and DOM (Solution C and C_1). The 10 mL of aliquots from solution C and C_1 were further diluted via using mobile phase to attain a concentration of 1 μg/mL (1000 ng/mL) (labeled as Solution D and D_1). Here, **Figures 5.1** and **5.2** illustrates a summary of the prepared dilutions.
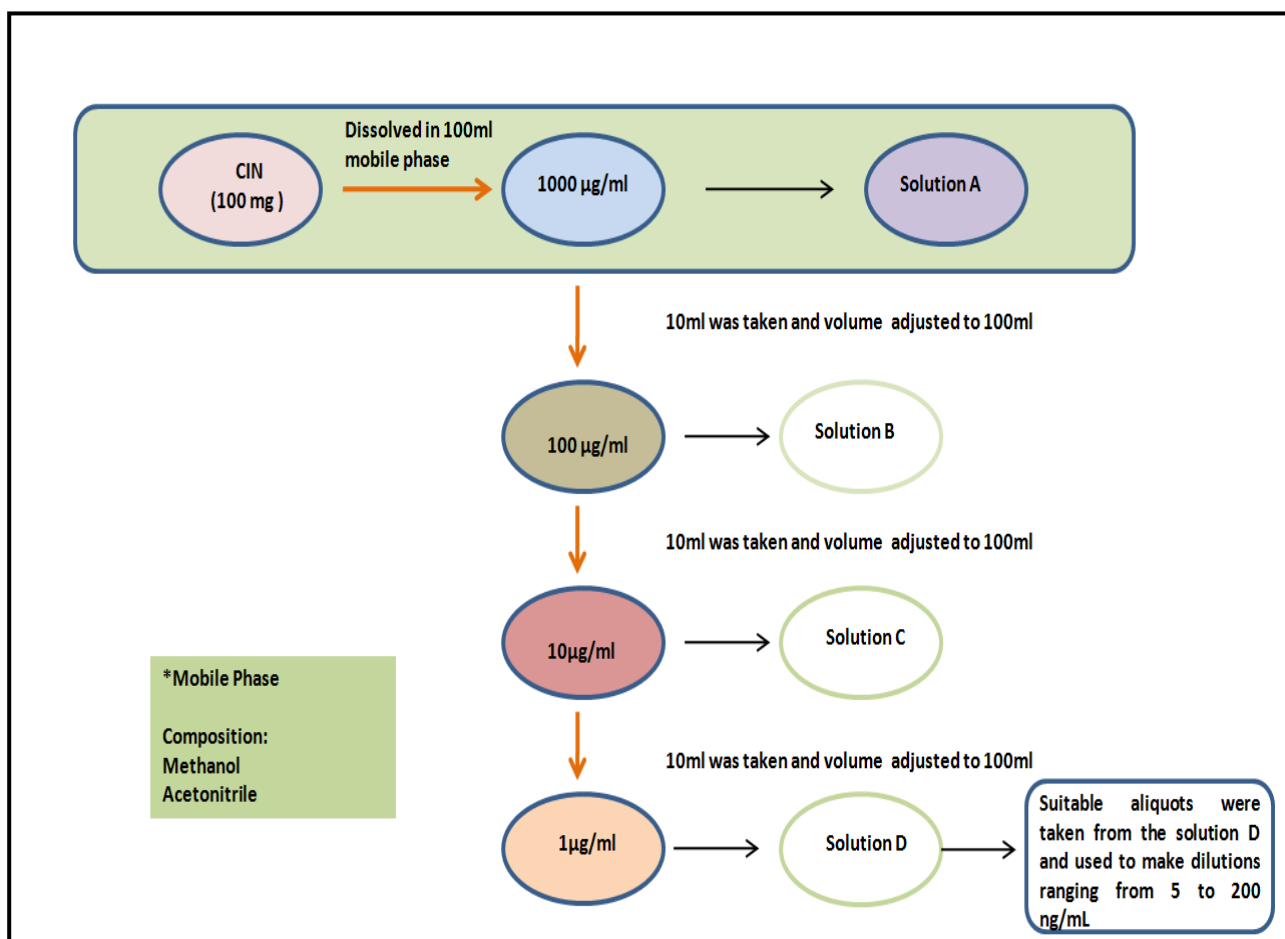
Figure 5.1: Schematic diagram of the dilutions prepared for CIN without plasma
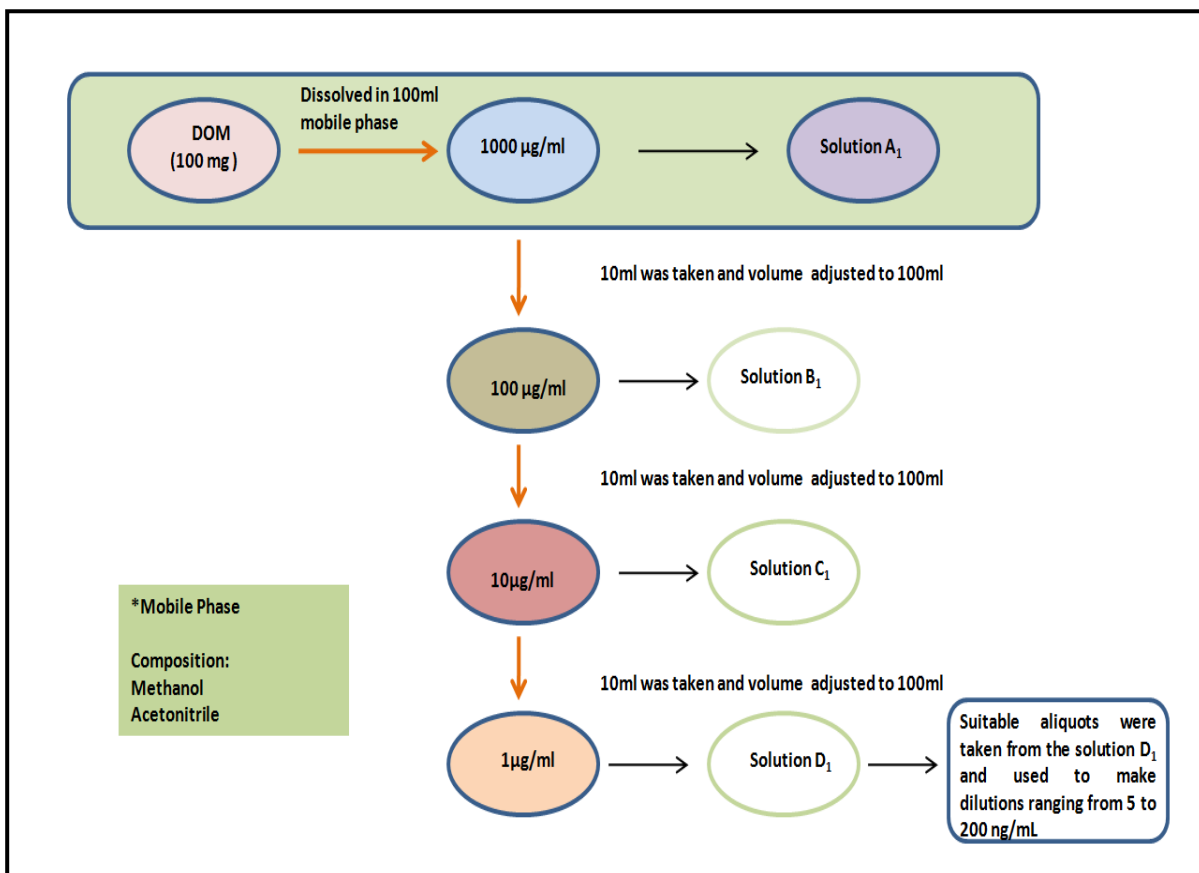
Figure 5.2: Diagrammatic illustration of DOM dilutions prepared without plasma

5.2.13.1.4. Preparation of stock solution of internal standard in the mobile phase

In a 100 mL volumetric flask 10 mg of irbesartan (IRB) was precisely weighed and diluted with 50 mL of mobile phase. The obtained solution was ultrasonically agitated for 15 minutes and the volume was attuned to 100 mL using the mobile phase to get a solution 100 µg/mL concentration (labelled as Solution E). An aliquot of 10 mL from solution E was taken out into a 100 mL standard graduated flask, then the volume was raised to 100 mL with the mobile phase, yielding a desired outcome with a concentration of 10 µg/mL (Solution F), as represented in. **Figure 5.3**.
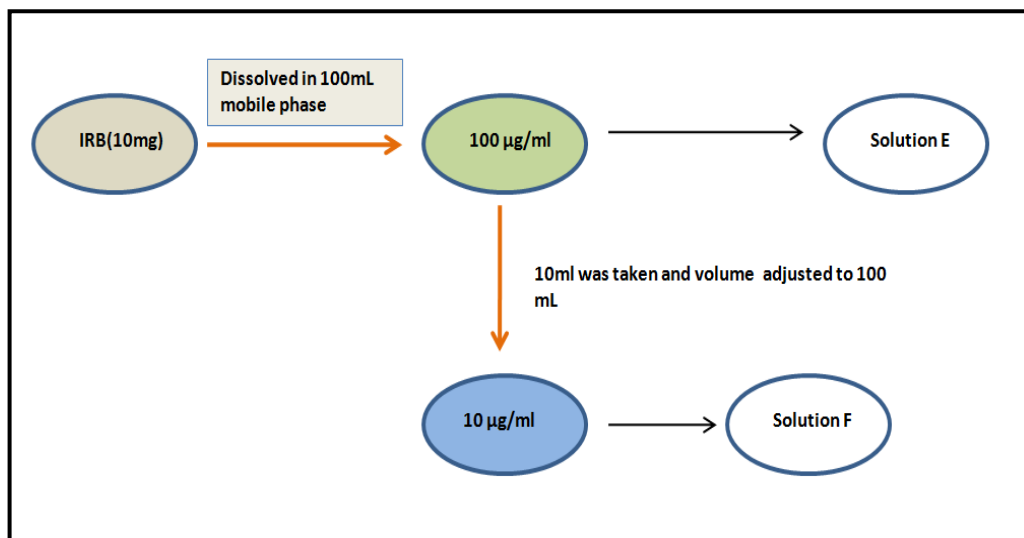
Figure 5.3: Diagrammatic representation of the dilutions prepared for IRB.

5.2.13.1.5. Method specificity

By pipetting off 0.5 mL of blank plasma with a concentration of 1 µg/mL and diluting it by 100 ml of mobile phase, a blank plasma concentration of 5 ng/mL was achieved. Further, 20 µL of this plasma solution was used as a blank sample in HPLC to assess the specificity of the method. Furthermore, 5 ng/mL solutions of CIN and DOM were generated independently from the stock solution in the mobile phase with the spiked matrix. The 50 ng/mL solutions of CIN-DOM (with plasma) were made by diluting 0.5 mL of the 1 µg/mL stock solutions D and D1 to 10 mL. To get a final concentration of 5 ng/mL for CIN, DOM and 10 µg/mL for IRB, a 1 mL aliquot from these obtained solutions was pipetted into two 10 mL standard volumetric flasks. This was followed by the addition of 1 mL of internal standard from its stock solution (100 µg/mL). Finally, each flask's volume was increased to 10 mL. Further, 20 µL of these solutions were put into HPLC and evaluated at 270 nm [160].

5.2.13.1.6. Development of calibration curve of CIN in the mobile phase (nanogram level)

Aliquots (0.05, 0.1, 0.25, 0.5, 1.0, 1.5 and 2.0 mL) of solution D were taken out and placed in a 10 mL volumetric flask to construct the calibration curve for CIN. These aliquots were further diluted with the mobile phase to concentrations of 5, 10, 25, 50, 100, 150, and 200 ng/mL. For the construction of a calibration curve, the dilutions were injected into HPLC. Each of the five working standard solutions was added to the RP-HPLC in a volume of about

25μL. The experiment was run five times, with the mean data being documented at a wavelength of 270 nm.

5.2.13.1.7. Development of calibration curve of DOM in the mobile phase (nanogram level)

The calibration curve for DOM was created by placing aliquots from solution D1 in a 10 mL volumetric flasks (0.05, 0.1, 0.25, 0.5, 1.0, 1.5 and 2.0 mL) and diluting them with the mobile phase to obtain concentrations of 5, 10, 25, 50, 100, 150 and 200 ng/mL. The dilutions were injected into HPLC for calibration curve development. Each of the five working standard solutions was added to the RP-HPLC in a volume of about 25μL. The experiment was run five times, with the mean data being recorded at a wavelength of 270 nm.

5.2.13.1.8. Development of calibration curve of CIN in plasma (nanogram level)

To construct the calibration curve for CIN, aliquots (0.05, 0.1, 0.25, 0.5, 1.0, 1.5, and 2.0 mL) from solution D were placed in volumetric flasks with10 mL capacity. Then, 0.5 mL of rat plasma was introduced, followed by 1 mL of solution F (IRB, 10 μg/mL). 1 mL of acetone was added to the mixture, and then it was centrifugated at 35,000 rpm for 15 minutes. Before the samples were put into the HPLC for drug detection at 270 nm, the mobile phase was used to make dilutions of 5, 10, 25, 50, 100, 150, and 200 ng/mL, as shown in **Figure 5.4**.
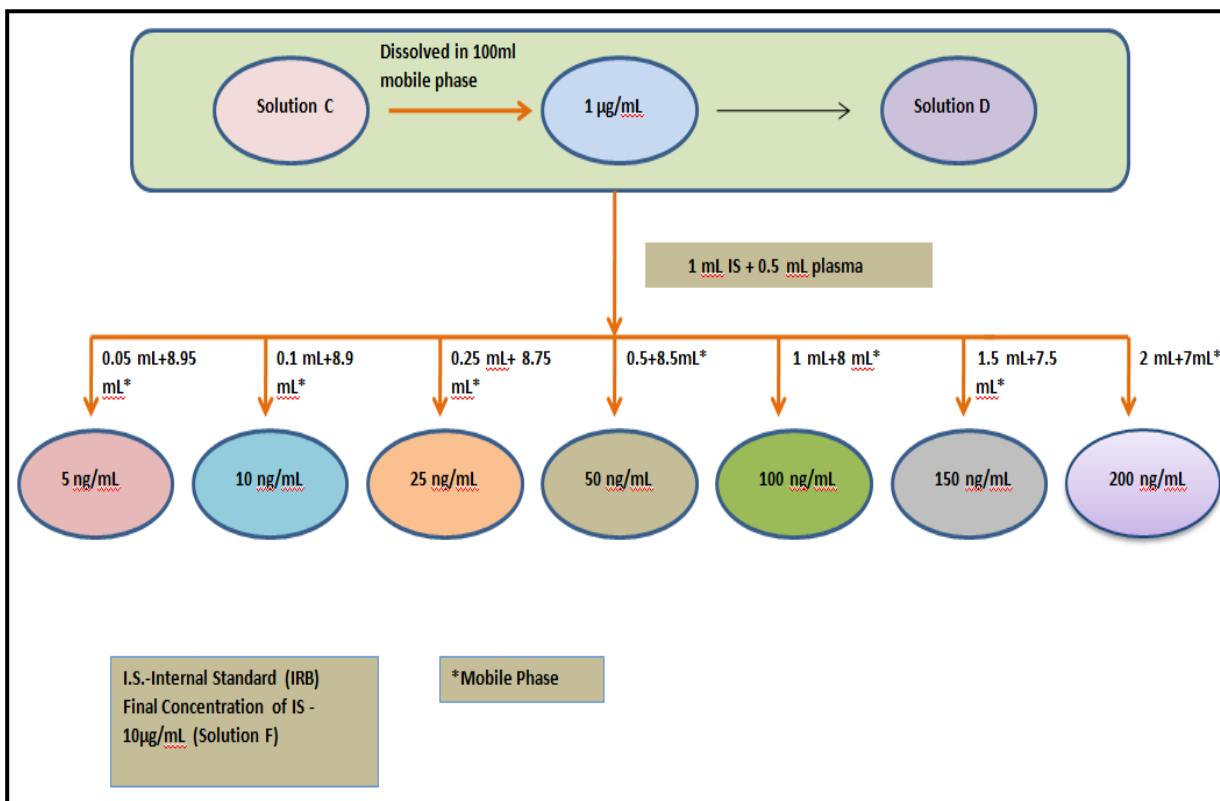
Figure 5.4: Diagrammatic representation of the dilutions prepared for CIN with plasma

5.2.13.1.9. Development of calibration curve of DOM in plasma (nanogram level)

To generate the DOM calibration curve, aliquots of 0.05, 0.1, 0.25, 0.5, 1.0, 1.5, and 2.0 mL were taken from solution D1 and put in 10 mL volumetric flasks. After that, 1 mL of solution F (IRB, 10 µg/mL) and 0.5 mL of rat plasma were introduced. The obtained solutions were mixed with 1 mL of acetone individually and centrifugated at 35000 rpm For 15 minutes. The resulting supernatant was gathered and allowed to evaporate. To get the concentrations of 5,10, 25, 50, 100, 150 and 200 ng/mL. Using the mobile phase, all samples were resurrected to a volume of 10 mL and introduced into HPLC for measurement at 270 nm, as represented in **Figure 5.5**.
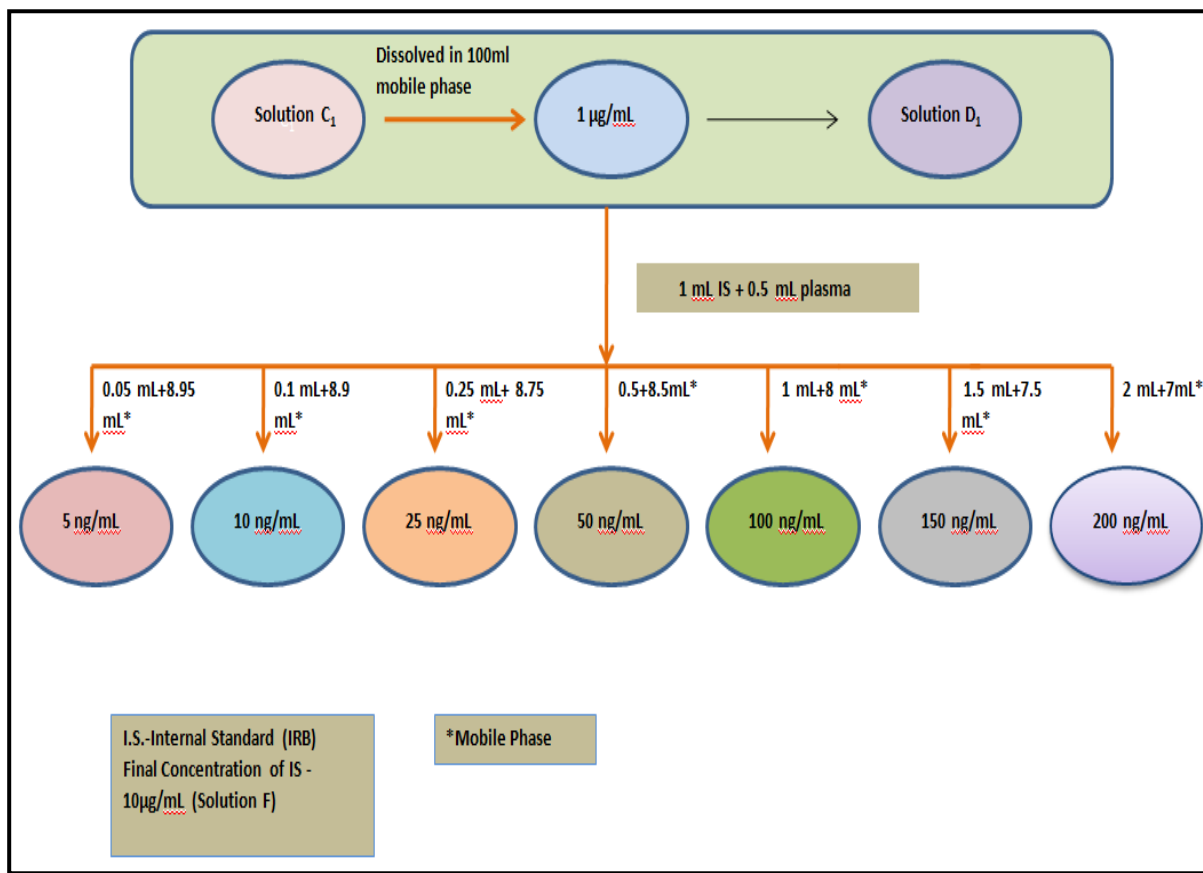
Figure 5.5: Diagrammatic illustration of the DOM dilutions prepared with plasma

5.2.13.1.10. Accuracy study and recovery

The percentage of CIN and DOM that were successfully recovered from the solution at each of the three distinct QC levels, such as LQC, MQC, and HQC, was used to assess the accuracy of both samples (CIN and DOM). The values for the LQC, MQC, and HQC were 15, 100 and 150 ng/mL respectively (for CIN and DOM each). All of these solutions had the internal standard added to them, and its strength was upheld at 10 µg/mL throughout. The experiment was carried out for six times and the average data were chronicled. We were able to determine the percentage of absolute recovery using equation 5.1. For every concentration, the average, standard deviation, and percent RSD were determined. Accuracy within 85–115 percent of the nominal values was considered acceptable [153].

5.2.13.1.11. Precision studies, determination of LOD and LOQ

LQC, MQC, and HQC samples were employed for intraday, interday, and interanalyst precision analyses. All solutions had a 10µg/mL concentration of the internal standard added to them. Section 5.2.2.1.5 describes the process for carrying precision and LOD, LOQ of CIN and DOM. Each concentration's average, standard deviation, and % RSD were assessed.

5.2.13.1.12. Stability study

DOM and CIN spiked plasma samples were tested at the room temperature for 3 h, -20 °C for 3 weeks, and three freeze-unfreeze rotations were run for the stability investigation. For freeze-unfreeze stability, 3 mL of plasma were collected in a single vial. To achieve a concentration of 1000 µg/mL, 3 mg of CIN and DOM were added to this vial and five minutes were spent vortexing the resultant solution. A deep freezer was used to keep this test tube at -20 °C. The sample was frozen, and then the test tube was taken out and let to defrost at room temperature. Cycle 1 involved extracting 1 mL of plasma from the thawed samples, while for Cycle 2 remaining 2 mL of plasma was placed in deep freezer again. The supernatant was centrifuged after precipitating plasma that included drugs (1 mL). After centrifugation, the transparent and clear supernatant was taken out and adjusted with mobile phase up to 1000 mL to achieve a concentration of 1 µg/mL. In addition, dilutions were produced to obtain concentrations of 15 ng/mL (LQC), 100 ng/mL (MQC) and 150 ng/mL. (HQC). Furthermore, 2 mL of the leftover frozen plasma sample was taken out and defrosted at room temperature before being extracted for Cycle 2. The remaining portion was immediately returned to the deep freezer for Cycle 3 processing. The same procedure was followed for Cycle 2 and 3 to get LQC, MQC, and HQC samples as for Cycle 1. The internal standard was incorporated to all of these solutions at a concentration of 10 µg/mL. Each dilution was made in triplicate, put into the HPLC, and its retention time was recorded at 270 nm. For each concentration, the average, standard deviation, and percent RSD were computed [159].

Additionally, the short-term stability of plasma samples spiked with CIN and DOM was judged. Stability was checked one hour, two hours, and three hours before extraction. For the short-term stability assessment, 3 mL of plasma was put in a vial with 3 mg of CIN and DOM each (to reach a concentration of 1000 µg/mL), and the mixture was mixed thoroughly

for five minutes. Room temperature was maintained for the vial. A spiked plasma sample of 1 mL was gleaned out after each time interval, and the drugs were retrieved from the same. Furthermore, it underwent processing to create LQC, MQC, and HQC samples before being mixed with IS (10 µg/mL). Each dilution was made in triplicate, loaded into the HPLC, and their retention periods were all measured at 270 nm. For every concentration, the average, standard deviation and percent relative standard deviation were assessed. 1 mL plasma was collected in three vials for long-term stability assessment, and 1 mg of CIN and DOM were introduced to each container to achieve a concentration of 1000 µg/mL. All three vials were frozen at -20 °C after the mixture had been vortexed for five minutes. The three vials had been frozen for one, two, and three weeks before they were took out. Each interval was followed by the isolation of the medications from the plasma, processing them to create the LQC, MQC, and HQC samples and then IS (10 µg/mL) was incorporated. All dilutions were made in triplicate, added to the HPLC, and their retention duration was tracked at 270 nm. For every concentration, the average, standard error, and percent RSD were estimated.[161].

5.2.13.1.13. System suitability

In order to assess the parameters like tailing factor, HETP and theoretical plate, for system suitability characteristics, the lowest level of drug in the calibration curve (LLOQ, as 5 ng/mL) was injected in hexaplicate.

5.2.14. In vivo testing

5.2.14.1.Pharmacokinetic studies

The Institutional Animal Ethics Committee of the PBRI, Bhopal, reviewed the protocol prior to the experiment's execution and sanctioned it for its ethical conduct. PBRI/IAEC/29-03/010 was the study's protocol number. A single dose, randomized block study design was opted for to conduct this study. This investigation was conducted by employing albino Wistar rats (Male) weighing 250-300 g and approximately 6 weeks old. Prior to treatment, the Wistar rats were fasted for 24 hours [162]. Five groups of six animals each were created out of the study animals. Group I was considered as the positive control group who received an oral dose of the combination of pure drug (cinnarizine+ domperidone) suspension in distilled

water. Group II was considered a negative control group which received plain nanosponges (carrier system) in distilled water. Group III animals were administered with the oral marketed tablet formulations of cinnarizine and domperidone combination, by oral gavage. Tablet was orally administered after dispersing in distilled water. Group IV and V received cinnarizine and domperidone-loaded nanosponge formulations prepared by microwave and ultrasonication synthesis methods, respectively. Both groups (IV and V) have an equivalent amount of cinnarizine and domperidone compared to a market tablet formulation and are also designated as cinnarizine and domperidone control group. Details of all groups are given below in **Table 5.11.**

Blood from each rat's retro-orbital plexus vein was collected at 1 hr, 2 hr, 3 hr, 8 hr, 12 hr, 24 hr, 36 hr, and 48 hr intervals continuously [116]. Heparinized containers were used to collect the blood samples, and RBCs were whirled at 3000 rpm for 30 minutes to enable them to settle. After being collected in tubes, the supernatant plasma was housed at -20°C before being assessed using the established HPLC technique [102]. The plasma concentration-time measurements were utilized to calculate the pharmacokinetic characteristics of the cinnarizine and domperidone combination after its oral intake.

Table 5.11: Details of groups used in the pharmacokinetic evaluation of the optimized CDNS

Group no.	Type of Formulation	Total no of animals	Dose
1	The Positive Control group will receive plain drug suspension orally.	6	2.03 mg/ Kg CIN + 1.54 mg/Kg DOM
2	The Negative Control group will receive plain CDNS suspension orally.	6	10 mg/Kg
3	Oral marketed tablet formulations of CIN and DOM combination [Vertigil] (20 mg + 15 mg), Cipla Pvt. Ltd. (India)] by oral gavage.	6	2.03 mg/ Kg CIN + 1.54 mg/Kg DOM

4	CIN and DOM loaded MW-NS having an equivalent amount of CIN and DOM compared to the marketed tablet formulation.	6	8.71 mg/Kg
5	CIN and DOM loaded US-NS having an equivalent amount of CIN and DOM compared to the marketed tablet formulation.	6	10.51 mg/Kg
Total animals		**30** **Note:** Same animals and groups will be reused for pharmacodynamic study	

5.2.14.2. Pharmacodynamics study

Male albino Wistar rats ranging between 250 and 300 g were employed in the investigation. Prior to administration, the Wistar rats were fasted for 24 hours. This pharmacodynamics study with respect to cinnarizine and domperidone-loaded nanosponges, synthesized by microwave and ultrasonication method, were carried out by using the rat emesis model. The animals and the groups made for the pharmacokinetic studies were used for this study too after giving them a sufficiently long washout period of 72 hrs.

5.2.14.2.1. Rat emesis model

In this investigation, Male albino Wistar rats ranging between 250 and 300 g were employed. Rats, which don't have an emetic reaction [163], are observed to consume non-nutritive substances like clay after exposure to emetic compounds such as cisplatin, and copper sulphate. Often referred to as 'nausea', pica is thought to indicate gastrointestinal malaise [164]. The effectiveness of anti-emetic medications was tested using pica in Wistar rats, which have no emetic reflex. Pica is quantified as the amount of kaolin (clay) consumed by rat in grams [165]. In this experiment, rats were given an oral dose of copper sulphate (40 mg/kg) in distilled water, which was administered intragastrically (IG) using a brusque oral needle, as an emetic inducer for quantifying pica in rats. [162, 166]. In humans, dogs, cats, and ferrets, intragastric administration of copper sulphate induces vomiting by triggering the

endings of the visceral afferents innervating the stomach wall. As a result, rats' afferent impulses from their stomach also appear to cause pica in them. Increased kaolin intake after giving copper sulphate indicates motion sickness or nausea whereas decreased kaolin intake in rats which are pretreated with the drug indicates an anti-emetic effect. Pica was constantly monitored for 48 hours after receiving test materials (drug-loaded nanosponges in 1 mL distilled water suspension) orally 10 minutes before emetic stimulation. The pica data were obtained from the consumption of clay or kaolin within 24 hours and 48 hours following drug administration; the control group's consumption was subtracted from the drug-treated group's consumption.

5.2.14.2.2. Preparation of Kaolin pellets

Acacia gum and hydrated aluminium silicate (kaolin) were blended togather (1:100 w/w) with distilled water until they formed a thick paste. To mimic rats' normal laboratory diet, kaolin pellets were shaped to resemble their usual diet. Drying of the pellets was carried out at room temperature.

5.2.14.3. Statistical analysis

The statistical test was performed by GraphPad Prism version 9.4.1 (GraphPad Software Inc, USA). An Independent t-test was performed to contrast between the two groups, while one-way ANOVA was trailed by post hoc Tukey's test for numerous group comparisons. As long as the p-value was under 0.05, the findings were deemed statistically significant.

Chapter 6

Results and Discussion

6. RESULTS AND DISCUSSION

6.1. Analytical method development

The RP-HPLC method used in the current investigation is the same as that published by Naga Sirisha and Shanta Kumari [167]. The two drugs were isolated chromatographically using a C-18 column (25 cm lengthwise and inner diameter of 0.46 cm, size of silica particles: 5 µm). A combination of ethyl nitrile and methyl alcohol in the proportion of (3:7 v/v) was pumped at the rate of 1 mL/min. Drugs were individually weighed and diluted with methanol. The resulting mixture was sonicated for 15 mins. An autosampler was used to inject 10 µl of this solution, and the drugs were detected at 270 nm. The eluent vehicle and tester mixtures were degassed and clarified through a 0.45 µm membrane filter (Millipore, USA). DOM and CIN showed retention times of 3.38 and 4.49 minutes, respectively. The chromatogram that was obtained is presented in **Figure 6.1**.
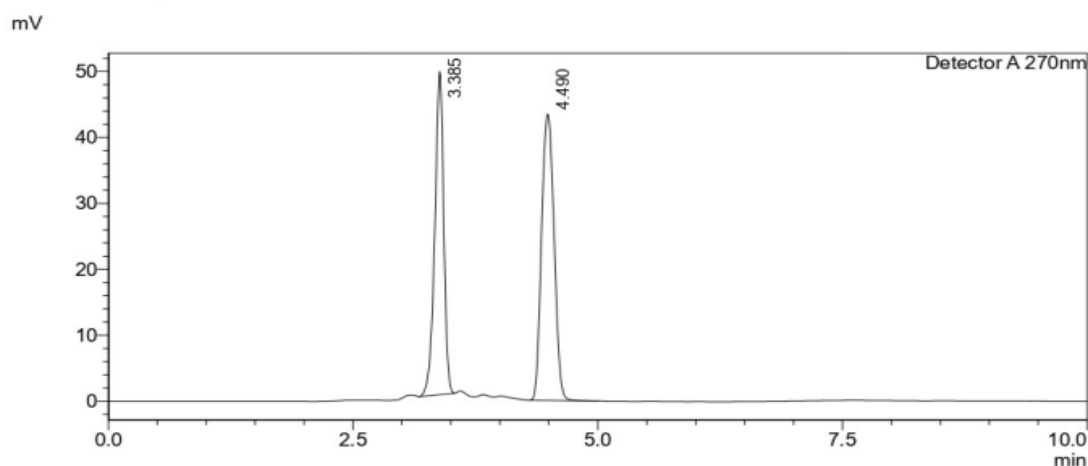
Figure 6.1: Representative HPLC chromatogram of cinnarizine plus domperidone

6.2. Analytical method validation

The HPLC process was authenticated as per the guiding principle laid down under ICH Q2(R2) guidance document. The precision of the system was verified six times by carrying out the analysis of the drugs using the described method. Precision studies were also done on an intraday and interday basis. Multiple samples of the mixture of both drugs were injected to confirm repeatability. To assess accuracy, percent recovery trials were done at three different concentrations (decided to add 80, 100, and 120 percent of the label claim of both drugs). The specificity of the method was assessed by examining the resolution factor of the principal drug peak from the adjacent peak. Further, the LOD

and LOQ were established as a measure of the sensitivity of the method. The robustness of the procedure was assessed by systematically varying the wavelength (270 ± 5 nm), flow rate (1 ± 0.2 mL/min) and eluent composition ($\pm 5\%$ v/v). The ruggedness of the method was tested by allowing three different analysts to carry out the same procedure. The system appropriateness constraints such as resolution, number of theoretical plates and tailing aspect were studied by analysing six replicates of the samples. The results of the aforementioned parameters used for the validation of the method are shown here.

6.2.1. Linearity and Range

Using the graph between concentration and mean peak area, the calibration curves were generated. Linearity was detected between 2 and 14 µg/mL, with regression coefficients between 0.994 and 0.996. The linearity of the method for the individual drugs are given in **Figures 6.2** and **6.3** respectively.
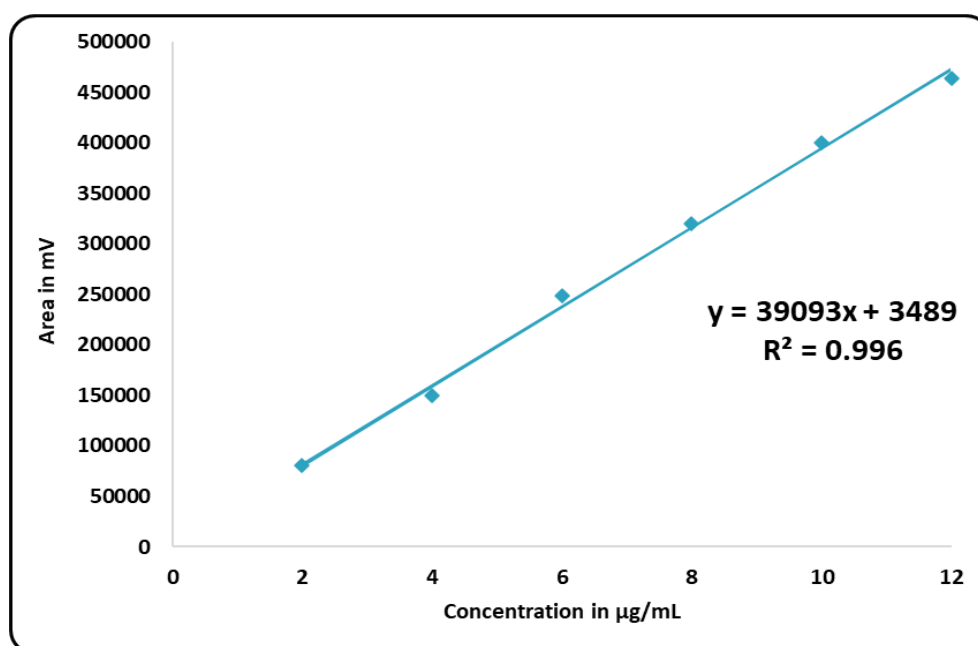
Figure 6.2: Plot of linearity of cinnarizine
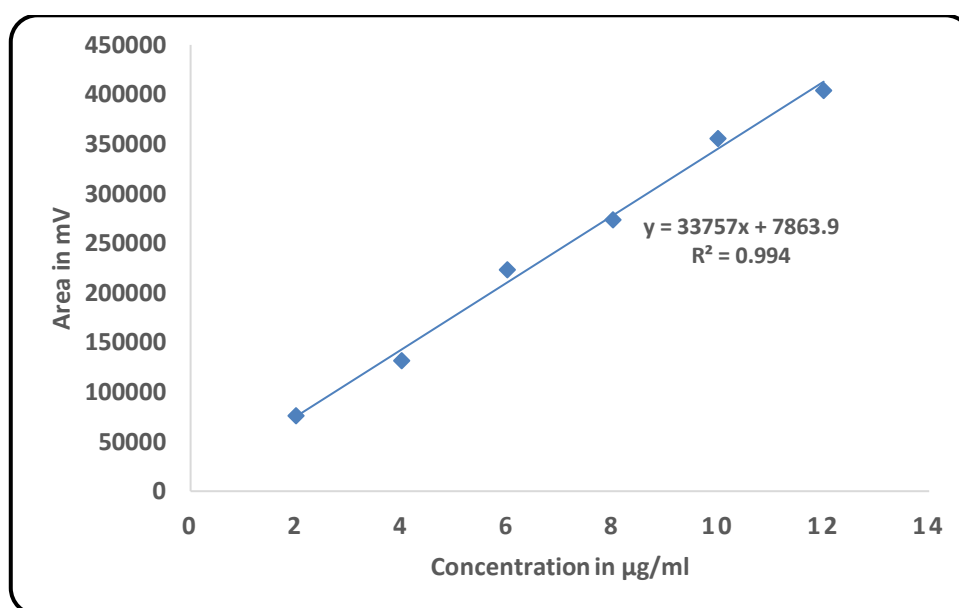
Figure 6.3: Plot of linearity of domperidone

6.2.2. Precision

Under identical experimental conditions, the exactness of the fostered process was concluded by estimating the percentage RSD for the 6 determinations of HQC, MQC, and LQC solutions at the interday, intraday, and interanalyst levels. For each sample, the observed percentage relative variation was less than two percent. The precision study results for CIN and DOM are presented in **Tables 6.1** and **6.2** below.

Table 6.1: The results of precision studies for CIN

Parameters	Level	Conc(µg/mL)	Analytical Responses(area), injections						Mean	SD	%RSD
Repeatability											
LQC		4.8	189931	187931	189490	190068	187295	190992	188951.2	1451.002	0.76
MQC		6	243709	244581	249807	240986	239153	235986	242370.3	4378.173	1.8
HQC		7.2	281009	277841	272328	274292	283383	282742	278599.2	4169.522	1.49
Intermediate precision											
Day 1	LQC	4.8	185633	190931	189360	188068	192305	193952	190041.5	2738.633	1.44
	MQC	6	242519	245661	242107	241725	237738	236916	241111	2972.909	1.23
	HQC	7.2	283849	283141	272810	281213	275361	273500	278312.3	4555.75	1.63
Day 2	LQC	4.8	189177	190064	184717	189214	192260	188500	188988.7	2252.041	1.19
	MQC	6	248849	249007	250295	249371	247389	241194	247684.2	3027.044	1.22
	HQC	7.2	284824	293977	290359	285157	287446	290869	288772	3276.716	1.13
Day 3	LQC	4.8	181262	178824	181628	185900	181569	180090	181545.5	2182.294	1.2
	MQC	6	243207	247967	239249	235520	247674	247445	243510.3	4739.48	1.94
	HQC	7.2	280311	280493	281935	288614	287642	285851	284141	3367.295	1.18
Intermediate precision (inter analyst)											
Analyst 1	LQC	4.8	184538	179931	179490	180168	183273	182718	181686.3	1911.555	1.05
	MQC	6	243709	234581	230837	240676	239053	236306	237527	4191.019	1.76
	HQC	7.2	284319	279337	280028	274567	279889	272139	278379.8	3972.187	1.42
Analyst 2	LQC	4.8	189639	191176	189984	186853	193264	198516	191572	3646.14	1.9
	MQC	6	248857	251377	249984	246853	243578	251174	248637.2	2725.892	1.09
	HQC	7.2	284824	280367	279359	291467	284346	291735	285349.7	4833.787	1.69
Analyst 3	LQC	4.8	182132	179960	189672	182425	179993	181163	182557.5	3318.71	1.81
	MQC	6	241432	246134	237892	242881	241984	237644	241327.8	2924.852	1.21
	HQC	7.2	289356	291189	290043	282346	286289	285436	287443.2	3049.351	1.06

Table 6.2: Results of precision studies for DOM

Parameters	Level	Conc(µg/mL)	Analytical Responses(area), injections						Mean	SD	%RSD
Repeatability											
LQC		4.8	155674	150324	155692	156231	151089	153567	153763	2548.7	1.65
MQC		6	212892	218799	219933	212236	210899	211234	214332	3979.33	1.85
HQC		7.2	249872	252234	251976	252108	250034	247994	250703	1697.96	0.67
Intermediate precision											
Day 1	LQC	4.8	167476	164007	160530	168136	165188	163039	164729	2841.6	1.72
	MQC	6	221727	227938	225226	223268	222254	225216	224272	2315.09	1.03
	HQC	7.2	246674	247270	247717	240060	242948	247006	245279	3082.47	1.25
Day 2	LQC	4.8	153669	155136	150238	153503	158037	153191	153962	2559.03	1.66
	MQC	6	218054	211393	216953	212294	213382	219078	215192	3240.37	1.5
	HQC	7.2	244108	242285	248229	240266	242165	240327	242897	2977.72	1.22
Day 3	LQC	4.8	153501	153849	153755	156302	151871	153086	153727	1452.79	0.94
	MQC	6	212686	213741	217071	213265	217233	218492	215415	2465.26	1.14
	HQC	7.2	240126	243550	241085	244865	243349	249357	243722	3259.24	1.33
Intermediate precision (inter analyst)											
Analyst 1	LQC	4.8	148964	150453	144556	149777	148788	151345	148981	2366.73	1.58
	MQC	6	212887	223349	219902	223312	217998	220785	219706	3921.57	1.78
	HQC	7.2	241290	249936	247755	252031	251132	247451	248266	3866.99	1.55
Analyst 2	LQC	4.8	149978	148779	149933	150155	148873	151332	149842	939.551	0.62
	MQC	6	216334	217835	218977	210021	218886	211443	215583	3902.31	1.81
	HQC	7.2	241133	242759	248871	243347	248873	248599	245597	3563.91	1.45
Analyst 3	LQC	4.8	151764	150789	150777	156733	150342	151138	151924	2403.18	1.58
	MQC	6	218872	217745	212246	213351	219983	218892	216848	3234.65	1.49
	HQC	7.2	240031	244433	247745	247339	244338	248897	245464	3235.81	1.31

6.2.3. Accuracy

The accurateness of the built scheme was gauged by determining the average percent retrieval of the HOQ, MQC, and LQC solutions in the mobile phase. The data demonstrated that the mean percentage recovery in the mobile phase for all three levels was inside the recommended boundaries of 95-105 percent. The developed method's accuracy was confirmed by a percent RSD below 2%. **Table 6.3** summarizes the results of the precision study.

Table 6.3: Results of accuracy studies for CIN and DOM

Levels	Actual conc of drug (ng/mL)	Conc of drug recovered in the plasma sample (ng/mL) *(N=6)	Recovery (%)	Mean Recovery (%)
CIN				
LQC	4.8	Mean= 4.78; S.D.= 0.04; RSD (%) = 0.93	99.58	
MQC	6	Mean= 5.98; S.D.= 0.08; RSD (%) = 1.39	99.66	99.65
HQC	7.2	Mean= 7.18; S.D.= 0.05; RSD (%) =0.75	99.72	
DOM				
LQC	4.8	Mean= 4.75; S.D.= 0.05; RSD (%) = 1.25	98.95	
MQC	6	Mean= 5.94; S.D.= 0.03; RSD (%) = 0.60	99.16	98.99
HQC	7.2	Mean= 7.12; S.D.= 0.08; RSD (%) =1.17	98.88	

6.2.4. Robustness

The robustness of the procedure that was established was investigated by modifying the detecting wavelength (265, 270 and 275 nm), the rate of pumping the mobile phase (0.8, 1, and 1.2 mL/min) and the eluent (Met: ACN) mixture ratio (75:25, 70:30 and 65:35 v/v). The observed percent RSD was not found to be more than 2 percent for all of the samples, signifying that the method was sufficiently tough and that the responses were impervious to these changes. Both **Tables 6.4** and **6.5** provide a concise summary of the findings from the robustness study that was conducted on CIN and DOM.

Table 6.4: Robustness results of various parameters tested for CIN

Value	Peak aera (mean ± SD) *	Mean of peak areas **	Retention time (mean ± SD) *	Mean of retention times **	% Recovery (mean ± SD) *	Mean of % recoveries **
Varying detecting wavelength (λ)						
265	227874 ± 6057.39	228417 ± 758.78 %RSD= 0.33	4.57 ± 0.01	4.58 ± 0.01 %RSD= 0.21	98.66 ± 0.16	98.93 ± 0.39 %RSD = 0.39
270	229284 ± 7464.92		4.59 ± 0.01		99.38 ± 0.20	
275	228093 ± 4079.88		4.59 ± 0.01		98.76 ± 0.10	
Varying rate of flow (mL/min)						
0.8	228689 ± 3772.57	229096 ± 1091.01 %RSD = 0.47	4.52 ± 0.02	4.49 ± 0.02 %RSD = 0.44	99.00 ± 0.10	99.13 ± 0.61 %RSD = 0.61
1	230332 ± 5932.46		4.49 ± 0.01		99.80 ± 0.16	
1.2	228267 ± 3569.17		4.47 ± 0.01		98.60 ± 0.07	
Varying mobile phase ratio (Met: ACN)						
75:25	227320 ± 4905.65	226981 ± 1317.62 %RSD = 0.58	3.57 ± 0.02	3.59 ± 0.02 %RSD = 0.53	98.33 ± 0.13	98.44 ± 0.57 %RSD = 0.58
70:30	225527 ± 6622.13		3.60 ± 0.01		97.50 ± 0.17	
65:35	228096 ± 4845.77		3.62 ± 0.02		98.60 ± 0.12	

*N = 6, **N = 3

Table 6.5: Robustness results of various parameters tested for DOM

Value	Peak aera (mean ± SD) *	Mean of peak areas **	Retention time (mean ± SD) *	Mean of retention times **	% Recovery (mean ± SD) *	Mean of % recoveries **
Varying detecting wavelength (λ)						
265	202825 ± 4260.85	203315.4 ± 714.83 %RSD= 0.05	3.58 ± 0.01	3.57 ± 0.01 %RSD= 0.28	98.66 ± 0.12	98.94 ± 0.34 %RSD = 0.34
270	204135.6 ± 4095.59		3.56 ± 0.01		99.33 ± 0.12	
275	202985.6 ± 2211.05		3.57 ± 0.02		98.83 ± 0.06	
Varying rate of flow (mL/min)						
0.8	200721 ± 1536.49	201694 ± 6262.19 %RSD = 1.09	3.42 ± 0.01	3.39 ± 0.02 %RSD = 0.58	97.73 ± 0.04	98.48 ± 0.88 %RSD = 0.89
1	200129 ± 2460.38		3.38 ± 0.02		98.26 ± 0.13	
1.2	204232 ± 6262.19		3.37 ± 0.02		99.46 ± 0.18	
Varying mobile phase ratio (Met: ACN)						
75:25:00	203583 ± 4927.18	203229 ± 1283.34 %RSD = 0.63	3.41 ± 0.01	3.38 ± 0.02 %RSD = 0.59	99.00 ± 0.14	98.94 ± 0.58 %RSD = 0.58
70:30:00	201897 ± 6868.97		3.38 ± 0.02		98.33 ± 0.20	
65:35:00	204416 ± 6337.29		3.37 ± 0.02		99.50 ± 0.19	

*N = 6, **N = 3

6.2.5. LOD and LOQ

For CIN, the LOD and LOQ were 0.244 and 0.742 mg/mL, respectively, whereas for DOM the values were 0.105 and 0.32 mg/mL.

6.2.6. System suitability

Both drugs were injected in hexaplicate form and the results were within the conventional range. CIN and DOM were continually kept and well distinguished at 4.48 ± 0.106 min and 3.36 ± 0.108 min, which shows that there is a good resolution between the two peaks. The percent RSD of the documented retention times was less than 2, which shows that the integral HPLC system used had excellent repeatability of replicate injections. In all chromatographic runs, the number of theoretical plates was always more than 2000. This was done to make sure that the column worked well throughout the whole separation process. The outcomes of the validation, together with the system suitability parameters, are segmented and reported in **Table 6.6** below.

Table 6.6: Validation and system suitability parameters

Parameter	Cinnarizine	Domperidone
Range (µg/mL)	2 - 12	2 - 12
Slope	39093	33757
Intercept	3489	7863
Coefficient of correlation (R^2)	0.9966	0.9945
Retention time (min)	4.48 ± 0.106	3.36 ± 0.108
Intraday precision (%)	1.35	1.39
Interday precision (%)	1.43	1.33
Accuracy (%)	98.63- 99.91	98.18 -99.66
LOD (µg/mL)	0.244	0.105
LOQ (µg/mL)	0.742	0.32
Tailing factor	0.97 ± 0.03	1.01 ± 0.02
HETP	26.33	26.72
Theoretical plates	2275.91 ± 10.37	2583.61 ± 12.93
Theoretical Plates/meter	38302 ± 224	43488 ± 315
Resolution	2.66 ± 0.01	

6.3. Development of calibration curves

The calibration curves were developed in triplicate to aid in the selection of media for different evaluations to be performed during the course of the research work. The studies were performed on both the drugs using three different media, viz, distilled water, 0.1 N HCl, and methanol. The wavelength used to measure the absorbance was selected as 254 nm for cinnarizine and 287 nm for domperidone based on previous reports [168, 169] as well as scans run on-site. The calibration curve generated in distilled water would be used while performing the phase solubility studies of the drugs with different cyclodextrins. The one prepared in 0.1 N HCl would help with evaluating drug release from the system, while the other prepared in methanol, where the drugs showed good solubility, would help with evaluating entrapment efficiency and drug loading. The concentration range in which Beer-Lambert's law is obeyed, the equation of the straight line, and the coefficient of correlation for CIN and DOM are furnished in **Table 6.7**.

Table 6.7: Results of calibration curves of both drugs in three media each

Drug	Cinnarizine			Domperidone		
Medium	Distilled water	0.1 N HCl	Methanol	Distilled water	0.1 N HCl	Methanol
Concentration range (µg/ml)	2 – 12	2 – 12	2 – 12	2 – 22	2 – 22	2 – 20
Equation of the straight line	y = 0.0717x – 0.0129	y = 0.0745x – 0.0299	y = 0.0731x + 0.0409	y = 0.0361x – 0.031	y = 0.0365x – 0.039	y = 0.0405x + 0.0048
Coefficient of correlation (R^2)	0.9968	0.9984	0.9956	0.9967	0.9976	0.9932

Using UV-visible spectrophotometry, it is also possible to assess the release of CIN and DOM from loaded nanosponges. In the concentration span of 2 to 12 µg/mL, a linear response for CIN was observed, with correlation coefficient values (R^2) of 0.9968, 0.9984, and 0.9956 in distilled water, 0.1 HCl, and methanol, respectively **(Figure 6.4)**. In contrast, in distilled water and 0.1 HCl media, DOM showed a linear response in the concentration span of 2 to 22 µg/ml, alongside R^2 values of 0.9967 and 0.9976 (**Figure 6.5**). However, for methanol, the straight response was in the breadth of 2 to 20 µg/mL, with a correlation factor of 0.9932. High correlation values (R^2) indicate that concentration and absorbance of drug solutions are closely related. Beer's law was shown to be valid in these concentration ranges based on the results.
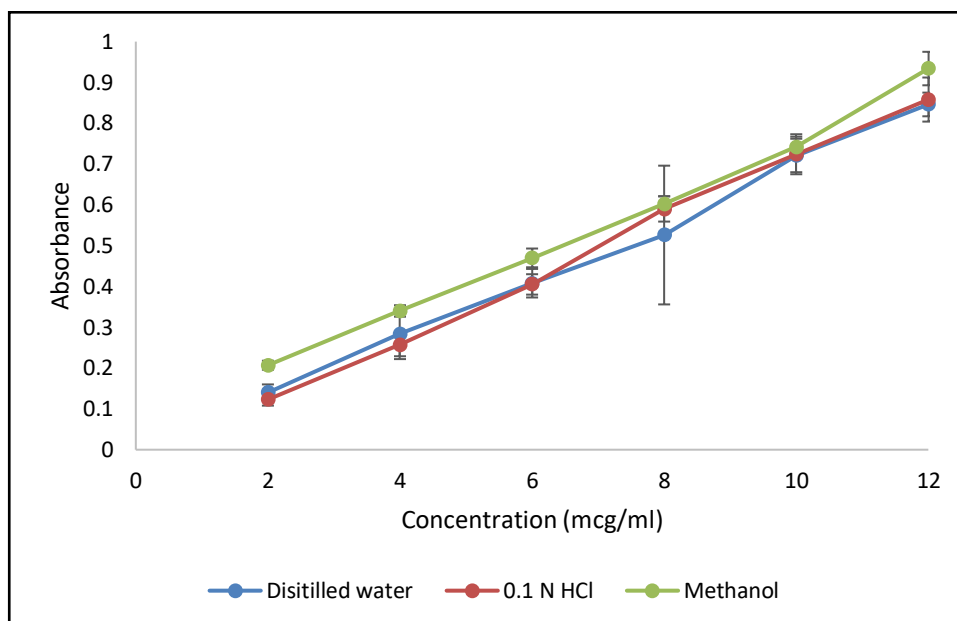
Figure 6.4: Calibration curves of CIN in distilled water, 0.1 N HCl, and methanol
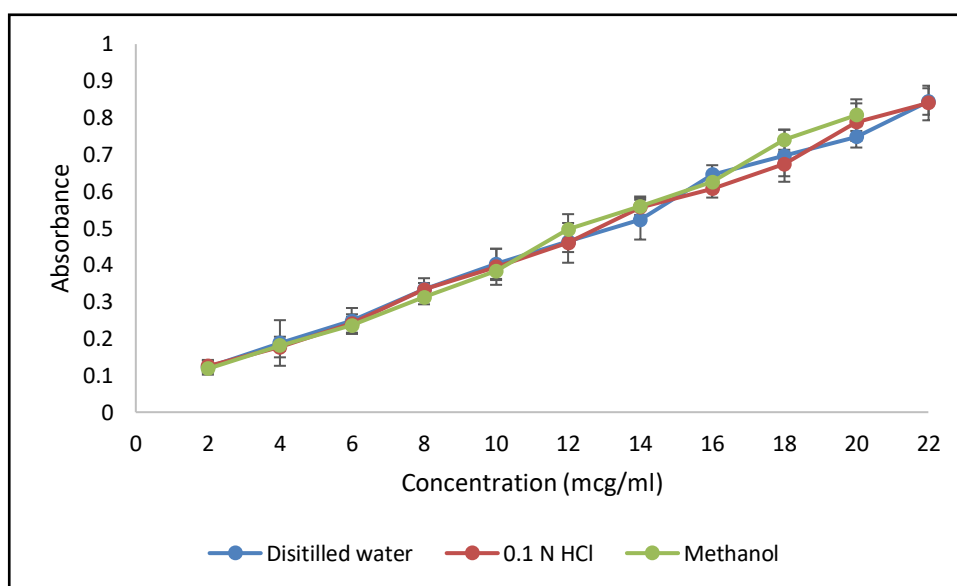
Figure 6.5: Calibration curves of DOM in distilled water, 0.1 N HCl, and methanol

6.4. Solubility analysis of CIN and DOM

6.4.1. Aqueous solubility

The aqueous solubility for CIN and DOM was experimentally determined to be 2.349 µg/mL and 1.039 µg/mL correspondingly. These solubility estimates were close to the values reported by previous researchers. The value reported for cinnarizine is around 2 µg/mL [170] and for domperidone is 0.986 µg/mL [171].

6.4.2. pH-dependent solubility

Both drugs showed better solubility in the acidic media with maximum solubility at pH 4. The solubility in the alkaline medium was negligible. This has also been reported by other researchers for cinnarizine[172, 173] as well as domperidone [174, 175]. The results are shown in **Figure 6.6.**
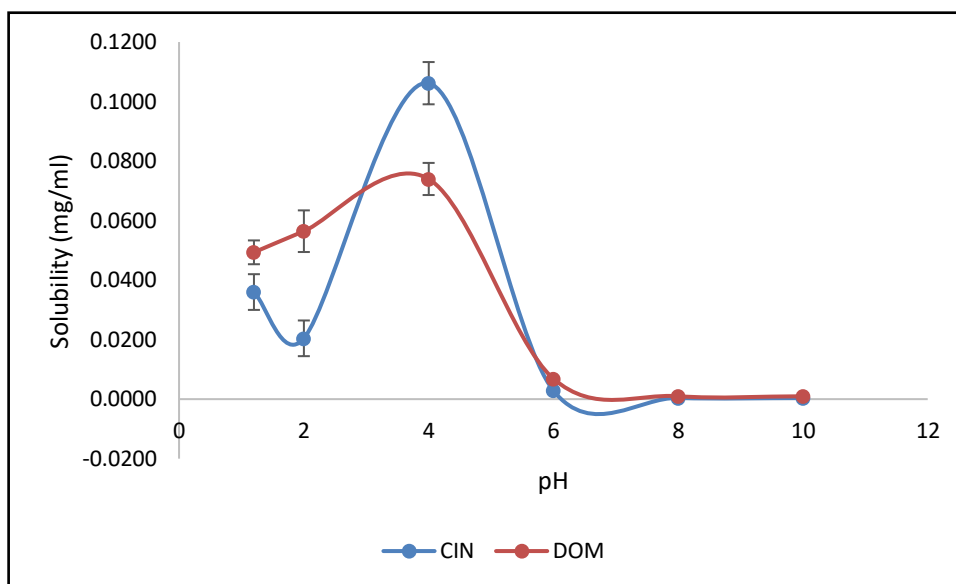
Figure 6.6: pH solubility profiles of CIN and DOM

6.5. Synthesis of cyclodextrin-based nanosponges

6.5.1. Selections of the polymer

The phase solubility contours of CIN and DOM in aqueous mixtures of CDs (β-CD, HPβ-CD and Mβ-CD) are illustrated in **Figures 6.7 and 6.8** respectively. The solubility of the drugs improved directy as a function of CDs' concentrations, yielding A_L (Linear diagram) type phase solubility plot in all the three cyclodextrins except A_N type for Mβ-CD with respect to CIN. These A type curves are pointing toward formation of a complex, where the complex-forming molecules, CDs were existing in first-order degree with regard to the drug. As the slopes of all of these plots were less than 1, it was possible to appraise a 1:1 stoichiometry and determine the apparent stability or binding constant (K_S) of the binary complexes sourcing the equation laid down by Higuchi and Connors [124]. The appraised values of regression coefficients, slopes of the plots, and binding constant (Ks) are presented in **Table 6.8**. The apparent stability constants of both drugs with various CDs understudy increased in the order HPβ-CD >β-CD>Mβ-CD.
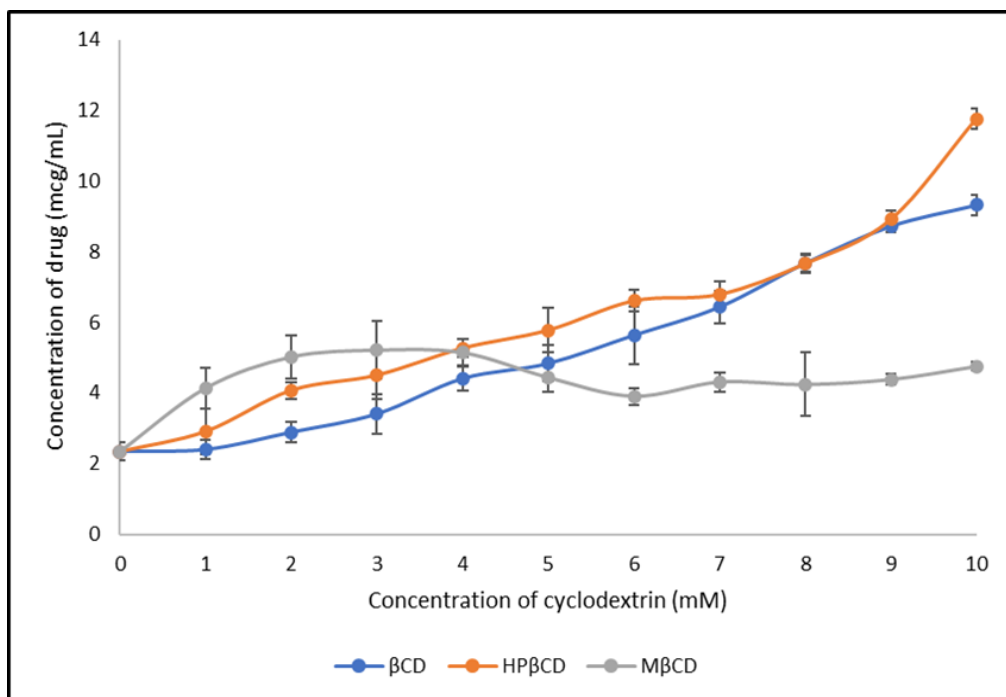
Figure 6.7: Phase solubility diagram of CIN with different cyclodextrins
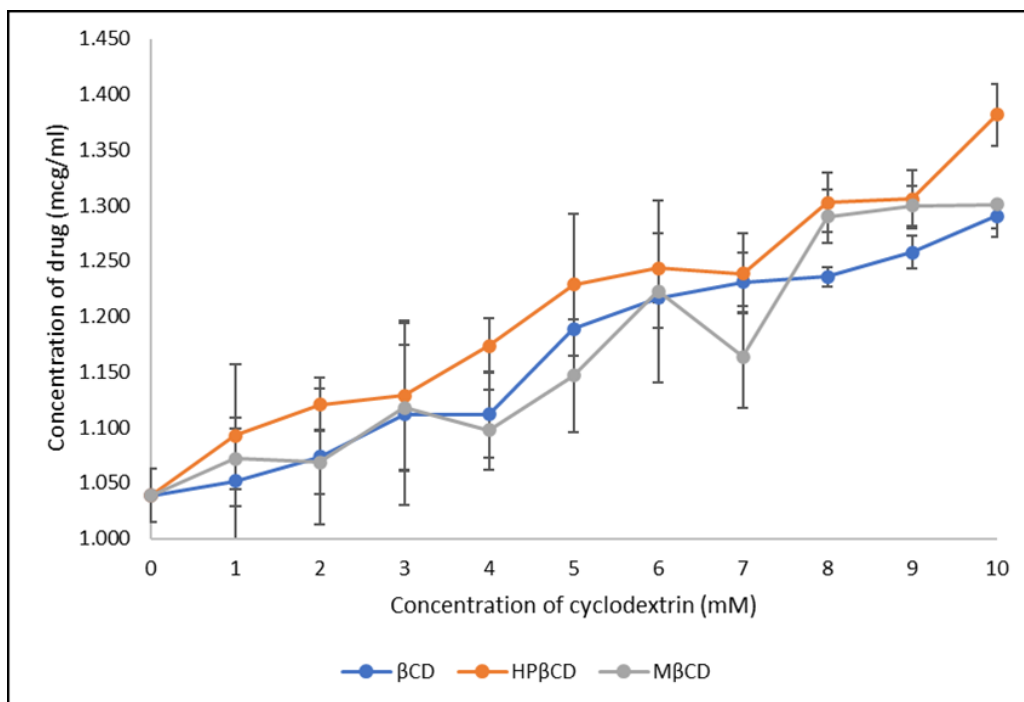
Figure 6.8: Phase solubility diagram of DOM with different cyclodextrins

Table 6.8: Results of phase solubility studies on both drugs with three cyclodextrins

Sample	Regression coefficient	Slope	Curve Type	Binding constant (K_S) (M^{-1})
Cinnarizine				
β-CD in D/W (Distilled Water)	0.9739	0.0744	A_L	1000.03
HPβ-CD in D/W	0.9355	0.0797	A_L	1003.009
Mβ-CD in D/W	0.9739	0.0069	A_N	935.954
Domperidone				
β-CD in D/W	0.9674	0.0020	A_L	140.3157
HPβ-CD in D/W	0.9723	0.0021	A_L	143.1434
Mβ-CD in D/W	0.9068	0.0018	A_L	128.8033

Ks of the complexes (due to their linear curves, AL types) reflect the potency of collaboration among the chemical host and the boarder. In supramolecular relationships, the K_s in the array of 100–5000 M^{-1} suggests sturdy host-guest interfaces [176]. Based on the stability constants obtained during the phase solubility studies of both the drugs with different cyclodextrins, HPβ-CD was deemed to improve the solubility of both the drugs CIN (1003.009 M^{-1}) and DOM (143.14 M^{-1}). A similar improvement in the aqueous solubility by β-CD and its derivatives, namely HPβ-CD has been reported previously [177, 178].

Thus, synthesis of nanosponges using HPβ-CD was undertaken at the onset. Despite numerous attempts, the product obtained was slimy and could not be processed further. Thus, the focus was shifted to synthesizing nanosponges of β-CD. The stability constants for CIN and DOM with β-CD were found to be 1000.03 and 140.31 M^{-1}. As these values are also high enough thus the next trials were conducted using β-CD. The factors that aided in making this choice were its low cost, easy availability, and convenience to handle while synthesis of CD-NS.

6.5.2. Selection of Cross-linkers

The next crucial step in the synthesis of CD-NS was the selection of the linker. A comprehensive literature review assisted us in shortlisting two carbonyl-based linkers, to

begin with. They were carbonyldiimidazole and diphenyl carbonate. The usage of carbonyldiimidazole resulted in the formation of greasy nanosponges that required days-long post-synthesis processing. Diphenyl carbonate yielded a solid product that could be separated and evaluated. Other benefits associated with diphenyl carbonate, such as cost-effectiveness, ease of handling the product, and formation of the product with desired characteristics helped seal its selection.

6.6. Wave-assisted synthesis of nanosponges

6.6.1. Microwave-assisted synthesis of CD-NS (MW-NS)

According to the design, experiments were conducted and responses were obtained. Employing Stat-Ease Design Expert® software package V13.0, we analyzed the response surfaces of the parameters within the investigational sphere to determine the Analysis of Variance (ANOVA). A Box-Behnken design was chosen because it can be used to explore quadratic response surfaces and to create 2nd-degree algebraic simulations. In order to develop the response surface methodology, seventeen experiments were necessary centered on the Box-Behnken layout. According to the experimental design, different permutations of factors produced diverse reactions, as shown in **Table 6.9** below. There is a wide variation between all 17 batches, indicating a strong dependence of the dependent variables on the independent variables.

Table 6.9: Box–Behnken experimental design and experimental results

Run	Autonomous Parameters			Reliant Parameters	
	Microwave power level	Reaction time	Stirring speed	Yield	Particle size
	Watt	Min	rpm	%	Nm
1	560	60	1500	77.8	204.12
2	560	40	1000	74.3	231.86
3	350	80	1000	57.6	487.32
4	455	60	1000	66.4	332.35
5	455	80	1500	68.1	297.28
6	455	60	1000	64.9	331.28
7	455	60	1000	65.3	327.17
8	350	60	1500	55.6	507.83

Run	Autonomous Parameters			Reliant Parameters	
	Microwave power level	Reaction time	Stirring speed	Yield	Particle size
	Watt	Min	rpm	%	Nm
9	455	40	500	61.7	384.69
10	455	60	1000	65.8	327.56
11	560	60	500	75.2	213.93
12	350	40	1000	52.7	560.46
13	455	40	1500	62.2	359.16
14	455	60	1000	65.2	325.45
15	455	80	500	67.4	308.42
16	560	80	1000	79.6	194.72
17	350	60	500	54.1	530.37

In **Table 6.10**, mathematical relationships are shown for the variables mentioned above using multiple linear regression. Based on these equations, we can determine the quantitative effects of power level of the microwave (A), time required for the completion of the reaction (B) and speed of stirring the recation mixture (C) on percentage yield (Y1) and size of particles (Y2). These coefficients indicate the effect of the autonomous parameters on Y1 and Y2. Multiple-factor coefficients and higher-order coefficients represent quadratic relationships and interaction terms respectively. Positive signs indicate synergistic effects, whereas negative signs indicate antagonistic effects. According to ANOVA, both polynomial equations have statistically significant coefficients (p<0.01) **(Table 6.11 and 6.12)**, as per the stipulations of DesignExpert® package.

Table 6.10: The regression formulas for the reliant parameters — percent yield and particle size

Parameter	Equation
Yield (%)	$65.52 + 10.8625 * A + 2.725 * B + 0.6625 * C + 0.1 * AB + 0.275 * AC + 0.05 * BC + 0.6775 * A^2 + -0.1475 * B^2 + -0.5225 * C^2$
Particle size (nm)	$328.762 - 155.169 * A - 31.0538 * B - 8.6275 * C + 9 * AB + 3.1825 * AC + 3.5975 * BC + 33.2515 * A^2 + 6.5765 * B^2 + 2.049 * C^2$

Table 6.11: The ANOVA outcomes of the quadratic model for the parameter: % yield

Source	Sum of Squares	df	Mean Square	F-value	p-value	
Model	1010.24	9	112.25	291.50	< 0.0001*	Significant
A-Microwave power level	943.95	1	943.95	2451.37	< 0.0001*	
B-Reaction time	59.40	1	59.40	154.27	< 0.0001*	
C-Stirring speed	3.51	1	3.51	9.12	0.0194*	
AB	0.0400	1	0.0400	0.1039	0.7566	
AC	0.3025	1	0.3025	0.7856	0.4049	
BC	0.0100	1	0.0100	0.0260	0.8765	
A²	1.93	1	1.93	5.02	0.0601	
B²	0.0916	1	0.0916	0.2379	0.6406	
C²	1.15	1	1.15	2.99	0.1277	
Residual	2.70	7	0.3851			
Lack of Fit	1.31	3	0.4358	1.26	0.4012	Not significant
Pure Error	1.39	4	0.3470			
Cor Total	1012.93	16				
R²						0.9973
Adjusted R²						0.9939
Predicted R²						0.9772

* p-value under 0.05 were deemed significant

In the statistical model constructed for % yield (Y1), the F-value was 291.50 (P < 0.0001), and the R^2 value was 0.9973. The individual autonomous parameters and the quadratic terms AB, AC, BC, and A^2 have momentous impacts on the yield(%), seeing as the "p" scores, lesser than 0.05 signify the significant model terms as shown in **Table 6.11.** The influence of A on yield(%) is significantly greater than those of B and C, as indicated by the equation. We further investigated the interaction between autonomous parameters and practical yield by using perturbation and three-dimensional response surface charts. Based on the perturbation chart (**Figure 6.9**) it can be seen that A, B and C

all had the principal bearing on the yield(%) of CDNS. According to this plot, A has the largest and most direct impact on Y1, tailed by B and C, both of which have a small impact on Y1. A 3D response surface plot was used to clarify the correlation between the dependent and autonomous variables.
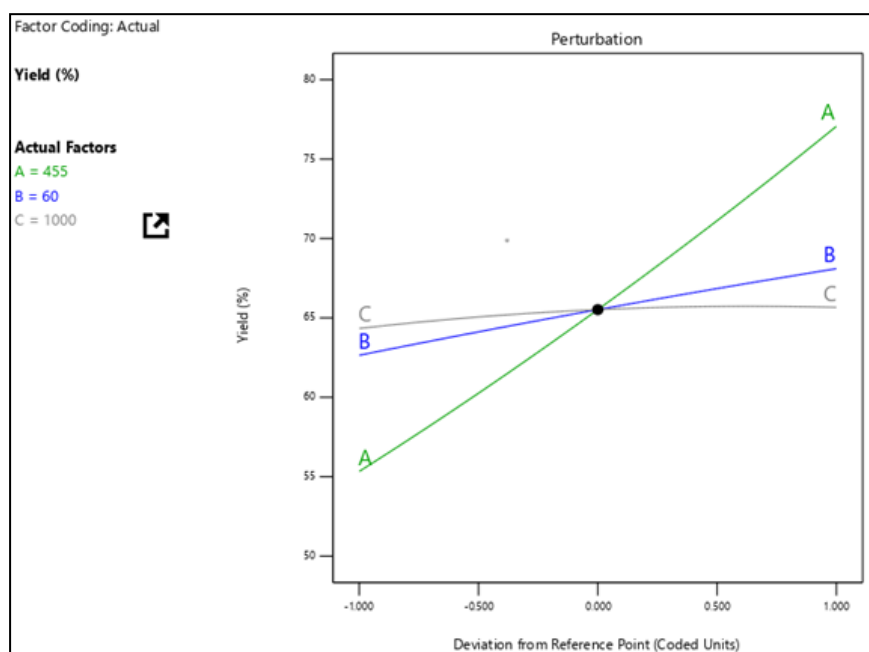
Figure 6.9: The plot disclosing the principal consequences of the power level of the microwave, time for completion of the reaction, and speed of stirring on the yield(%)

The synergistic impact of A and B on the yield (%) at a constant value of C is depicted in **Figure 6.10**. At minimal level of the microwave power, the yield increased from 52 to 57 %. Comparably, at high levels of the microwave power, the yield increased from 74 to 80 %. A higher percent yield was obtained as the level of B factor (reaction time) was raised from 40 minutes to 80 minutes.
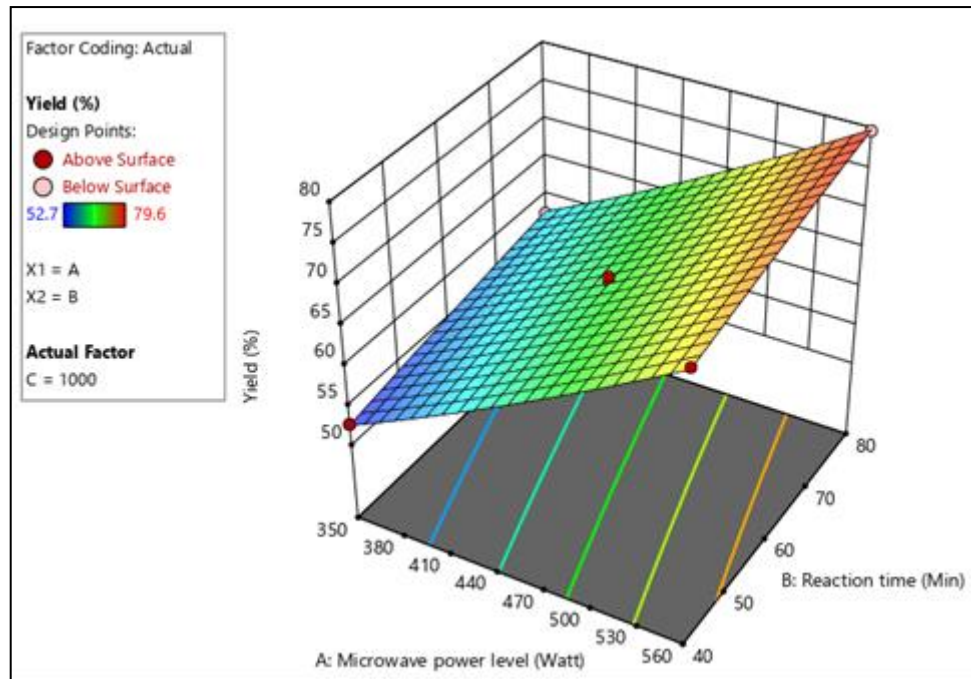
Fig 6.10: Response surface chart representing the collaborations amongst the power level of the microwave and time of reaction influencing the yield (%) at a unvarying speed of stirring

Table 6.12: The ANOVA outcomes of the quadratic model for the parameter: particle size

Source	Sum of Squares	df	Mean Square	F-value	p-value	
Model	2.064E + 05	9	22930.03	1200.30	< 0.0001*	Significant
A-Microwave power level	1.926E + 05	1	1.926E+05	10082.83	< 0.0001*	
B-Reaction time	7714.68	1	7714.68	403.83	< 0.0001*	
C-Stirring speed	595.47	1	595.47	31.17	0.0008*	
AB	324.00	1	324.00	16.96	0.0045*	
AC	40.51	1	40.51	2.12	0.1887	
BC	51.77	1	51.77	2.71	0.1437	
A²	4655.42	1	4655.42	243.69	< 0.0001*	
B²	182.11	1	182.11	9.53	0.0176*	
C²	17.68	1	17.68	0.9253	0.3681	
Residual	133.73	7	19.10			

Lack of Fit	99.56	3	33.19	3.89	0.1114	Not significant
Pure Error	34.16	4	8.54			
Cor Total	2.065E+05	16				
R^2						0.9994
Adjusted R^2						0.9985
Predicted R^2						0.9920

* p-value under 0.05 were deemed significant

The particle size of the NS was uncovered to be in the span of 194.72–560.46 nm as displayed in **Table 6.9**. The factorial equation for particle size demonstrated a superior correlation coefficient (0.9994) and the Model F-value of 1200.30 that infers that the model is significant. Model requirements may be substantial if values of "Prob>F" are lower than 0.0001. The statistically meaningful model terms in this instance are A, B, and C as well as the quadratic term of AB, A2, and B2 as illustrated in Table 6.12. The particle size is utmost affected by factor A (Microwave power), and it can be said that as the applied power goes up, nanosponges with smaller particle sizes are produced. With the help of the perturbation and 3D response surface plots, we learned more about how the main effects and interactions of the independent variables affected the practical yield. **Figure 6.11** (perturbation plot) demonstrates how A, B, and C each have distinct outcomes on particle dimension. It is found that all of the variables affect the response Y2 in different ways. Factor A has the most significant and inverse impact on Y2, followed by C and B, which have little impact on Y2. **Figure 6.12** is a plot of the 3D response surfaces of the response Y2 (particle size) that shows how the independent variables affect the response Y2. A variable was kept the same whereas the other 2 changed within a certain scope. The response surface plot depicts the interaction effect of A and C on particle size (Y2) at a constant B level. Y2 decreases from 560 nm to 400 nm at low values of A (power level of the microwave). Similarly, at high A levels, Y2 decrease from 350 nm to 195 nm. The C factor (stirring speed) was raised from 500 rpm to 1500 rpm, and this resulted in a reduction in particle size.
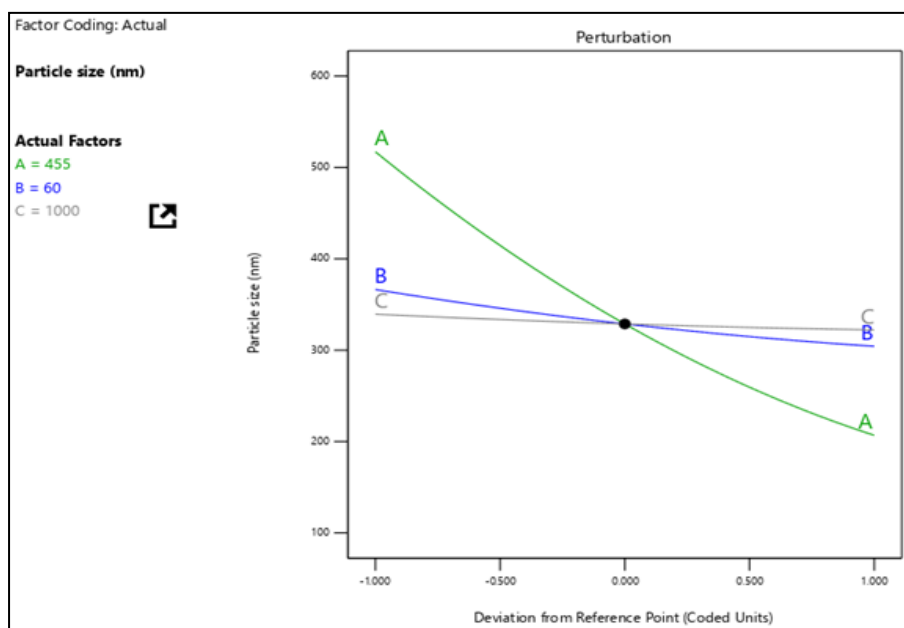
Figure 6.11: The plot disclosing the principal consequences of the power level of the microwave, time for completion of the reaction, and speed of stirring on the particle size
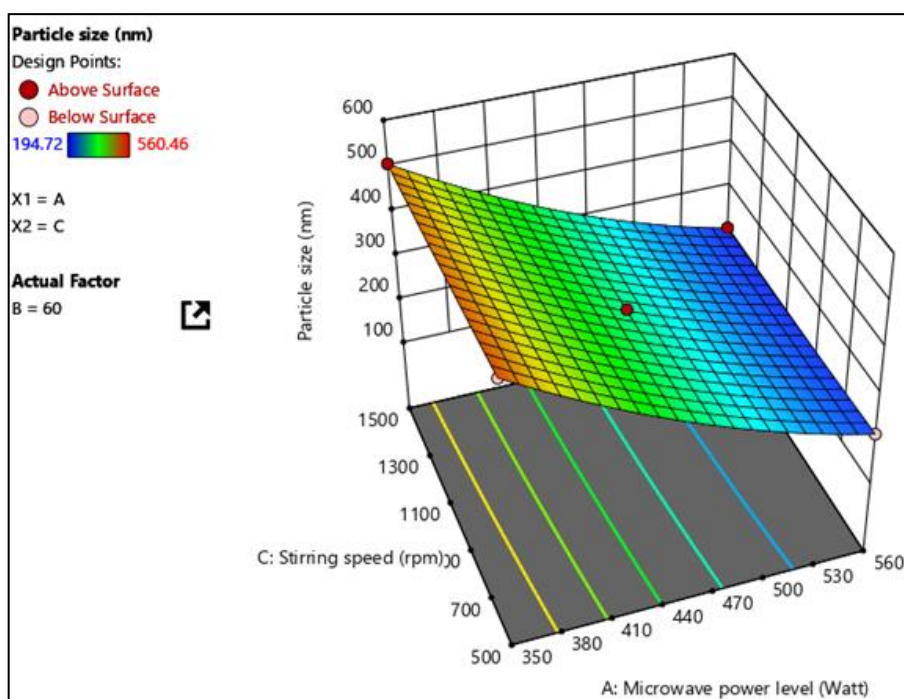
Figure 6.12: Response surface chart representing the collaborations amongst the microwave power levels and speed of stirring influencing the particle size at a fixed reaction time

Subsequently, mathematical optimization was accomplished by desirability function using Design Expert® Software. The targets elected for the optimization of MW-NS were power level of the microwave, time for reaction, and the speed of stirring to be within the study range to obtain the least particle size with maximum yield. Hundred of solutions were found that contained distinctive values of the autonomous variables. The outcome with the maximum desirability value was opted for as the optimized processing condition. The final batch was subjected to a power of 560 W for 80 mins and the stirring was carried out at 1000 rpm. This predicted the formation of a batch of nanosponges having a particle size of 191.368 nm and the total yield to be 79.73% of the total starting material. The batch was scaled up and the actual yield was found to be 78.4% the MW-NS were found to have an average particle size of 193.64 ± 1.24 nm. The portrayal of the synthesis of CD-NS using the microwave-assisted technique is given in **Figure 6.13.**
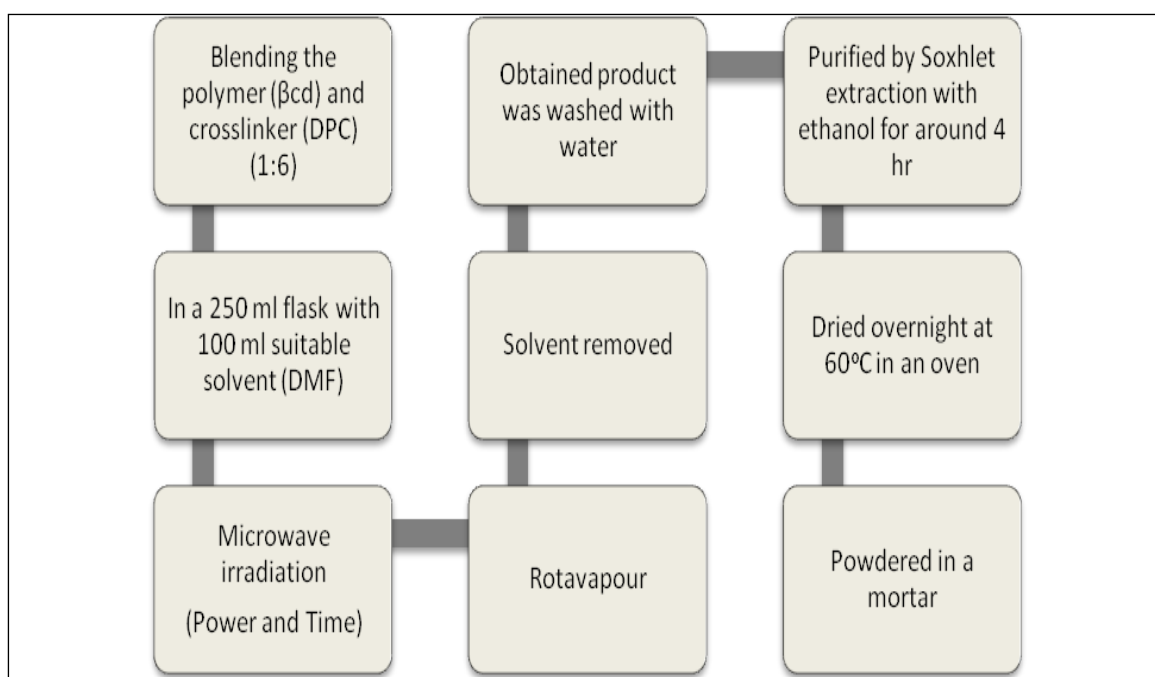
Figure 6.13: Scheme for the synthesis of MW-NS

6.6.2. Ultrasound-assisted synthesis of CDNS (US-NS)

According to the design, experiments were conducted and responses were obtained. Using Stat-Ease Design Expert® software V13.0, we analyzed the response surfaces of the parameters inside the investigational sphere to determine the Analysis of Variance (ANOVA). A Box-Behnken design was chosen because it can be used to delve into the

quadratic response surfaces and to erect 2nd-degree algebraic simulations. In order to develop the response surface methodology, seventeen experiments were necessary founded on the Box-Behnken blueprint. According to the investigational blueprint, different permutations of factors produced distinctive responses, as shown in **Table 6.13** below. There is a wide variation between all 17 batches, indicating a strong dependence of the dependent variables on the autonomous variables.

Table 6.13: Box–Behnken experimental design and the detected responses

Run	Autonomous Parameters			Reliant Parameters	
	Sonication time	Power intensity	Duration of pulse	Yield	Particle size
	Hr	Watt	sec	%	nm
1	2	375	8	64.7	163.45
2	3	250	8	48.3	332.56
3	3	500	8	60.6	142.94
4	1	375	10	53.6	176.87
5	2	375	8	65.3	167.25
6	2	250	6	45.9	362.17
7	2	500	6	68.2	163.8
8	1	375	6	47.6	198.72
9	2	500	10	69.7	147.89
10	1	500	8	55.6	154.21
11	2	250	10	53.4	335.67
12	2	375	8	63.2	165.39
13	1	250	8	35.4	356.14
14	2	375	8	66.4	168.41
15	3	375	10	58.1	154.75
16	2	375	8	65.1	162.96
17	3	375	6	53.6	168.43

Multiple linear regression analysis was used to find mathematical relationships between the mentioned variables, as shown in **Table 6.14**. These equations show how the sonication time (A), power intensity (B) and the duration of pulse (C), as well as how they affect each other, affect the yield percentage (Y1) and particle size (Y2) too. The

effects of the autonomous parameters on the responses Y1 and Y2 are shown by the magnitude of their indices. Multi-factor coefficients and higher-order coefficients represent quadratic relationships and interaction terms, respectively. A +ve sign symbolizes a collaborative effect, while a -ve sign represents an hostile effect. ANOVA findings revealed that both polynomial models were statistically significant with P values less than 0.01 (**Table 6.15 and 6.16**), as per the provisions of DesignExpert® software.

Table 6.22: Regression equations for the responses viz yield (%) and particle size

Response	Code	Equation
Yield (%)	Y1	$64.94 + 3.55 * A + 8.8875 * B + 2.4375 * C - 1.975 * AB + - 0.375 * AC + - 1.5 * BC - 10.52 * A^2 - 4.445 * B^2 - 1.195 * C^2$
Particle size (nm)	Y2	$165.492 - 10.9075 * A - 97.2125 * B - 9.7425 * C + 3.0775 * AB + 2.0425 * AC + 2.6475 * BC + 1.64025 * A^2 + 79.3303 * B^2 + 7.56025 * C^2$

Table 6.15: The ANOVA results of the quadratic model for the response: yield (%)

Source	Sum of Squares	df	Mean Square	F-value	p-value	
Model	1394.29	9	154.92	63.23	< 0.0001*	significant
A-Sonication time	100.82	1	100.82	41.15	0.0004*	
B-Power intensity	631.90	1	631.90	257.93	< 0.0001*	
C-Duration of pulse	47.53	1	47.53	19.40	0.0031*	
AB	15.60	1	15.60	6.37	0.0396*	
AC	0.5625	1	0.5625	0.2296	0.6464	
BC	9.00	1	9.00	3.67	0.0968	
A²	465.98	1	465.98	190.20	< 0.0001*	
B²	83.19	1	83.19	33.96	0.0006*	
C²	6.01	1	6.01	2.45	0.1612	

Residual	17.15	7	2.45			
Lack of Fit	11.78	3	3.93	2.92	0.1635	Not significant
Pure Error	5.37	4	1.34			
Cor Total	1411.44	16				
R^2						0.9878
Adjusted R^2						0.9722
Predicted R^2						0.8605

* p-value below 0.05 were deemed statistically relevant

The statistical model developed for yield (%) was unearthed to be relevant with an F-value of 63.23 (p<0.0001) and an R^2 score of 0.9878. The individual autonomous variables and the quadratic terms of AB, A^2 and B^2 have substantial influences on the yield (%) as the p-values were below 0.05 representing the significance of the model terms as displayed in **Table 6.14**. According to the equation, B has a more profound effect than A and C. Using perturbation and 3D response surface charts, we were able to further examine the outcome of autonomous parameters on practical yield. The perturbation chart **(Figure 6.14)** shows the principal consequences of the autonomous parameters on the yield (%) of NS. The chart unmistakably illustrates that factor B has a major and direct impact on Y1, tailed by factor A, which initially has a direct influence and then an indirect one, and finally factor C has the smallest influence on Y1. We further elucidated the correlation between the autonomous and reliant parameters using 3D response surface chart. **Figure 6.15** (Response Surface plot) illustrates the interaction impact of A and B on the yield (%) when C is held constant. At low values of B (level of power intensity), Y1 increased from 35 to 45 %. Analogously, at high values of B, Y1 increased from 55% to 70%. As factor A (sonication time) was increased from 1 hour to 3 hours, the yield percentage increased.
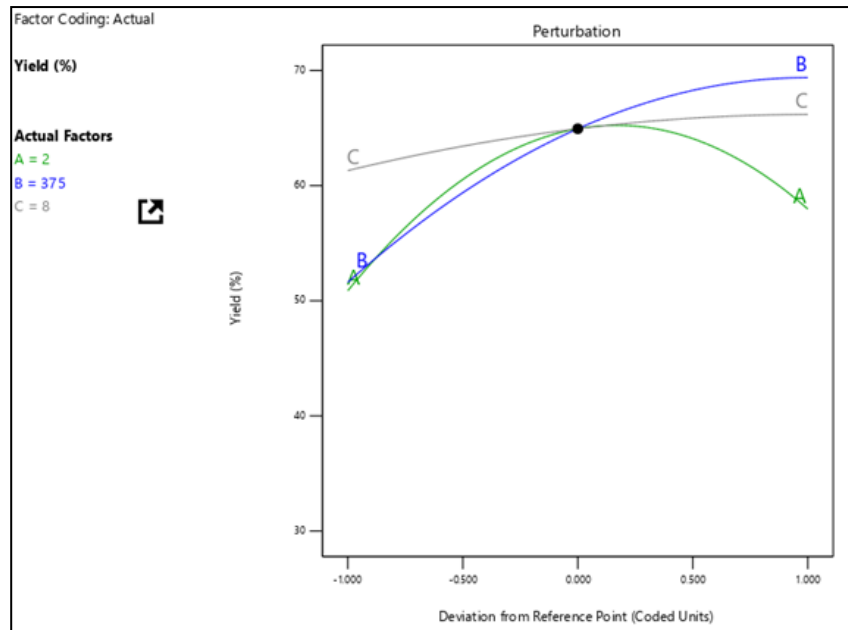
Fig 6.14: The perturbation chart exhibiting the principal outcomes of sonication time, power intensity, and the duration of a pulse on the yield (%)
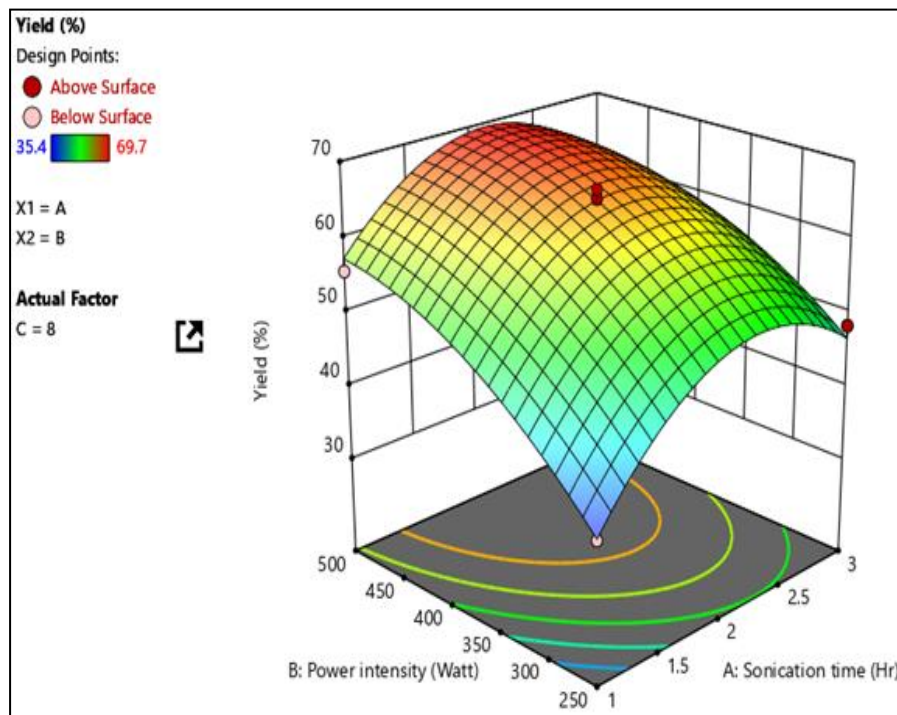
Fig 6.15: Response surface chart illustrating the interactions of the sonication time and power intensity influencing the yield (%) at a constant pulse duration

Table 6.16: The ANOVA results of the quadratic model for the response: particle size

Source	Sum of Squares	df	Mean Square	F-value	p-value	
Model	1.047E+05	9	11628.07	1157.80	< 0.0001*	Significant
A-Sonication time	951.79	1	951.79	94.77	< 0.0001*	
B-Power intensity	75602.16	1	75602.16	7527.69	< 0.0001*	
C-Duration of pulse	759.33	1	759.33	75.61	< 0.0001*	
AB	37.88	1	37.88	3.77	0.0932*	
AC	16.69	1	16.69	1.66	0.2384	
BC	28.04	1	28.04	2.79	0.1387	
A^2	11.33	1	11.33	1.13	0.3235	
B^2	26498.06	1	26498.06	2638.40	< 0.0001*	
C^2	240.66	1	240.66	23.96	0.0018*	
Residual	70.30	7	10.04			
Lack of Fit	48.11	3	16.04	2.89	0.1659	Not significant
Pure Error	22.20	4	5.55			
Cor Total	1.047E+05	16				
R^2						0.9993
Adjusted R^2						0.9985
Predicted R^2						0.9923

* p-value below 0.05 were deemed significant

As reported in **Table 6.13**, the particle size of NS was discovered to range between 142.94 and 362.17 nm. The algebraic formula for particle size flaunted a sound regression coefficient (0.9993) and the Model F-value of 1157.80 that confers significance to the model. Model terms are deemed as statistically significant when their values for "Prob>F" are less than 0.0001. In this scenario, the individual autonomous parameters and the quadratic term of B^2 and C^2 are significant as shown in **Table 6.16**. Factor B (Power intensity) has the maximum effect on the particle size, and it can be concluded that as the

applied power increases, nanosponges with lesser particle sizes are generated. A perturbation plot and a 3D response surface plot were used to probe the principal and interactional effects of the autonomous parameters on practical yield. As shown in the perturbation chart, the autonomous parameters have individual main effects on particle size **(Figure 6.16).** Y2 is influenced most by factor B, while A and C do not affect particle size that much. The 3D response surfaces chart of the response Y2 is displayed in **Figure 6.17** to represent the interactional behavior of autonomous variables on responseY2, 1 parameter was kept constant while the other 2 fluctuated in a certain scope. **Figure 6.17** illustrates how A and B collaborated together to determine particle size at a constant C level. Y2 decreased from 362 nm to 250 nm at low B levels (power intensity). Similarly, Y2 decreased from 250 nm to 142 nm at high B levels. Factor A also contributes to particle size reduction when the sonication time limit was between 1 to 3 hours. However, a longer sonication time of 3 hours, produces slightly superior results in terms of smaller particle size.
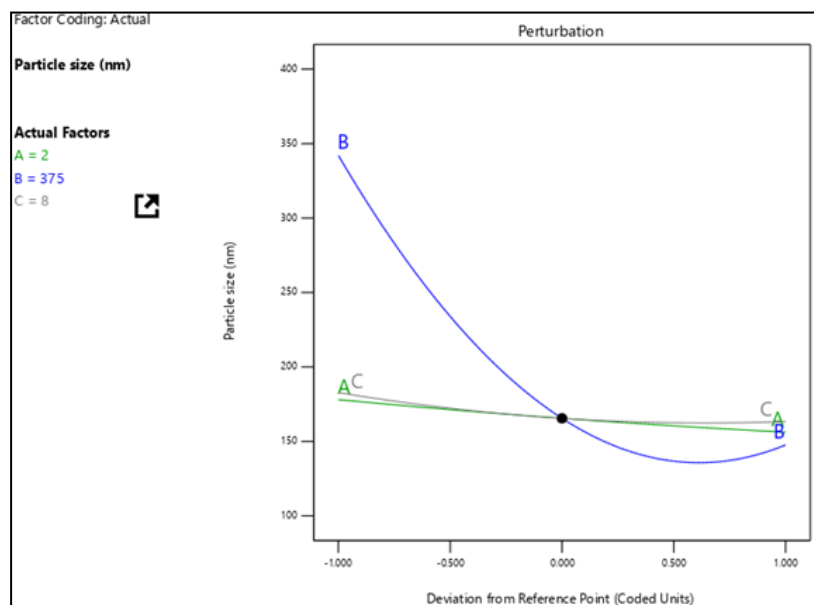
Figure 6.16: The perturbation chart exhibiting the principal outcomes of sonication time, power intensity, and the duration of a pulse on the particle size
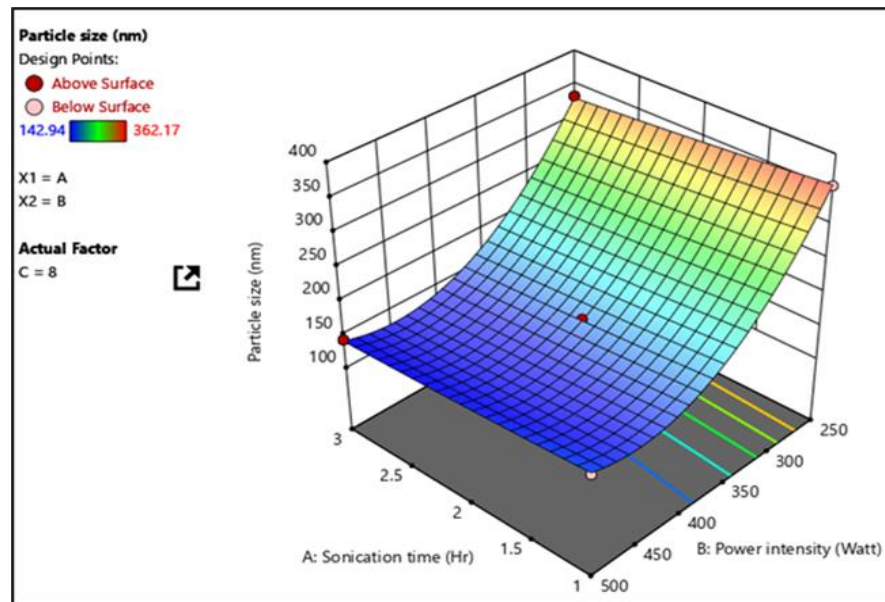
Figure 6.17: Response surface chart illustrating the interactions between the intensity of power and the duration of sonication influencing the particle size at unvarying duration of pulses

The desirability function was then used to do numerical optimization with Design Expert® Software. The targets chosen for US-NS optimization were sonication time, power intensity, and pulse duration to be within the study range to obtain the smallest possible particle size with the highest yield. Five distinct solutions were discovered, each with a different set of autonomous parameters. The result with the maximum desirability score was selected as the optimized processing scenario. The final batch was treated to a pulse cycle of 8.869 seconds (9 seconds on/ 5 seconds off) at a power level of 488.637 W (500 W) for 2.075 hours (2 hours). This anticipated the production of a batch of nanosponges having a size of 140.387 nm with a total yield of 69.64 percent of the total starting material. The final nanosponge batch was substantially increased with the ultrasonication method and the actual yield was determined to be 67.7 %, with an average particle size of 144.18 ± 2.63 nm. The schematic illustration of CDNS synthesis utilizing the ultrasound-assisted approach is shown in **Figure 6.18.**
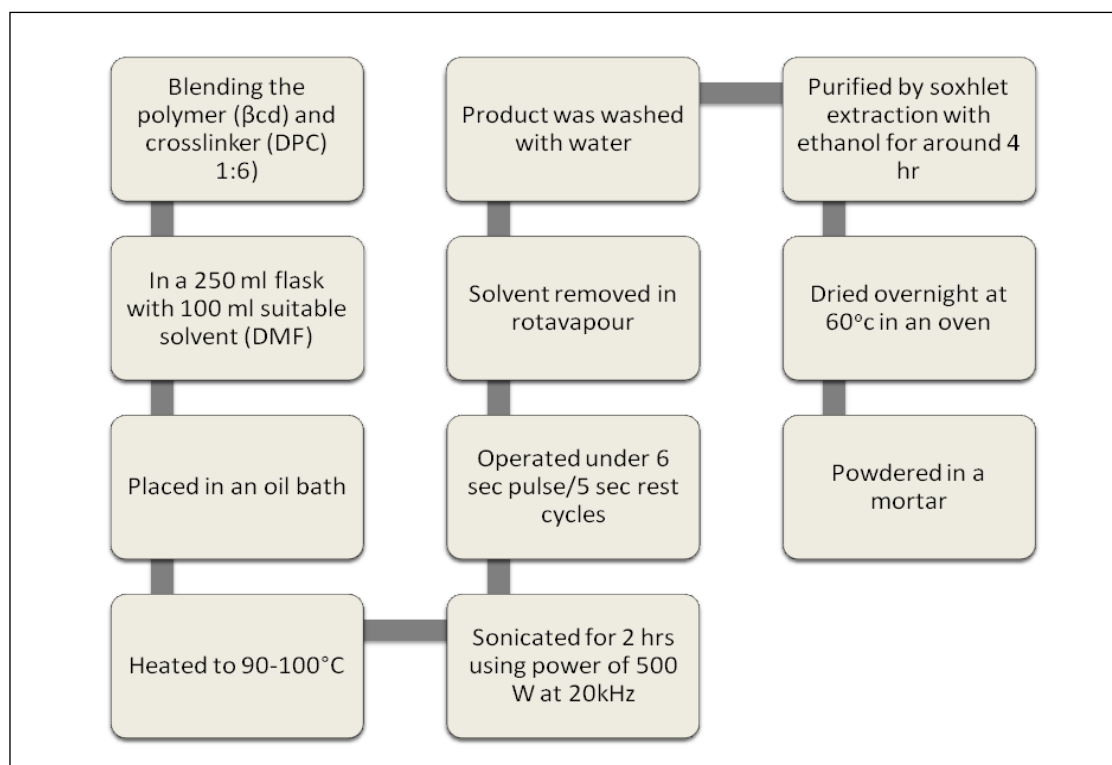
Figure 6.18: Scheme for the synthesis of MW-NS

6.7. FTIR-ATR of the blank nanosponges

Nanosponges are prepared by the crosslinking reaction carried out between β-CD and DPC. The reaction involved is:
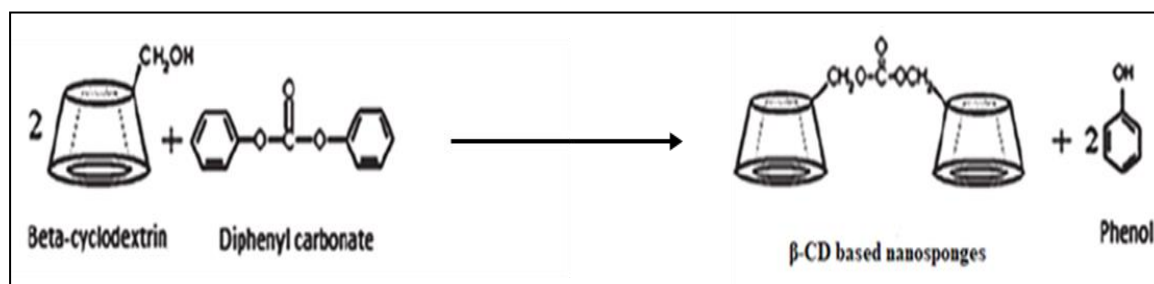
FTIR ATR spectra was recorded in the frequency span of 4000-600 cm^{-1} for nanosponges prepared by both methods. The FTIR spectra of carbonate linker-based NS flaunted a unique peak of carbonate bond joining two β-cyclodextrin molecules at 1740-1780 cm^{-1} which corroborates the creation of CDNS. The other characteristic NS peaks were also discovered at 2918 cm^{-1}, 1418 cm^{-1} and 1026 cm^{-1} distinctly, which were attributed to the C-H stretching vibration, C-H bending vibration, and primary alcohol's C-O stretching vibration, respectively. According to the published literature, the range between 1700 and 1800 cm^{-1} is acknowledged as being suitable to establish CDNS's crystallinity [150,179,180]. In the case of conservatively amalgamated NS, the prominent peak caused

by the carbonate connection between CD units was identified at 1740 cm^{-1}, which was increased to 1780 cm^{-1} for the wave-amalgamated NS [181].
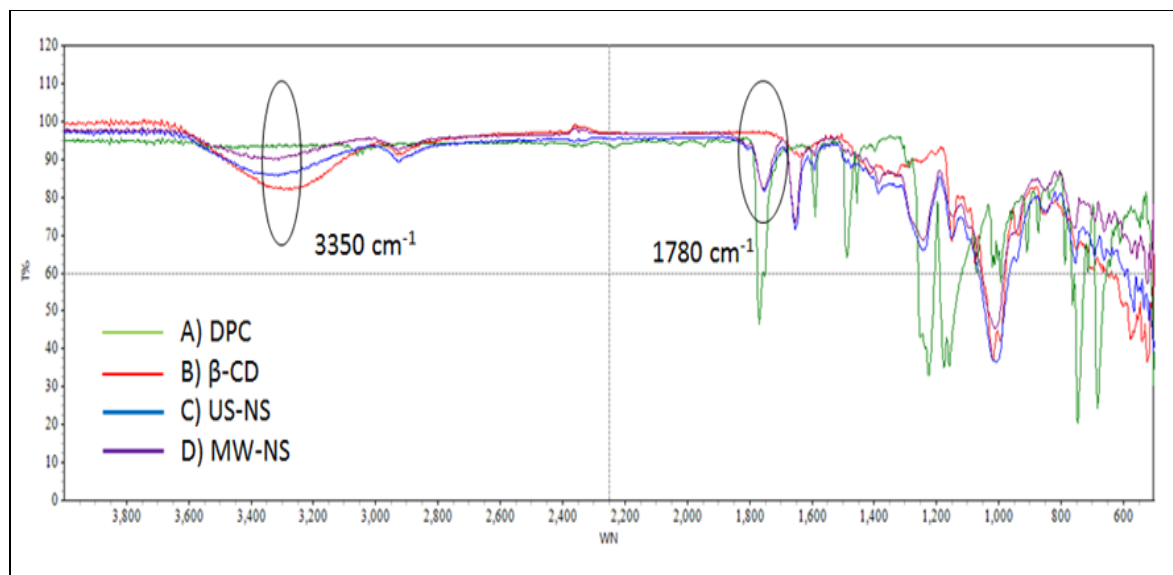
Figure 6.19: FTIR spectra of A) DPC, B) β-CD, C) US-NS, and D) MW-NS

The nonexistence of the archetypal non-hydrogen-bonded O-H stretching at 3350 cm^{-1} furthered by the primary alcohol group in β-CD symbolized the comprehensiveness of the cross-linking procedure. The carbonate nanosponges prepared by the wave-assisted method showed a typical peak at around 1780 cm^{-1}. The synthesis of nanosponges with a crystalline character is confirmed by all these changes in FTIR spectra, as illustrated in **Figure 6.19.**

6.8. Loading of the drug into nanosponges

With the help of the freeze-drying loading technique, individual drugs CIN and DOM as well as both drugs in combination (40 mg CIN+ 30 mg DOM) were simultaneously loaded into nanocavities of synthesized nanosponges [102,182]. The details of the formulations tested further are shown in **Figure 6.20.** The drug loading and entrapment competence results of these nanocarriers could indicate whether microwave or ultrasonication-assisted nanosponges are superior. The difference in drug loading in different nanosponges is attributed to the degree of crosslinking, which ultimately affect

the complexation capacity of nanosponges. Additionally; we would be able to determine whether drugs are to be loaded concurrently or separately.
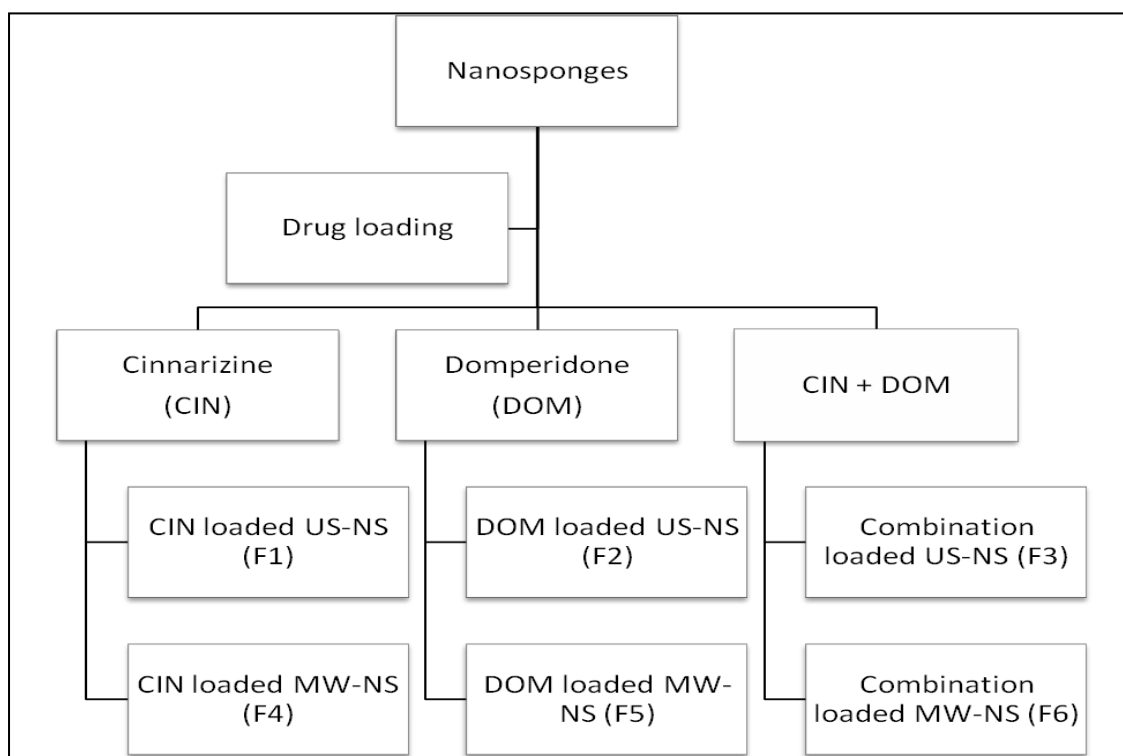
Figure 6.20: Details of formulations of drug-loaded CDNS

6.9. Characterization of drug-loaded nanosponges

6.9.1. Particle size, PDI and zeta potential

In all formulations, zeta potential values ranged from -10.1 ± 0.25 to -7.12 ± 0.32 mV, which were considered sufficient for preventing particle colliding due to electric repulsion. The particle size of each formulation was less than 200 nm confirming its nano-size, and PDI values ranged from 0.2 to 0.3. A value below 0.4 indicates a moderately disperse nature and is a generally accepted value for nanocarriers [183]. The obtained results showed that all of these drug-loaded nanosponge formulations were nano-sized and moderately dispersed. **Table 6.17** displays the data for particle size, PDI, and zeta potential for the batches.

Table 6.17: Particle size, PDI, and zeta potential of individual and combination-loaded MW-NS and US-NS

Batch number	Particle size (nm)	Polydispersity index	Zeta potential (mV)
F1	151.3 ± 1.3	0.302 ± 0.07	-7.12 ± 0.32
F2	146 ± 4.9	0.240 ± 0.02	-8.22 ± 0.17
F3	145.5 ± 1.3	0.251 ± 0.02	-9.17 ± 0.43
F4	197.4 ± 3.2	0.218 ± 0.05	-10.1 ± 0.25
F5	192.5 ± 2.7	0.257 ± 0.04	-7.74 ± 0.12
F6	198.3 ± 1.7	0.242 ± 0.05	-8.69 ± 0.36

6.9.2. Drug loading and entrapment efficiency

All the drug-loaded NS were cleansed appropriately with methanol to eliminate any uninhibited drug. They were dried and then ground with methanol and sonicated for 15 mins to discharge the captured drug. It was then filtered and the solutions were analysed spectrophotometrically at 254 and 287 nm. The drug loading and entrapment competence of all NS were as given in **Table 6.18**. Good encapsulation efficiencies of formulations could be conceivably as a result of the embedding of actives in the non-polar voids present in the arrangement of NS molecule. It can further be attributed to the development of hydrogen bonds due to the existence of hydrogen atoms on actives or collaboration involving aromatic rings with protons of β-CD by means of strong Van der Waals forces.

Table 6.18: Values for % drug loading and % entrapment efficiency for individual drug-loaded as well as the combination of drugs-loaded US-NS and MW-NS

Formulation	% Drug Loading		% Entrapment Efficiency	
F1 (Ultrasonic method)	30.5 %		61%	
F2 (Ultrasonic method)	32.3 %		64.6%	
F3 (Ultrasonic method)	33.5 %	CIN= 19.3 %	67%	CIN=68%
		DOM= 14.2%		DOM= 66%

F4 (Microwave method)	31.6 %		63.2 %	
F5 (Microwave method)	42 %		84%	
F6 (Microwave method)	40 %	CIN= 23%	80%	CIN=80.6%
		DOM= 17%		DOM= 79%

In formulations F1 - F3, where nanosponges were generated using ultrasonic procedures, CIN was only loaded in F1, DOM was loaded in F2, and both were loaded in F3. Similarly, formulations F4-F6 featured nanosponges generated using the microwave technique, with CIN only present in F4, DOM solely present in F5, and both drugs present in F6. When CIN and DOM were loaded simultaneously into nanosponges in formulations F3 and F6, the results for percent drug loading and percent entrapment efficiency were nearly identical to those obtained when the drugs were loaded separately. Thus, nanosponges are an effective nanocarrier for the administration of combination drugs. When compared to the ultrasonication method, nanosponges synthesised using the microwave approach (F4-F6) displayed superior drug loading and entrapment efficiency of both CIN and DOM individually as well as concurrently.

6.9.3. Fourier transformed infrared-attenuated total reflectance spectroscopy (FTIR-ATR)

The potential encapsulation of the drug by the nanosponges was assessed using FTIR. The FTIR spectra of both drugs, blank US-NS, nanosponges loaded with individual drugs, and combination-loaded nanosponges are shown in **Figure 6.21** whereas **Figure 6.22** depicts the spectra of the aforementioned drugs and nanosponges prepared by microwave assistance (MW-NS). CIN showed characteristic peaks at 2959, 1597, 1490, 1448, and 1134 cm^{-1} corresponding to (C-H) stretching (aromatic, alkene, mono-substituted), (C=C) (aromatic stretch), (CH2) (alkane), and (C-N) stretching respectively. Peaks at 3126, 2933, 1718, and 1693 cm^{-1} due to N-H stretching, asymmetric C-H stretching, C = O stretching and N-H bending respectively were indicative of DOM. The non-existence of the emblematic non-hydrogen-bonded O—H stretching at 3350 cm^{-1} caused by the primary alcohol group in β-CD symbolized the totality of the cross-linking procedure. A peak at around 1750 cm^{-1} is also a distinctive feature of carbonate cross-linked nanosponges. During the process of drug loading and encapsulation, the characteristic drug peaks should disappear, decrease in intensity or show a shift in wave

number. All the prominent peaks of CIN were either absent or present at very low intensity in the spectrum of formulations F1, F3, F4, and F6 indicating encapsulation of CIN in the cavity of the nanosponges prepared by both methods. The same phenomena were observed in batches F2, F3, F5, and F6. Where the prominent characteristic peaks of DOM were absent and the intensity of the other significant peaks of DOM has reduced. These two characteristics contribute to the confirmation that DOM is encased within the cavity of nanosponges. All six spectra of drug-loaded nanosponges showed the distinctive peak at around 1780 cm^{-1} and a peak at 3350 cm^{-1} is either completely absent or present with very low intensity. These results point towards encapsulation of both the drugs individually as well as in combination by the nanosponges prepared by both the microwave and the ultrasound-assisted approaches.
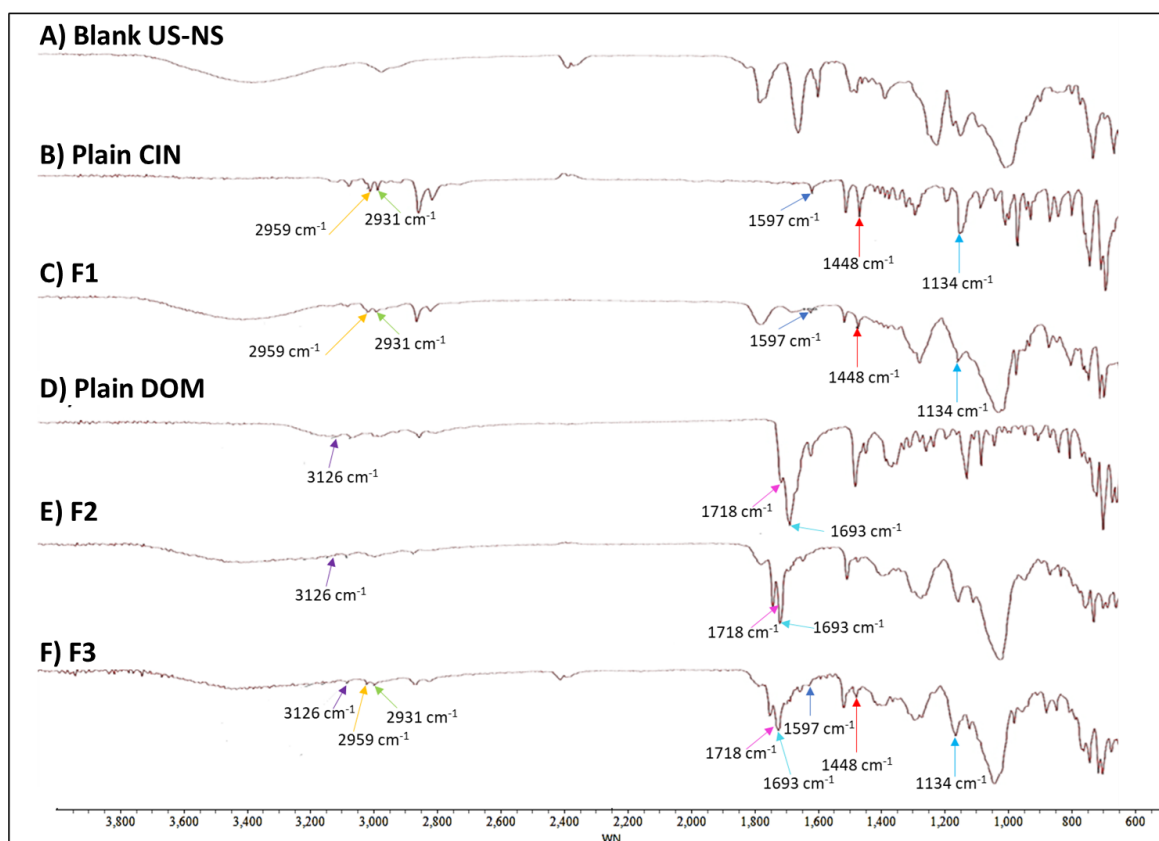
Figure 6.21: FTIR scan of A) Blank US-NS B) CIN, C) CIN loaded US-NS (F1), D) DOM, E) DOM loaded US-NS (F2), and F) Combination-loaded US-NS (F3)
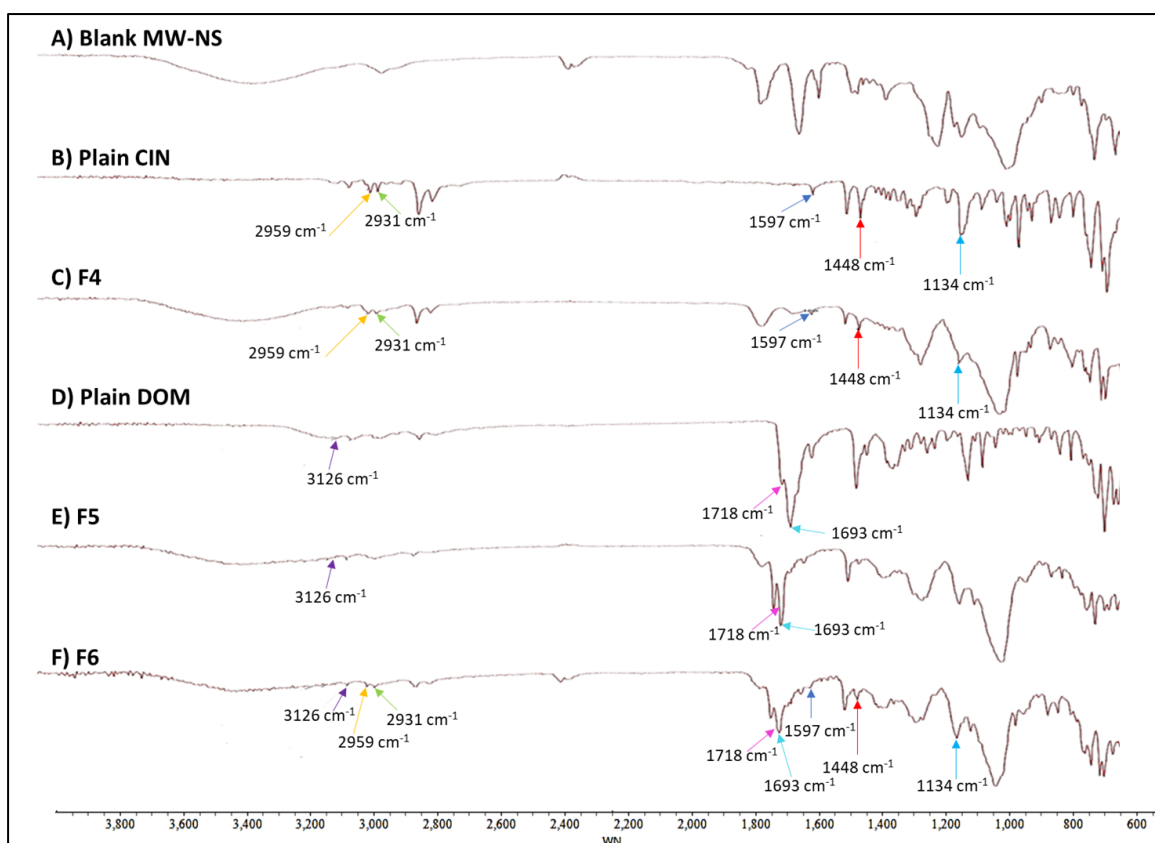
Figure 6.22: FTIR scan of A) Blank MW-NS B) CIN, C) CIN loaded MW-NS (F4), D) DOM, E) DOM loaded MW-NS (F5), and F) Combination-loaded MW-NS (F6)

6.9.4. Differential Scanning Calorimetry (DSC)

 The characteristic peaks of β-CD were observed at 316 – 328 °C and that of DPC (linker) was seen between 72 – 74 °C **(Figure 6.23).** These peaks were absent in the nanosponges prepared by both methods indicating that the individual components were not present and that the reaction had taken place. The drugs CIN and DOM show peaks at 118°C and 254°C respectively. Both peaks are present in the nanosponges prepared by the microwave-assisted method as well as ultrasound-assisted method indicating that the drugs did not react chemically **(Figure 6.30** and **6.31** respectively). The drug peaks have reduced indicating the entrapment of the drug in the nanosponges formed and their subsequent amorphization [184].
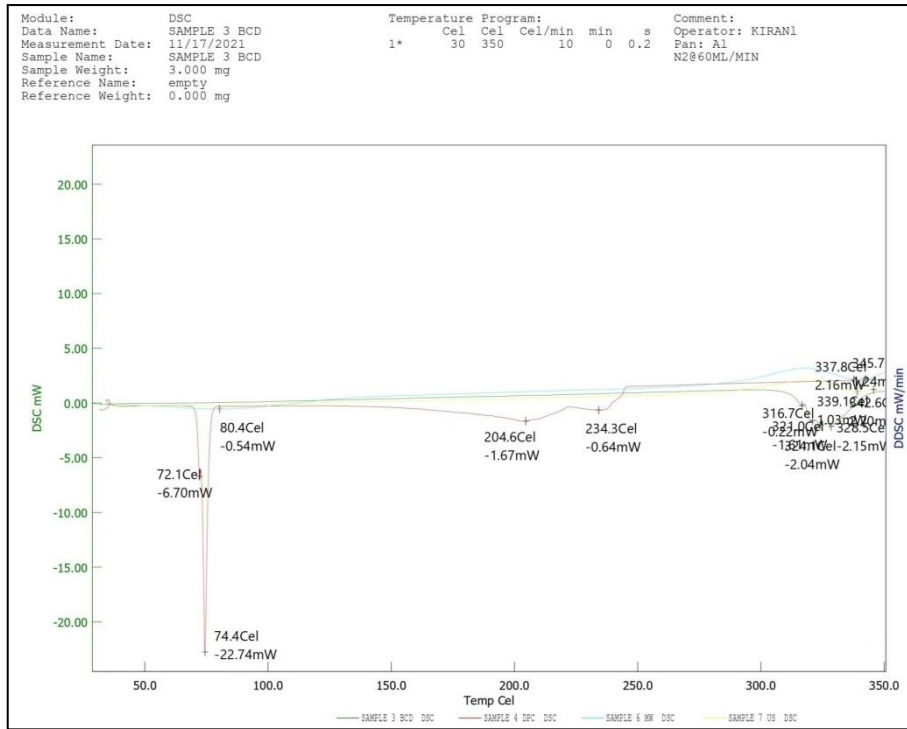
Figure 6.23: DSC thermograms of β-CD, blank MW-NS and blank US-NS
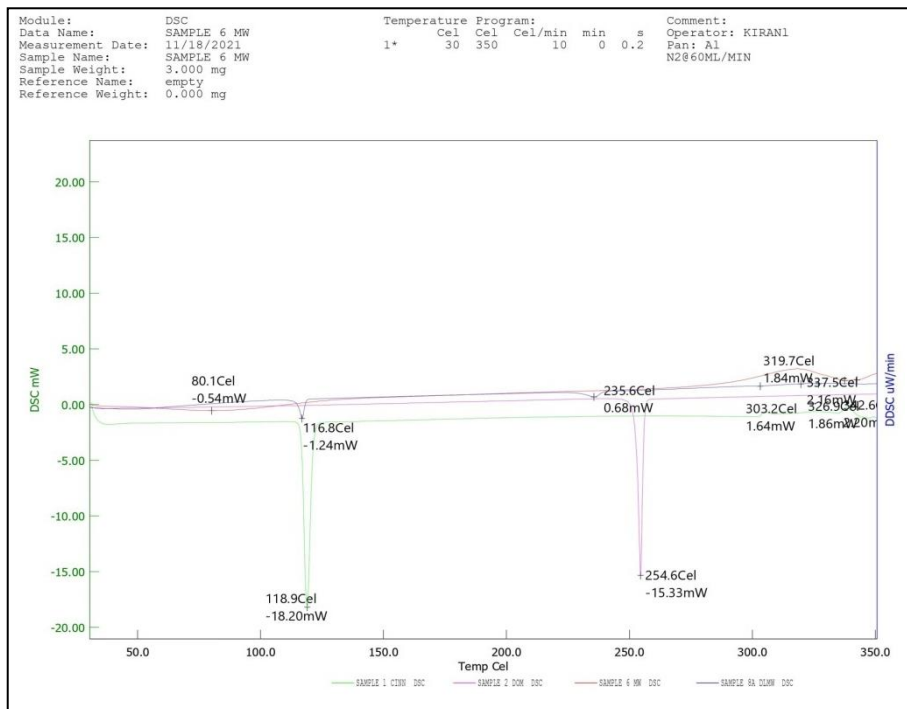
Figure 6.24: DSC thermograms of CIN, DOM and combination loaded MW-NS
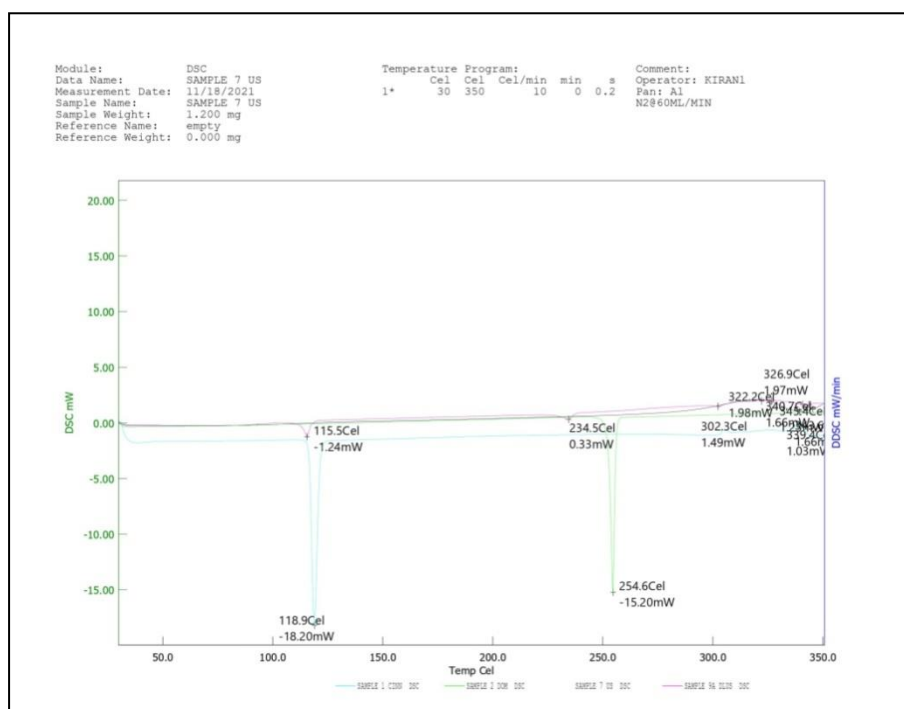
Figure 6.25: DSC thermograms of CIN, DOM and combination loaded US-NS

6.9.5. X-ray powder diffraction (XRPD)
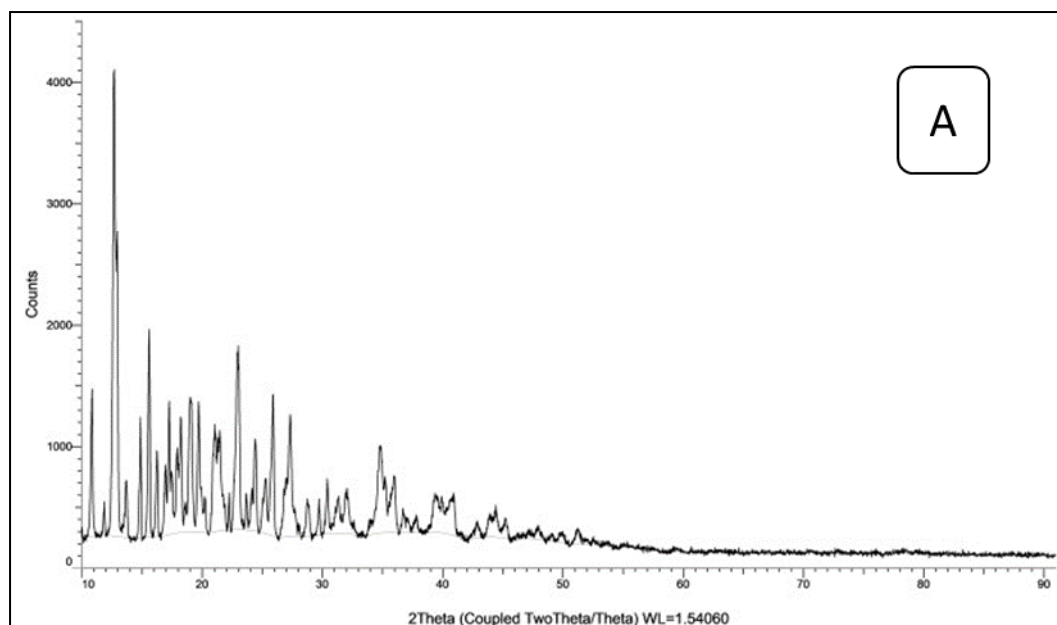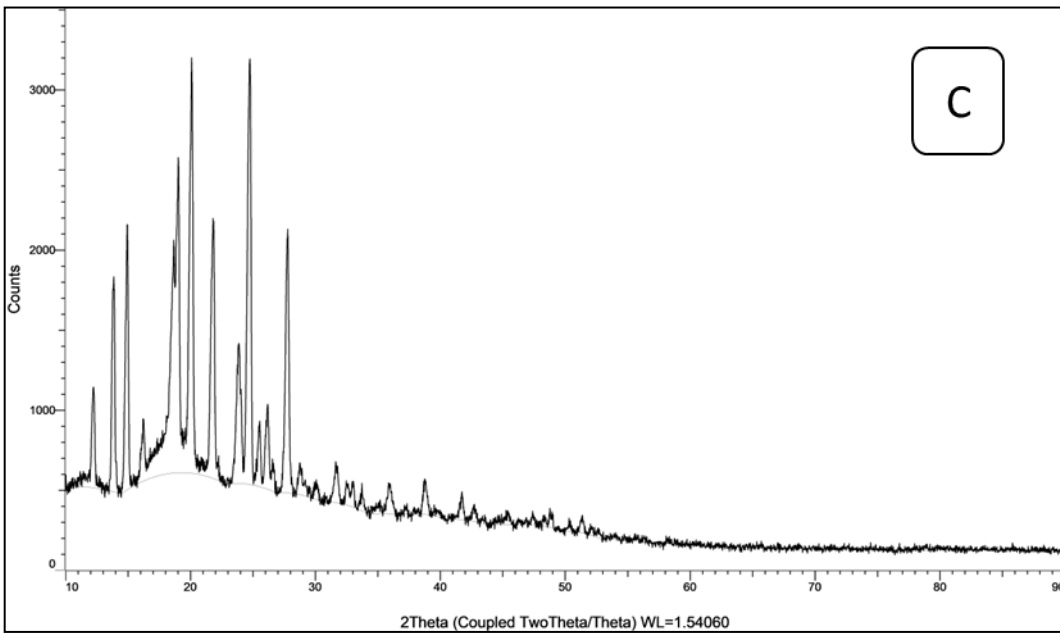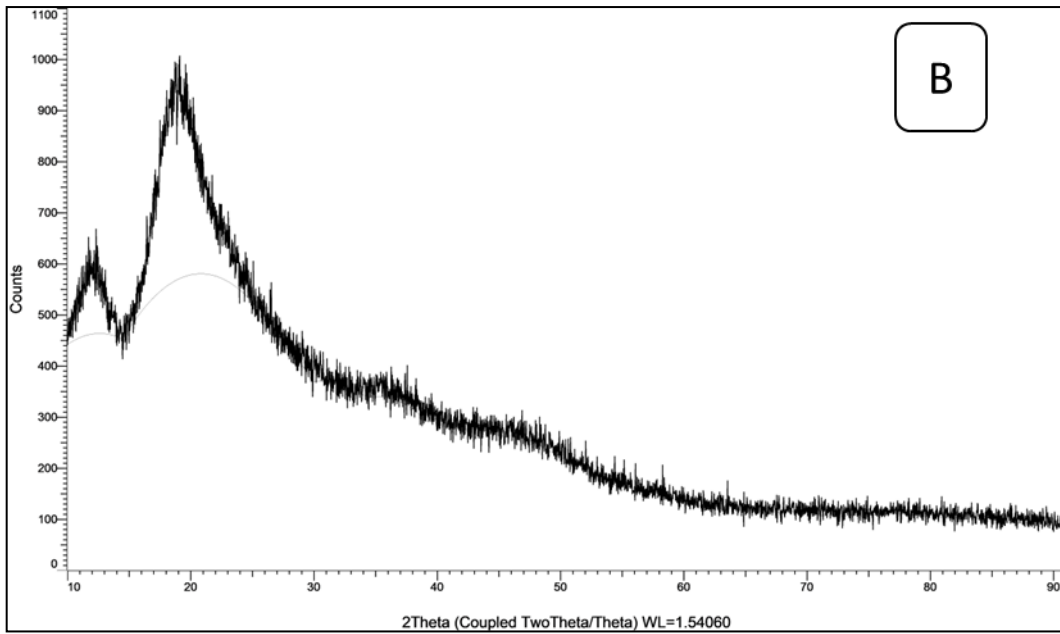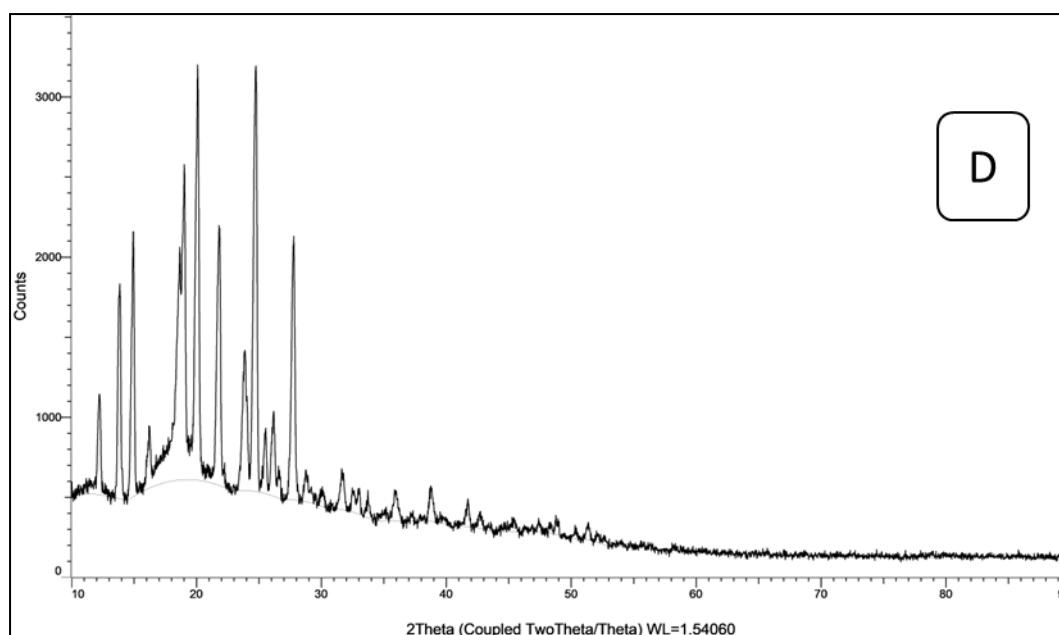
Figure 6.26: XRPD diffraction pattern of A) β-CD, B) CDNS prepared by the conventional method, C) blank MW-NS, and D) blank US-NS

The X-ray diffraction pattern **(Figure 6.26A)** of β-CD confirms its crystalline form. The XRD pattern of the CDNS prepared by the conventional methods **(Figure 6.26B)** was diffused without any characteristic peaks implying the amorphous disposition of the polymer formed. The diffractive profile of the NS prepared by the green methods **(Figure 6.26C and Figure 6.26D)** showed changes in peaks and a sharp peak pattern intimating the crystalline/para-crystalline nature of the formed NS [185]. The key 2θ values of the diffractograms with respect to β-CD and nanosponges prepared by wave-assisted methods (microwave and ultrasonication) are enumerated in **Table 6.19.**

Table 6.19: 2θ values of diffractograms of β-CD, MW-NS, and US-NS

BCD		MW-NS		US-NS	
2θ	Count	2θ	Count	2θ	Count
10.884	1473	12.251	1144	12.256	1026
12.685	4105	13.862	1832	13.857	1843

12.941	2771	14.962	2157	14.834	1987
14.885	1239	16.215	947	16.225	1015
15.576	1965	18.670	2061	18.254	2186
17.264	1372	19.028	2577	19.983	2863
18.235	1242	20.102	3199	21.748	2208
19.003	1406	21.816	2197	23.713	1457
19.719	1368	23.888	1417	24.725	2719
21.100	1115	24.757	3193	26.225	1102
21.330	1075	26.189	1037	27.665	1575
21.458	1132	27.801	2129		
22.992	1829				
24.425	1062				
25.883	1428				
27.315	1262				
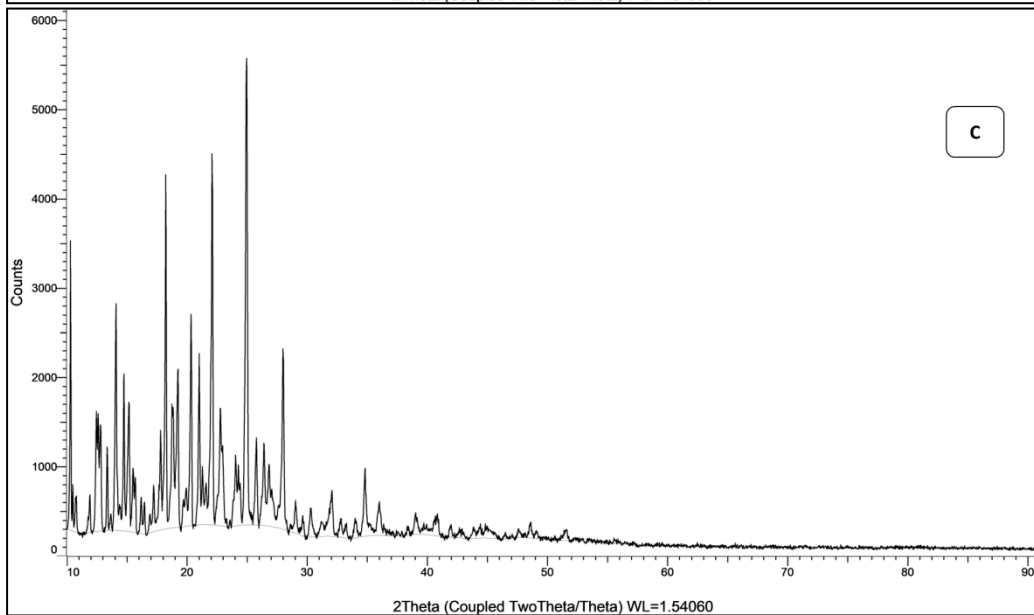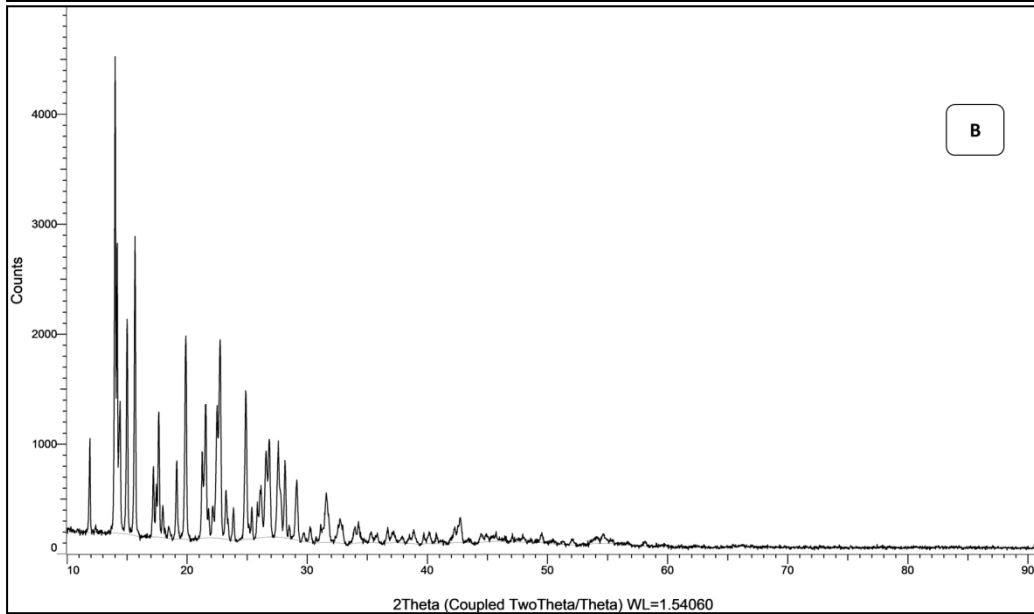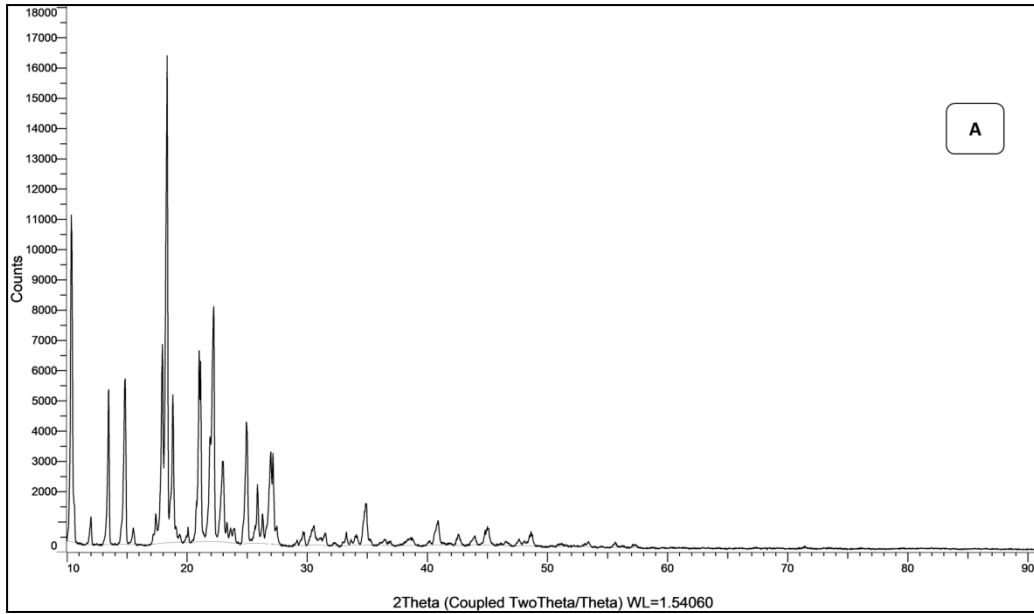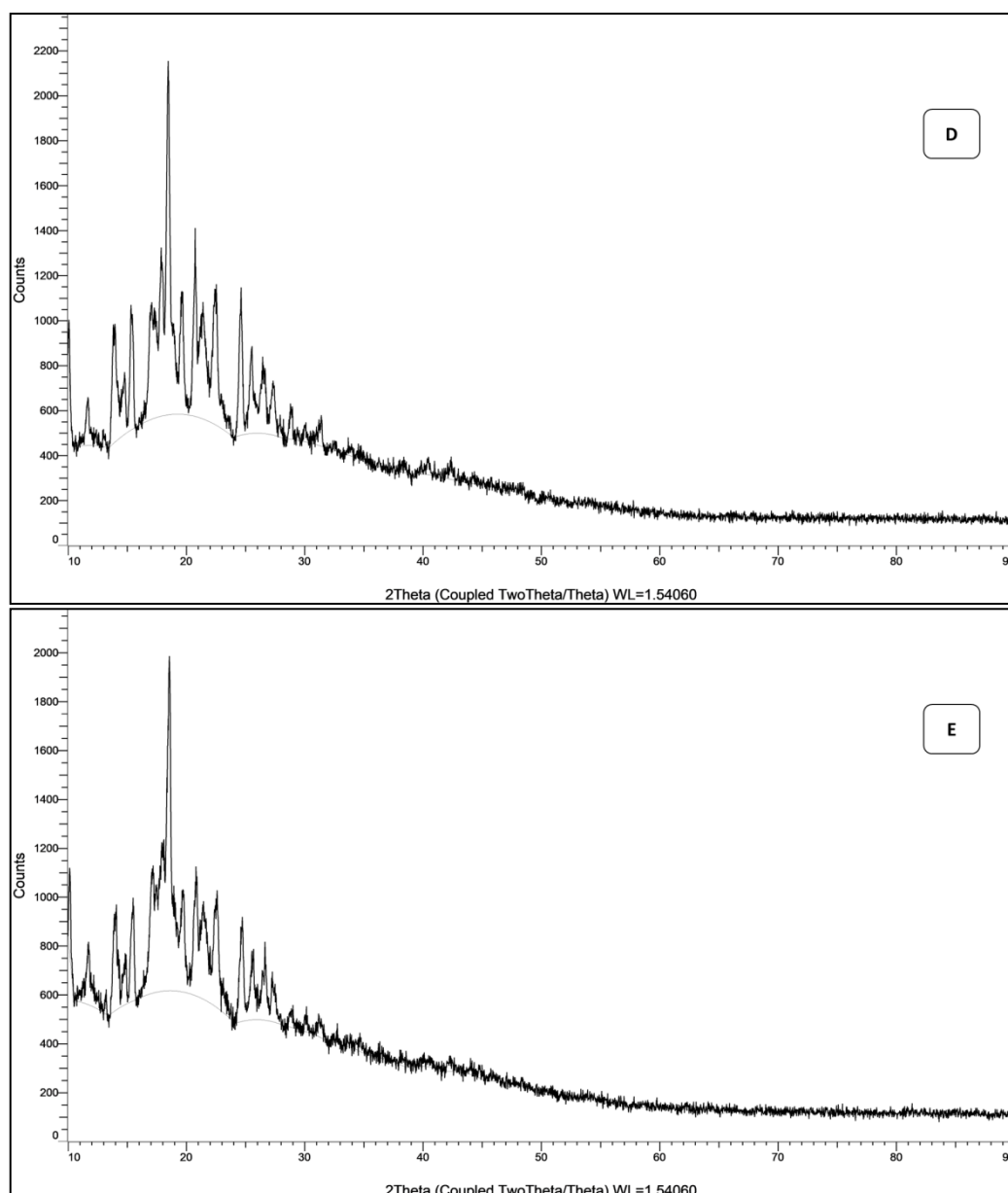
Figure 6.27: XPRD diffraction pattern of A) CIN, B) DOM C) physical mixture of drugs and β-CD, D) combination loaded MW-NS and E) combination loaded US-NS

The X-ray diffraction pattern of CIN **(Figure 6.27A)**, and DOM **(Figure 6.27B)** confirm their crystalline form. The XRD pattern of the physical mixture **(Figure 6.27C)** is a superimposition of the patterns of β-CD, CIN, and DOM. The diffraction pattern of the loaded CDNS prepared by both methods **(Figure 6.27D** and **E**) was confirming their crystalline/para-crystalline nature and different from that of CIN and DOM suggesting the encapsulation and probable amorphization of both the drugs [186]. The key 2θ values of the diffractograms with respect to cinnarizine, domperidone, physical mixture of both

drugs with β-CD and combination drug loaded nanosponge prepared by the wave-assisted approaches are enumerated in **Table 6.20.**

Table 6.20: 2θ values of diffractograms of CIN, DOM, physical mixture of drugs and β-CD, combination loaded MW-NS, and combination loaded US-NS

CIN		DOM		Physical mixture		MW-NS		US-NS	
2θ	Count	2θ	Count	2θ	Count	2θ	Count	2θ	Count
10.358	11138	11.918	1050	10.307	3531	10.051	1002	10.077	1042
11.995	1159	14.015	4523	12.455	1618	15.320	1068	17.238	1098
13.478	5369	14.194	2827	12.609	1592	15.448	1027	17.340	1013
14.859	5726	14.425	1388	12.788	1469	17.084	1050	17.468	1051
17.954	6863	15.013	2134	14.092	2827	17.289	1056	17.570	1002
18.338	16404	15.678	2889	14.757	2040	17.366	1043	17.775	1128
18.824	5196	17.647	1290	17.801	1407	17.877	1323	17.928	1223
20.998	6650	19.898	1982	18.235	4271	18.466	2153	18.108	1235
22.225	8113	21.586	1360	18.747	1701	19.616	1129	18.568	1985
22.941	2997	22.762	1947	19.258	2092	20.742	1410	18.824	1014
24.936	4292	24.885	1485	20.333	2706	21.407	1081	18.952	1045
25.857	2233	26.854	1042	21.023	2268	22.455	1139	19.744	1027
26.982	3313	27.596	1029	22.072	4505	24.629	1146	20.819	1124
				22.788	1653			22.609	1026
				24.092	1130				
				24.962	5573				
				25.780	1324				
				26.394	1263				
				26.829	1027				
				27.980	2320				

6.9.6. Morphological evaluation

The particles' geometry was evaluated by SEM studies. SEM topography images of β-CD and nanosponges after drug loading are shown in **Figure 6.28** at magnifications ranging from 5000 and 30,000X. A SEM image of β-CD demonstrates its crystalline nature. When β-CD is transformed into nanosponges with the aid of a linker by joining individual β-CD molecules, the distinctive sponge-like configuration of nanosponges was found in samples. According to a recent study, nanosponges retain their characteristic sponge-like morphology after the lyophilization process. The porous nature of our samples may be conducive to the increased loading and delivery of drugs [187].
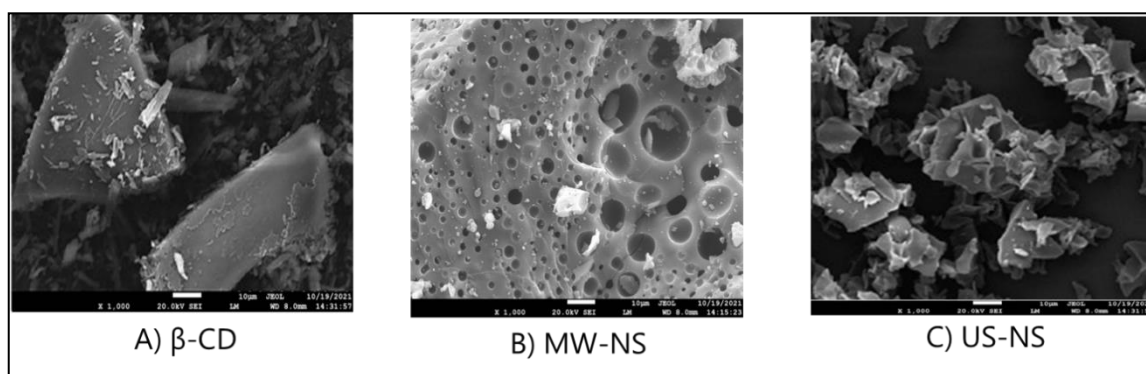
Figure 6.28: SEM scans of A) β-CD, B) MW-NS, and C) US-NS

6.9.7. In vitro drug release studies

The drug liberation profiles for cinnarizine and domperidone are illustrated in **Figures 6.29 and 6.30**, respectively, and their f1 and f2 values are presented in **Table 6.21.** The release of the plain CIN and the drug from the physical mixture attained a maximum value between 20 – 30% at the end of 24 hrs. Alternatively, a 60 – 70% drug release was observed in cases of nanosponges prepared by wave-assisted methods. The drug release was slightly faster and higher in the case of the MW-NS of CIN. But this difference was not considered significant.

According to the results of DOM, the initial release of drug from the powder of plain drug and the physical mixture was higher (~50%) but it achieved stagnation thereafter. The initial drug release of DOM from the nanosponges prepared by both the novel approaches showed slightly lower drug release ranging from 30 – 40% but over 80% released drug was achieved toward the end of 24 hours. The release from both nanosponges was very

close to each other showing no statistically significant difference making it impossible to gauge the better one of the two.

Thus, both nanosponges were taken further for formulation development and in-vivo testing.
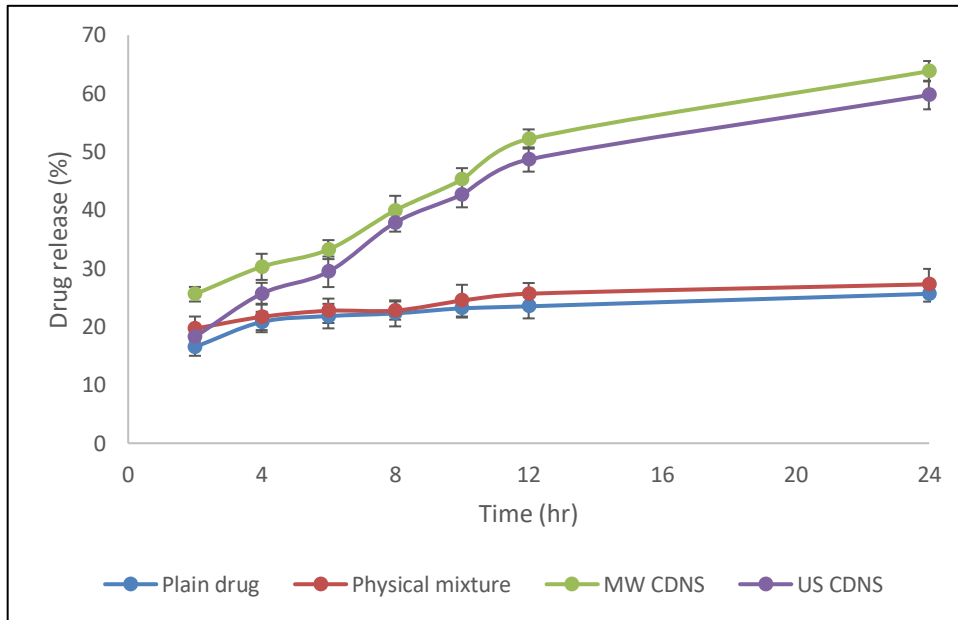
Figure 6.29: In vitro drug release of CIN from drug mixture, physical mixture with β-CD, MW-NS, US-NS
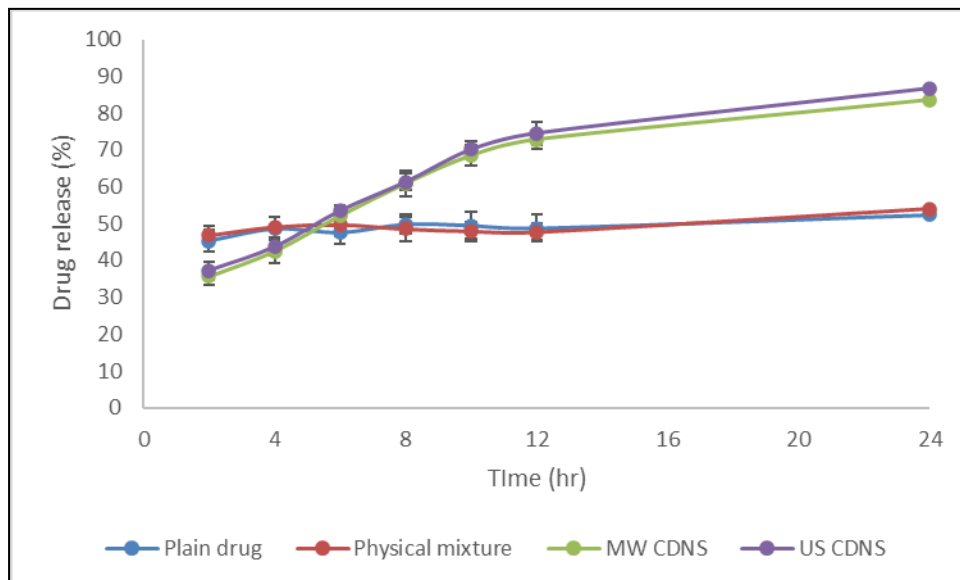
Figure 6.30: In vitro drug release of DOM from drug mixture, physical mixture with β-CD, MW-NS, US-NS

Table 6.21: Values of difference factor (f1) and similarity factor (f2) of the various nanosponge formulations as compared to that of the plain drug

Sample	Difference factor (f1) Limit: <15	Similarity factor (f2) Limit: 50-100
CIN loaded MW-NS	83	34
CIN loaded US-NS	64	38
DOM loaded MW-NS	26	42
DOM loaded US-NS	26	41

The values of f1 and f2 for the nanosponges prepared by both the methods (microwave and ultrasonication) did not lie in the prescribed range indicating that the profiles of the plain drug and the loaded nanosponges are entirely different and that there is a significant escalation in the amount of drug released from the nanosponges in case of both the drugs. Interestingly, in the case of cinnarizine, the nanosponges prepared by the microwave-assisted method showed a markedly greater dissimilarity as compared to those prepared by the ultrasound-assisted method. On the other hand, in the case of domperidone, nanosponges prepared by both methods had the values of the different factors the same. This clues that the microwave-assisted method might have an edge over the ultrasound-assisted method of synthesis with respect to the release of cinnarizine.

The mechanism of drug release from cyclodextrin-based nanosponges depends on several factors, including the physicochemical properties of the drug, the structure and composition of the nanosponge, and the environmental conditions. In general, the drug release from cyclodextrin-based nanosponges could occur through diffusion or desorption of the drug molecules from the nanosponge matrix. The drug molecules can be released from the nanosponge through the cavities or pores formed by the cyclodextrin molecules in the nanosponge structure. The size and shape of the cavities or pores can affect the rate and extent of drug release. Overall, the release mechanism of the drug from cyclodextrin-based nanosponges is a complex process that involves various factors have to be considered in the design and optimization of these nanocarriers.

6.9.8. Kinetic modelling

Based on in vitro release data, a number of kinetic models were fitted, as shown in **Table 6.22.**

Table 6.22: In vitro drug release kinetics – model fitting

Model	R^2 value of CIN-loaded MW-NS	R^2 value of CIN-loaded US-NS	R^2 value of DOM-loaded MW-NS	R^2 value of DOM-loaded US-NS
Zero-order	0.8934	0.9462	**0.9900**	**0.9922**
First-order	**0.9612**	**0.9817**	0.9715	0.9777
Higuchi square root	0.8238	0.8972	0.9877	0.9845
Korsmeyer-Peppas	0.8451	0.9393	0.9781	0.9726

Based on the release kinetics studies, it was observed that cinnarizine release is dependent on the amount of drug remaining to be released from either nanosponge. Whereas, in the case of domperidone, the release of the drug from both nanosponges showed a concentration-independent behaviour by following the zero-order kinetics as seen from the highest values of coefficient of correlation in the table above.

6.10. Formulation of the orally disintegrating tablets (ODTs)

ODT was chosen as the vehicle to deliver the drug-loaded NS. This was owing to the purpose of the usage of the drugs. The combination of the two drugs is recommended for motion sickness and vertigo. Both the conditions and the circumstances surrounding them make swallowing tablets difficult, hence ODT was selected. ODTs offer all the benefits of a solid unit dosage form like the uniformity of dose, convenience in storage and handling, etc., and at the same time, it does not require swallowing. The tablets have to be placed on the tongue, where they would disintegrate into a sweet, palatable suspension within 30 secs, which can then be gulped down easily.

The results of the trials taken to formulate the oral dispersible tablets (ODTs) of CIN and DOM-loaded CDNS are given in **Table 6.23.**

Table 6.23: Results of preliminary trial batches of ODTs

Batch No.	Hardness (kg/cm^2)	In vitro disintegration test (s)	Batch No.	Hardness (kg/cm^2)	In vitro disintegration test (s)
A 1	3	37	B 1	3	38
A 2	3	25	B 2	3	24
A 3	3	40	B 3	3	39
A 4	3	42	B 4	3	37
A 5	3	32	B 5	3	34
A 6	3	46	B 6	3	48
A 7	3.5	53	B 7	3.5	55
A 8	3.5	40	B 8	3.5	43
A 9	4	63	B 9	4	62

From the trials conducted, it was evident that the combination of Galen IQ 720 as the diluent and Primojel as the superdisintegrant showed a good balance between hardness and in vitro disintegration time. Choosing Galen IQ 720 as the diluent also offers added advantage of having a good mouth-feel. Thus, to decide the quantity of Primojel and Galen IQ to be used to give a robust ODT which disintegrates in vitro within 30 secs, various trials were conducted. Batches A2 and B2 containing 1% Primojel showed a good balance between hardness and in-vitro disintegration time. Thus, those batches were shortlisted for further in-vivo and stability testing.

6.11. Characterization of prepared ODT containing CIN and DOM

The results of the evaluation of the ODT of the CIN and DOM loaded MW-NS and US-NS based on all parameters are summarized in **Table 6.24**. The flow and compaction properties of blends to prepare ODTs of both MW-NS and US-NS were realised to be appropriate for direct compression. A Carr's index value of less than 20% and a Hausner's ratio of 1.25 is deemed excellent. Both the blends adhered to the limits and are thus suitable for direct compression. **Figures 6.31** and **6.32** show the in vitro drug release profile from the tablets. The drug release of CIN from the MW-NS and ODT of MW-NS was found to be 63.82 and 63.07 % respectively and that of DOM was 83.54 and 83% respectively. The release of CIN and DOM from US-NS was 59.73 and 86.79 % whereas the ODT of US-NS was 61.58 and 89.63% respectively. The non-interference of the tablet

ingredients and processing could be ascertained from the near similar profile obtained between the CDNS and the ODT of the CD-NS obtained by both waves-assisted methods.

Table 6.24: Results of in-vitro evaluation of the blend used and the prepared ODTs of drug-loaded MW-NS and US-NS

Sr. No	Parameter	ODT of MW-NS	ODT of US-NS
1.	Bulk density	0.427 ± 0.002 g/mL	0.432 ± 0.004 g/mL
2.	Tapped density	0.377 ± 0.003 g/mL	0.380 ± 0.007 g/mL
3.	Carr's index	11.70 ± 0.3 %	12.13 ± 1.12 %
4.	Hausner's ratio	1.13 ± 0.003	1.14 ± 0.012
5.	Angle of repose	20.11 ± 1.04 °	19.49 ± 1.23 °
6.	Hardness	3 ± 0.5 kg/cm^2	3 ± 0.5 kg/cm^2
7.	Dimensions	Thickness – 3 ± 0.2 mm Diameter – 8 ± 0.2 mm	Thickness – 3 ± 0.2 mm Diameter – 8 ± 0.2 mm
8.	Assay	98.62 ± 1.59 %	99.47 ± 1.59 %
9.	Weight variation	Passes	Passes
10.	In-vitro disintegration time	25 ± 2 s	24 ± 2 s
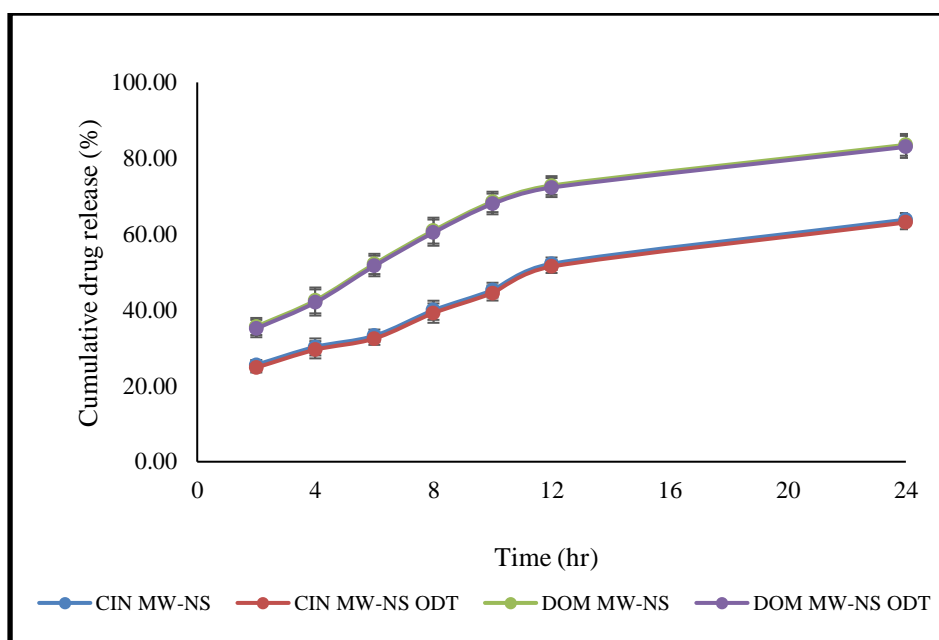
Figure 6.31: In vitro drug release profile of CIN plus DOM from MW-NS and ODT of MW-NS
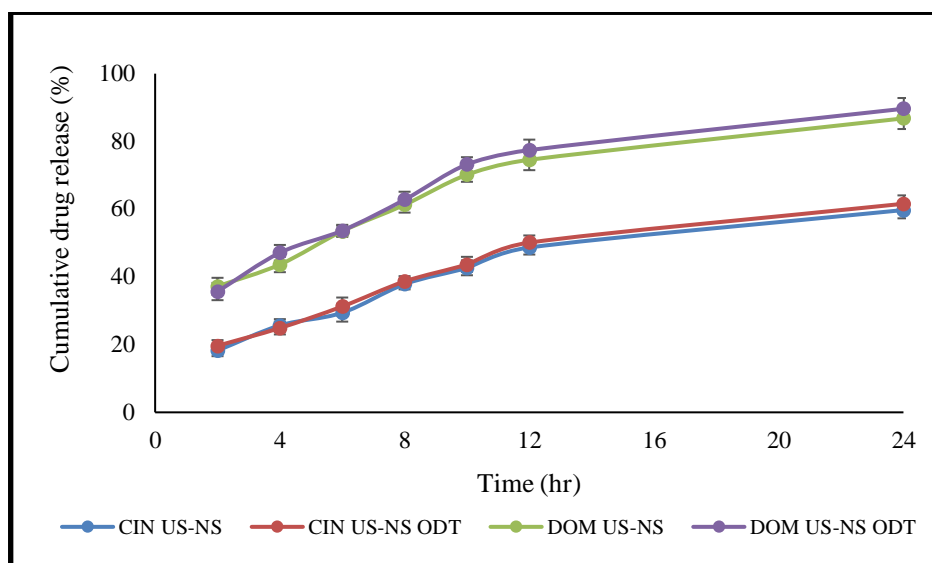
Figure 6.32: In vitro drug release profile of CIN plus DOM from US-NS and ODT of US-NS

6.12. Stability studies

The physical parameters after the 30th, 90th, and 180th day were as mentioned in **Tables 6.25** and **6.26.** All the physical parameters were within the acceptable limits which showed that both formulations were stable over 180 days.

Table 6.25: Physical parameters of ODT of combination loaded MW-NS subjected to stability studies

Physical Parameter	Storage conditions	0	30	90	180
Appearance	40ºC/75% RH	+++	+++	+++	+++
	30ºC/65% RH	+++	+++	+++	+++
Disintegration Time(s)	40ºC/75% RH	25	25	23	24
	30ºC/65% RH	25	24	25	25
Drug content (%)	40ºC/75% RH	99.57	99.65	99.48	99.61
	30ºC/65% RH	99.57	99.42	99.36	99.17
In vitro drug release of CIN at the end of 24 hrs	40ºC/75% RH	63.07	64.12	63.89	64.87
	30ºC/65% RH	63.07	63.21	63.48	63.74
In vitro drug release of DOM at the end of 24 hrs	40ºC/75% RH	83.00	83.64	83.21	83.49
	30ºC/65% RH	83.00	82.94	83.62	83.71

+++ Excellent, ++ Good, + Satisfactory, and – Poor

Table 6.26: Physical parameters of ODT of combination loaded US-NS subjected to stability studies

Physical Parameter	Storage conditions	0	30	90	180
Appearance	40ºC/75% RH	+++	+++	+++	+++
	30ºC/65% RH	+++	+++	+++	+++
Disintegration Time(s)	40ºC/75% RH	24	24	25	23
	30ºC/65% RH	24	24	26	27
Drug content (%)	40ºC/75% RH	100.62	100.43	100.25	99.67
	30ºC/65% RH	100.62	100.47	100.35	99.52
In vitro drug release of CIN at the end of 24 hrs	40ºC/75% RH	61.58	62.17	62.84	63.25
	30ºC/65% RH	61.58	62.21	61.64	62.43
In vitro drug release of DOM at the end of 24 hrs	40ºC/75% RH	89.63	88.65	88.35	89.29
	30ºC/65% RH	89.63	88.97	88.64	88.78

+++ Excellent, ++ Good, + Satisfactory, and – Poor

6.13. Bioanalytical method development and validation using HPLC

Using protein precipitation - HPLC with ultraviolet detectors (PPT-HPLC-UV), this research sought to develop a single analytical scheme to determine CIN, DOM, and IRB as internal standards simultaneously in plasma samples. Since patients are exposed to two drugs concurrently, it is necessary to develop a method which is able to quantify both drugs, with a single sampling. This was built up utilizing identical chromatographical settings as used in developing the HPLC process used for routine analysis.

6.13.1. Chromatograms of the blend including CIN, DOM and IRB

The chromatogram of both the drugs along with the IS dissolved in the mobile phase is shown in **Figure 6.33**. The retention times for DOM, CIN, and IRB (as the IS) were 3.20, 4.58 and 6.1 minutes, respectively.
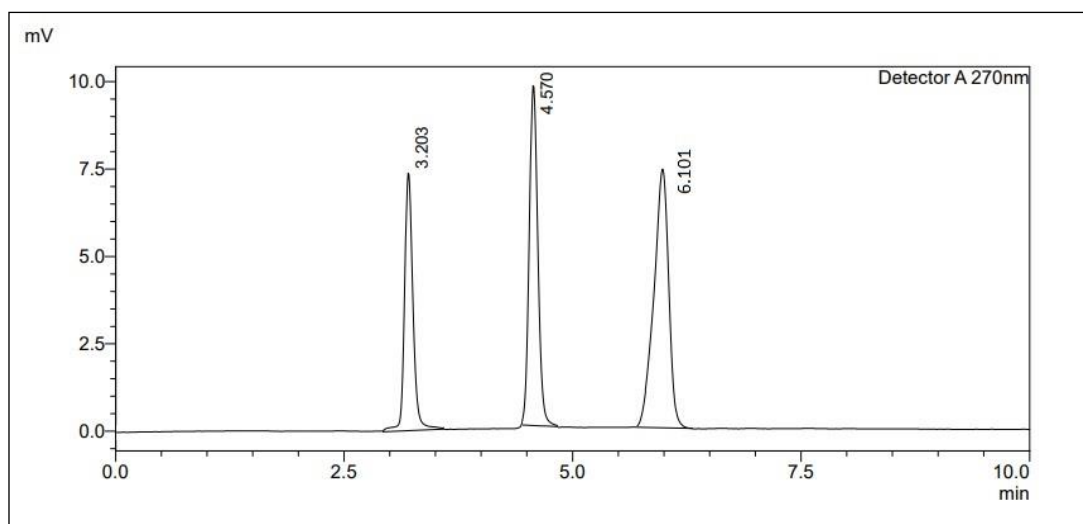
Figure 6.33: RP-HPLC chromatogram of DOM, CIN and IRB in the mobile phase

6.13.2. Specificity studies

Figures 6.34 and **6.35** show HPLC chromatograms of blank rat plasma (without analytes or internal standards) and blank rat plasma spiked with internal standards, respectively**.** It was evident from the nonappearance of spikes at the retention points of CIN, DOM, and IRB that the plasma matrix did not interfere with the quantitative estimation of both drugs.

Inversely, when CIN, DOM at their concentration of LLOQ (5 ng/mL) and irbesartan (as internal standard) at 10 µg/mL were added to the plasma, no peak of plasma components was detected at the retaining times of both drugs and the IS **(Figure 6.36).**
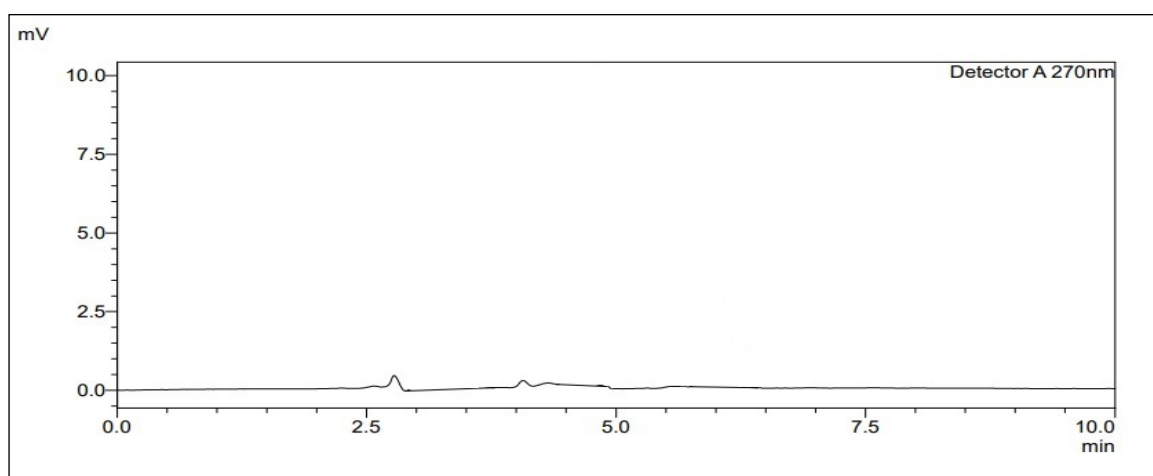
Figure 6.34: Chromatogram of the blank plasma of rat
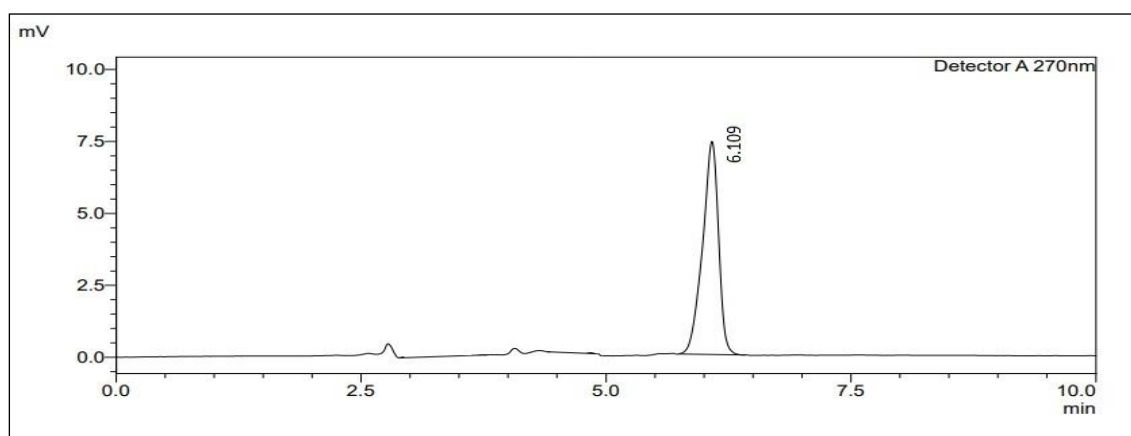
Figure 6.35: Chromatogram of the IS-spiked plasma of rat
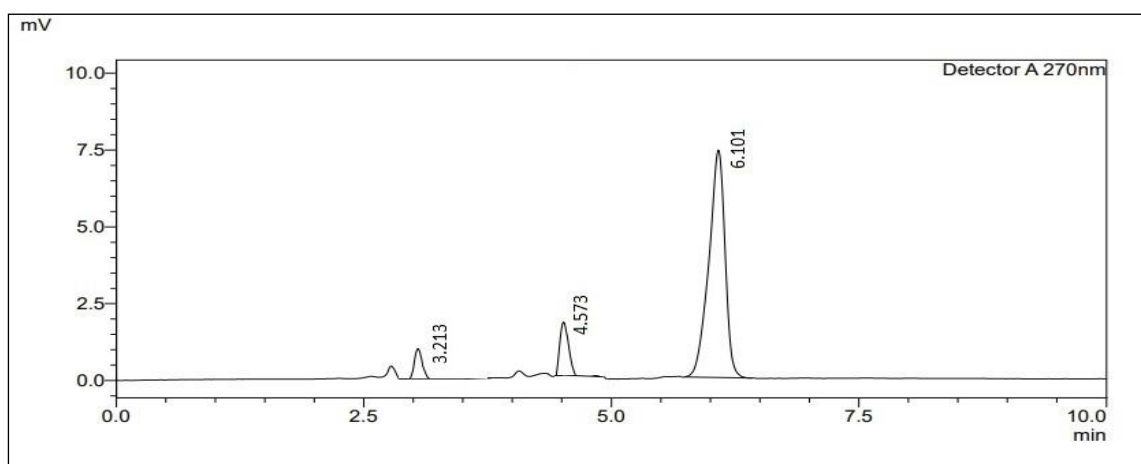
Figure 6.36: RP-HPLC chromatogram of DOM and CIN in plasma at LLOQ
concentration with IRB as internal standard

6.13.3. Linearity and Range

The method that is outlined in section 6.2.1 was followed to produce the calibration curves of CIN and DOM in the plasma of rat. The approach was shown to be rectilinear for both CIN and DOM within the concentration range of 5-200 ng/mL, exhibiting a regression coefficient of 0.999 for CIN and 0.998 for DOM, respectively, as demonstrated in **Figures 6.37** and **6.38**.
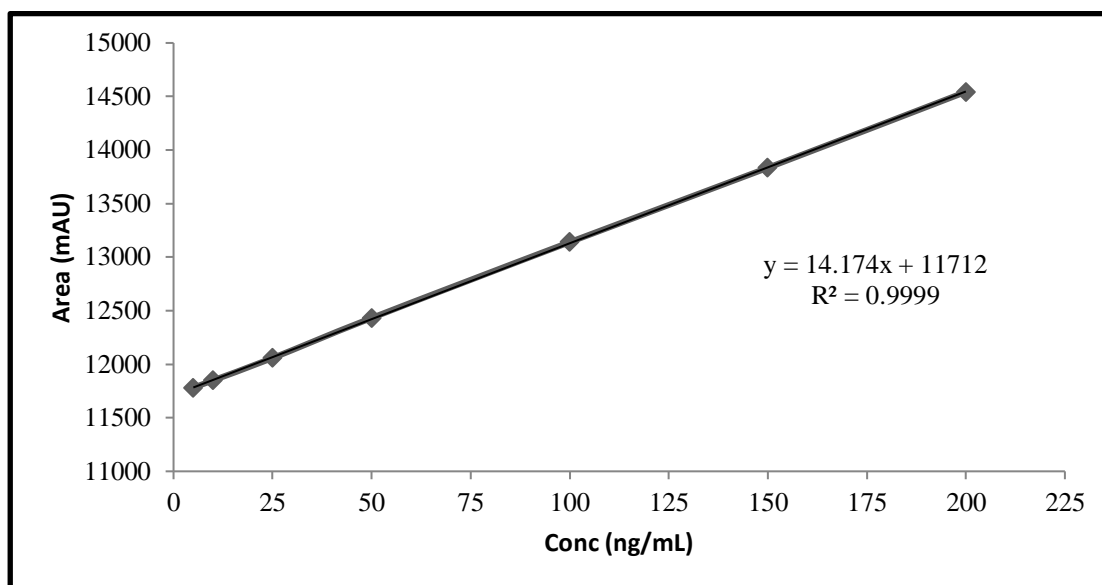
Figure 6.37: Calibration plot of CIN

In the CIN plot: $y = 14.174x + 11712$, $R^2 = 0.9999$
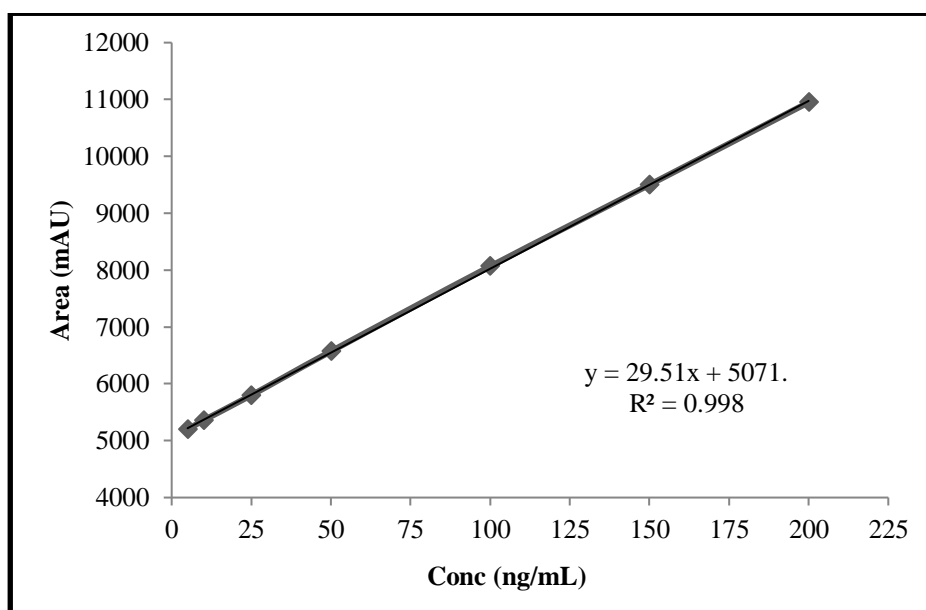
Figure 6.38: Calibration plot of DOM

In the DOM plot: $y = 29.51x + 5071.$, $R^2 = 0.998$

6.13.4. Accuracy studies

To determine the accurateness, we computed the % retrieval of the two drugs in plasma. There was a greater than 95% recovery of CIN and DOM in plasma, indicating that the developed approach was accurate **(Table 6.27)**. Additionally, the RSD was not more than 2, which points toward the results being echoable.

Table 6.27: Results of accuracy studies for CIN and DOM

Levels	Actual conc of drug (ng/mL)	Conc of drug recovered in the plasma sample (ng/mL) *(N=6)	Recovery (%)	Mean Recovery (%)
CIN				
LQC	15	Mean=14.88; S.D.= 0.14; RSD (%) = 0.94	99.20	
MQC	100	Mean=99.28; S.D.= 0.65; RSD (%) =0.65	99.28	99.24
HQC	150	Mean=148.89; S.D.= 1.28; RSD (%) =0.86	99.26	
DOM				
LQC	15	Mean=14.86; S.D.= 0.19; RSD (%) =1.27	99.06	
MQC	100	Mean=99.32; S.D.= 0.71; RSD (%) =0.71	99.32	99.3
HQC	150	Mean=149.32; S.D.= 0.96; RSD (%) =0.64	99.54	

6.13.5. Precision studies

CIN and DOM in plasma were studied intraday, interday and interanalyst precision **(Table 6.28 and 6.29)**. For HQC, MQC, and LQC samples, the percent RSD wasn't more than 2, demonstrating the precision of the scheme opted for.

6.13.6. Stability study of plasma samples

For spiking samples of CIN and DOM in plasma, 3 types of stability studies were performed: short term study **(Table 6.30)**, freeze-unfreeze rotations **(Table 6.31)**, and long-term study **(Table 6.32)** for HQC, MQC, and LQC samples. The findings showed that more than ninety five percent of the two drugs were recovered in each instance, with a percent RSD of less than 2. According to these investigations, we could conclude that the drugs in plasma were stable under all storage conditions.

6.13.7. System suitability

The trailing aspect for both CIN and DOM peaks was found to be less than 2 in any of the peaks, which demonstrated good peak regularity (acceptance limits were less than 2). All chromatographic runs had a theoretical plate count of at least 2000, ensuring effective column performance during the whole separation procedure. **Table 6.33** contains the results of the study.

6.13.8. LOD and LOQ

In plasma samples, the LOD and LOQ for CIN were determined to be 1.17 and 3.36, respectively. It was determined that the LOD and LOQ for DOM in plasma were 1.70 and 5.16, respectively **(Table 6.34)**. These results suggested that the approach was sensitive enough to detect both drugs at lower concentrations.

Table 6.28: Results of precision studies for CIN

Parameters	Level	Conc. (ng/mL)	Analytical Responses(area), injections						Mean (*N=6)	SD	% RSD
Repeatability	LQC	15	12055	12043	12065	12064	12033	12096	12059.33	21.81	0.18
	MQC	100	13229	13156	13205	13232	13205	13201	13204.67	27.28	0.21
	HQC	150	13819	13862	13847	13921	13793	13870	13852.00	44.23	0.32
Intermediate precision (Interday)											
Day 1	LQC	15	12065	12117	12041	12117	12098	12038	12079.33	36.25	0.30
	MQC	100	13232	13228	13205	13190	13197	13168	13203.33	24.08	0.18
	HQC	150	13821	13794	13809	13876	13865	13810	13829.17	33.33	0.24
Day 2	LQC	15	12016	12034	12115	12050	12178	12119	12085.33	62.11	0.51
	MQC	100	13130	13198	13245	13103	13342	13255	13212.17	87.91	0.67
	HQC	150	13799	13621	13835	13942	13851	13790	13806.33	105.7	0.77
Day 3	LQC	15	12087	12102	12089	12158	12096	12134	12111	28.65	0.24
	MQC	100	13200	13178	13297	13188	13316	13197	13229.33	60.56	0.46
	HQC	150	13802	13745	13915	13870	13856	13789	13829.50	61.95	0.45
Intermediate precision (Inter analyst)											
Analyst 1	LQC	15	12010	12178	12056	12134	12088	12005	12078.50	68.81	0.57
	MQC	100	13155	13200	13118	13109	13362	13158	13183.67	93.21	0.71
	HQC	150	13787	13727	13739	13851	13897	13875	13812.67	71.96	0.52
Analyst 2	LQC	15	12047	12099	12143	12005	12056	12075	12070.83	47.20	0.39
	MQC	100	13189	13056	13254	13168	13301	13245	13202.17	86.02	0.65
	HQC	150	13717	13791	13855	13870	13888	13802	13820.50	63.44	0.46
Analyst 3	LQC	15	11975	12186	11966	12145	12005	12158	12072.50	100.8	0.84
	MQC	100	13098	13139	13189	13119	13254	13320	13186.50	86.06	0.65
	HQC	150	13769	13936	13876	13791	13881	13797	13841.67	65.52	0.47

Table 6.29: Results of precision studies for DOM

Parameters	Level	Conc. (ng/mL)	Analytical Responses(area), injections						Mean (*N=6)	SD	% RSD
Repeatability	LQC	15	5778	5828	5789	5765	5686	5770	5769.33	46.62	0.81
	MQC	100	8069	8026	8123	8105	8058	7945	8054.33	63.67	0.79
	HQC	150	9445	9558	9514	9615	9510	9597	9539.83	62.93	0.66
Intermediate precision											
Day 1	LQC	15	5765	5713	5689	5834	5813	5789	5767.17	56.73	0.98
	MQC	100	8112	8077	8134	8078	8056	8097	8092.33	27.95	0.35
	HQC	150	9456	9555	9634	9542	9578	9617	9563.67	63.46	0.66
Day 2	LQC	15	5815	5860	5785	5743	5786	5814	5800.50	39.22	0.68
	MQC	100	8133	8008	8132	8115	8148	8071	8101.17	52.80	0.65
	HQC	150	9603	9456	9743	9612	9575	9548	9589.50	93.81	0.98
Day 3	LQC	15	5798	5716	5728	5808	5745	5789	5764.00	39.19	0.68
	MQC	100	8078	8161	8134	8098	8173	8266	8151.67	66.68	0.82
	HQC	150	9645	9466	9589	9607	9469	9614	9565.00	77.66	0.81
Intermediate precision (Inter analyst)											
Analyst 1	LQC	15	5780	5698	5711	5823	5785	5748	5757.50	47.64	0.83
	MQC	100	8104	8156	7978	8132	8204	8164	8123.00	78.48	0.97
	HQC	150	9587	9574	9607	9486	9554	9641	9574.83	52.70	0.55
Analyst 2	LQC	15	5796	5845	5795	5808	5879	5914	5839.50	49.00	0.84
	MQC	100	8015	8043	8116	7998	8103	8039	8052.33	47.39	0.59
	HQC	150	9474	9624	9565	9516	9597	9675	9575.17	73.03	0.76
Analyst 3	LQC	15	5769	5830	5790	5824	5716	5864	5798.83	52.31	0.90
	MQC	100	8176	8098	8113	8066	8137	8113	8117.17	37.08	0.46
	HQC	150	9465	9614	9586	9523	9683	9570	9573.50	75.00	0.78

Table 6.30: Short-term stability for CIN and DOM in plasma

Level	Area 1	Area 2	Area 3	Average	S.D.	RSD (%)	Conc of drug recovered in plasma (ng/ml)	Recovery (%)
CIN								
1 hour								
15	11928	11876	11968	11924.00	46.13	0.39	14.96	99.74
100	13215	13078	13130	13141.00	69.16	0.53	100.85	100.85
150	13822	13874	13798	13831.33	38.85	0.28	149.56	99.71
2 hours								
15	11946	11880	11945	11923.67	37.82	0.32	14.94	99.58
100	13124	13202	13054	13126.67	74.04	0.56	99.84	99.84
150	13885	13836	13781	13834.00	52.03	0.38	149.75	99.84
3 hours								
15	11873	11964	11932	11923.00	46.16	0.39	14.89	99.27
100	13066	13205	13104	13125.00	71.84	0.55	99.72	99.72
150	13788	13861	13813	13820.67	37.10	0.27	148.81	99.21
DOM								
1 hour								
15	5489	5549	5504	5514.00	31.22	0.57	15.01	100.08
100	8091	7970	7996	8019.00	63.69	0.79	99.90	99.90
150	9531	9455	9496	9494.00	38.04	0.40	149.88	99.92
2 hours								
15	5519	5464	5554	5512.33	45.37	0.82	14.96	99.70
100	8016	8079	7955	8016.67	62.00	0.77	99.82	99.82
150	9544	9434	9458	9478.67	57.84	0.61	149.36	99.57
3 hours								
15	5544	5513	5468	5508.33	38.21	0.69	14.82	98.80
100	8018	7951	8076	8015.00	62.55	0.78	99.76	99.76
150	9457	9414	9503	9458.00	44.51	0.47	148.66	99.11

Table 6.31: Freeze-thaw stability for CIN and DOM in plasma

Actual concentration of drug (ng/ml)	Area 1	Area 2	Area 3	Average	S.D.	RSD (%)	Conc of drug recovered in plasma (ng/ml)	Recovery (%)
CIN								
Cycle 1								
15	11861	11895	12015	11923.67	80.90	0.68	14.94	99.58
100	13086	13127	13171	13128.00	42.51	0.32	99.93	99.93
150	13835	13778	13893	13835.33	57.50	0.42	149.85	99.90
Cycle 2								
15	12005	11908	11855	11922.67	76.07	0.64	14.87	99.11
100	13105	13083	13177	13121.67	49.17	0.37	99.48	99.48
150	13761	13816	13903	13826.67	71.60	0.52	149.24	99.49
Cycle 3								
15	11903	12015	11848	11922.00	85.11	0.71	14.82	98.80
100	13181	13084	13115	13126.67	49.54	0.38	99.84	99.84
150	13745	13774	13890	13803.00	76.73	0.56	147.57	98.38
DOM								
Cycle 1								
15	5490	5502	5543	5511.67	27.79	0.50	14.93	99.55
100	8056	7975	8015	8015.33	40.50	0.51	99.77	99.77
150	9431	9489	9549	9489.67	59.00	0.62	149.73	99.82
Cycle 2								
15	5489	5495	5546	5510.00	31.32	0.57	14.88	99.18
100	7956	8007	8066	8009.67	55.05	0.69	99.58	99.58
150	9549	9418	9452	9473.00	67.98	0.72	149.17	99.45
Cycle 3								
15	5474	5497	5551	5507.33	39.53	0.72	14.79	98.57
100	7951	8006	8038	7998.33	44.00	0.55	99.20	99.20
150	9515	9450	9434	9466.33	42.90	0.45	148.94	99.30

Table 6.32: Long-term stability of CIN and DOM in plasma

Level	Area 1	Area 2	Area 3	Average	S.D.	RSD (%)	Conc of drug recovered in plasma (ng/ml)	Recovery (%)
CIN plasma								
Week 1								
15	12008	11919	11845	11924.00	81.61	0.68	14.96	99.74
100	13083	13168	13126	13125.67	42.50	0.32	99.76	99.76
150	13873	13821	13810	13834.67	33.65	0.24	149.80	99.87
Week 2								
15	11844	12016	11907	11922.33	87.02	0.73	14.84	98.96
100	13052	13171	13118	13113.67	59.62	0.45	98.92	98.92
150	13751	13822	13891	13821.33	70.00	0.51	148.86	99.24
Week 3								
15	11924	11823	12018	11921.67	97.52	0.82	14.80	98.64
100	13065	13164	13117	13115.33	49.52	0.38	99.04	99.04
150	13753	13796	13903	13817.33	77.24	0.56	148.58	99.05
DOM plasma								
Week 1								
15	5498	5561	5474	5511.00	44.93	0.82	14.91	99.40
100	7980	8071	8010	8020.33	46.37	0.58	99.94	99.94
150	9491	9527	9447	9488.33	40.07	0.42	149.69	99.79
Week 2								
15	5511	5466	5554	5510.33	44.00	0.80	14.89	99.25
100	7987	8068	7968	8007.67	53.11	0.66	99.51	99.51
150	9543	9411	9469	9474.33	66.16	0.70	149.21	99.48
Week 3								
15	5558	5470	5498	5508.67	44.96	0.82	14.83	98.87
100	8046	8009	7971	8008.67	37.50	0.47	99.55	99.55
150	9437	9511	9405	9451.00	54.37	0.58	148.42	98.95

Table 6.33: System suitability results for CIN and DOM in plasma

Parameters	Value (mean ± S.D.)	
	CIN	DOM
HETP (USP)	26.89	28.17
Theoretical plate	55772 ± 24.15	53242 ± 32.25
Tailing factor (Symmetry factor)	0.949 ± 0.14	0.877 ± 0.11

Table 6.34: Results of LOD and LOQ

Parameter	Cinnarizine(plasma)	Domperidone (plasma)
LOD (ng/ml)	1.110984	1.706082
LOQ (ng/ml)	3.36662	5.169945

6.14. In vivo testing

6.14.1. Pharmacokinetic studies

The plasma concentration-time profiles for both drugs are shown in **Figures 6.39 and 6.40.** The pharmacokinetic parameters were computed using PKSolver 2.0 add-in for Microsoft® Excel 2019. The results are shown in **Table 6.35.**
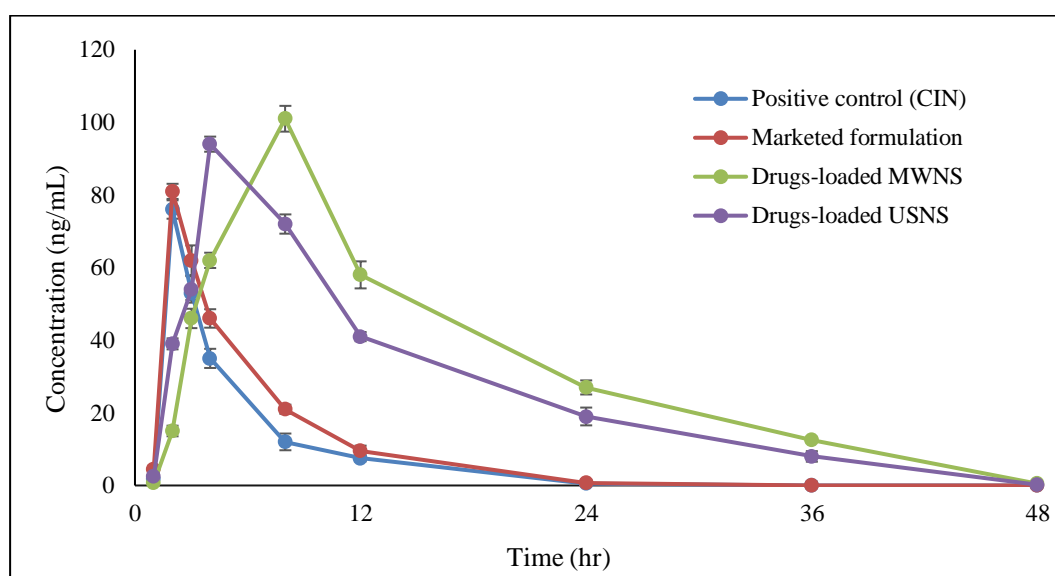
Figure 6.39: Comparative blood concentration-time curve for CIN
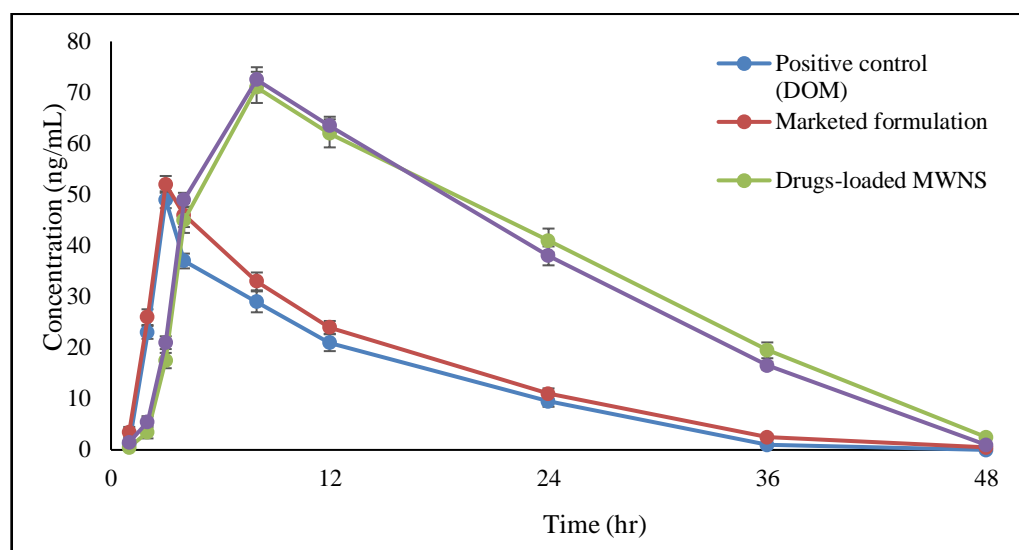
Figure 6.40: Comparative blood concentration-time curve for DOM

Table 6.35: Pharmacokinetics parameters of CIN and DOM

PK parameter	Positive control	Marketed formulation	Drugs-loaded MWNS	Drugs-loaded USNS
Cinnarizine				
$t_{1/2}$ (hr)	3.32 ± 0.36	3.32 ± 0.43	$6.58 \pm 0.45^{*\#}$	$5.59 \pm 0.52^{*\#}$
t_{max} (hr)	2 ± 0	2 ± 0	4 ± 0	4 ± 0
C_{max} (ng/mL)	76 ± 3.18	81 ± 2.47	$101 \pm 2.55^{*\#}$	$94 \pm 1.75^{*\#}$
$AUC_{0\ to\ \infty}$ (ng.hr/mL)	331.79 ± 49.67	430.59 ± 51.9	$1507.95 \pm 121.63^{*\#}$	$1273.31 \pm 108.29^{*\#}$
MRT (hr)	5.75 ± 0.54	6.05 ± 0.37	$14.80 \pm 0.89^{*\#}$	$12.96 \pm 1.06^{*\#}$
V_d (L)	7.41 ± 0.05	$5.69 \pm 0.07^{*}$	$3.22 \pm 0.06^{*\#}$	$3.24 \pm 0.05^{*\#}$
Cl (ng.hr.L^{-1})	1.54 ± 0.02	$1.19 \pm 0.04^{*}$	$0.34 \pm 0.02^{*\#}$	$0.40 \pm 0.03^{*\#}$
Domperidone				
$t_{1/2}$ (hr)	6.44 ± 0.38	5.38 ± 0.50	$5.95 \pm 0.35^{*}$	$4.57 \pm 0.27^{*}$
t_{max} (hr)	3 ± 0	3 ± 0	8 ± 0	8 ± 0
C_{max} (ng/mL)	49 ± 2.87	52 ± 3.75	$71 \pm 2.67^{*\#}$	$72.5 \pm 3.15^{*\#}$
$AUC_{0\ to\ \infty}$	$578.99 \pm$	$689.38 \pm$	$1676.45 \pm$	$1615.10 \pm$

(ng.hr/mL)	39.48	45.75	109.56[*#]	115.75[*#]
MRT (hr)	11.88 ± 0.88	12.53 ± 0.73	18.43 ± 0.59[*#]	17.15 ± 1.02[*#]
V_d (L)	6.17 ± 0.12	4.33 ± 0.08[*]	1.97 ± 0.04[*]	1.57 ± 0.02[*]
Cl (ng.hr.L^{-1})	0.66 ± 0.02	0.56 ± 0.01[*]	0.23 ± 0.02[*#]	0.24 ± 0.02[*#]

[*]Significant difference (p < 0.0001) when compared with plain drug (positive control).

[#]Significant difference (p < 0.0001) when compared with the marketed formulation.

In conclusion, MW-NS and US-NS released CIN and DOM in a controlled manner and were subsequently absorbed in-vivo. The difference in bioavailability between the NS and plain drugs was very significant. When a plain drug suspension or marketed formulation was administered, the absorption phase was quick and sharp, whereas when a drug-loaded NS was administered, absorption continued for a prolonged period of time. It is believed that the slow release of the drugs from the nanosponges in vivo and the elimination of already absorbed drugs are responsible for the post-absorption phase after Cmax.

The absorption of CIN and DOM from the reference tablet was rapid; the mean t_{max} was 2 and 3 hr respectively, while from the NS, the mean t_{max} of CIN from MW-NS as well as US-NS was 4 hr while in the case of DOM, the t_{max} of the drug in both nanosponges was 8 hr. The mean residence time (MRT) was considerably enhanced for both drugs. CIN and DOM plasma concentrations were prolonged by the controlled release tablet in vivo, which indicated that the controlled release tablet delayed peak plasma concentrations in vivo. The mean peak plasma concentration (C_{max}) of CIN from MW-NS and US-NS was 101 ± 2.55 and 94 ± 1.75 ng/mL, while that of the reference tablet at the same dose was 81 ± 2.47 ng/mL. As a result, the controlled release formulation effectively reduced drug release in vivo and subsequent absorption in the first phase.

The mean biological half-life ($t_{1/2}$) of CIN from the controlled release MW-NS, US-NS and the immediate release reference tablet was 6.58 ± 0.45, 5.59 ± 0.52 and 3.32 ± 0.43 h, respectively, whereas those for DOM in the aforementioned formulations was 5.95 ± 0.35, 4.57 ± 0.27, and 5.38 ± 0.50 respectively. The closeness in these values between the sustained release NS and the conventional marketed tablet suggests that the declining phase of the plasma concentration-time curve is only affected by the elimination function. Regardless of the dosage form, the plasma half-life was the same for the same drug substance.

The mean area under the plasma-time curve, $AUC_{0-\infty}$ of controlled release of CIN from MW-NS and USNS was 1507.95 ± 121.63 and 1273.31 ± 108.29 ng.hr/mL respectively, while the mean $AUC_{0-\infty}$ of CIN from the oral reference tablet was 430.59 ± 51.9 ng.hr/mL. The mean area under the plasma-time curve, $AUC_{0-\infty}$ of controlled release of DOM from MW-NS and US-NS was 1676.45 ± 109.56 and 1615.10 ± 115.75 ng.hr/ml respectively, while the mean $AUC_{0-\infty}$ of DOM from the oral reference tablet was 689.38 ± 45.75 ng.hr/mL.

Thus, the overall absorption of CIN from the MW-NS and US-NS was 4.54 and 3.84 times more than its reference tablet, while that of DOM was 2.90 and 2.79 times higher, indicating that the test formulation was more bioavailable than the reference product at the same dose. Thus, the higher bioavailability of NS can be attributed to its sustained release dissolution-enhanced nature.

To compare the in vivo performance of the pharmacokinetic parameters of both the drugs from MW-NS and USNS, a one-way ANOVA tailed by post hoc Tukey's test for multiple group comparisons was performed. The results are shown in **Table 6.36**.

<div align="center">

Table 6.36: PK parameters of CIN and DOM

</div>

PK parameter	Drugs-loaded MWNS	Drugs-loaded USNS
Cinnarizine		
$t_{1/2}$ (hr)	6.58 ± 0.45	$5.59 \pm 0.52^{*}$
t_{max} (hr)	4 ± 0	4 ± 0
C_{max} (ng/mL)	101 ± 2.55	$94 \pm 1.75^{**}$
$AUC_{0\,to\,\infty}$ (ng/mL*hr)	1507.95 ± 121.63	$1273.31 \pm 108.29^{**}$
MRT (hr)	14.80 ± 0.89	$12.96 \pm 1.06^{**}$
Vd (L)	3.22 ± 0.06	3.24 ± 0.05
Cl (ng.hr.L^{-1})	0.34 ± 0.02	$0.40 \pm 0.03^{*}$
Domperidone		
$t_{1/2}$ (hr)	5.95 ± 0.35	4.57 ± 0.27
t_{max} (hr)	8 ± 0	8 ± 0
C_{max} (ng/mL)	71 ± 2.67	72.5 ± 3.15
$AUC_{0\,to\,\infty}$ (ng/mL*hr)	1676.45 ± 109.56	1615.10 ± 115.75

MRT (hr)	18.43 ± 0.59	17.15 ± 1.02
Vd (L)	1.97 ± 0.04	$1.57 \pm 0.0^{**}$
Cl (ng.hr.L^{-1})	0.23 ± 0.02	0.24 ± 0.02

*Significant difference ($p < 0.05$) when compared with drug-loaded MWNS.

**Significant difference ($p < 0.01$) when compared with drug-loaded MWNS.

Based on the observations, it could be observed that there was a statistical difference between the Pharmacokinetic parameters of CIN from both the nanosponges. Based on this it could be concluded that for cinnarizine, nanosponges prepared by microwave-assisted technique proved to be better in enhancing the pharmacokinetic parameters of the drug. Though a similar comparison cannot be made for domperidone. It can still be emphatically said that CDNS, in general, can make a definite improvement in their in vivo performance.

6.14.2. Pharmacodynamics study

Mitchell and his colleagues discovered that gastrointestinal distress brought on by poison or motion causes rats to consume non-nutritive material such as kaolin (China clay), and they concluded that pica is a symptom of illness and is similar to vomiting in other animals [188]. Thus, a rat animal model was employed for assessing the effect of drug-loaded NS on the pica reflex as a direct correlation to emesis in humans. The release of 5-HT from enterochromaffin cells, increased expression of c-fos in the nucleus tractus-solitarian and delayed gastric emptying have all been shown to be associated with pica in humans.

The results in terms of consumption of the non-nutritive substance, kaolin by the rats of various groups have been listed in **Table 6.37.**

Table 6.37: Consumption of kaolin (in grams) by rats of five different groups

Duration	Positive control	Negative control	Marketed formulation	Drugs-loaded MWNS	Drugs-loaded USNS
24 hrs	12.164 ± 1.478	17.391 ± 1.563	10.573 ± 1.496	$3.440 \pm 1.521^{*\#\#}$	$6.121 \pm 1.453^{*\#}$
48 hrs	13.452 ± 1.632	19.987 ± 1.732	12.115 ± 1.648	$5.480 \pm 1.746^{*\#\#}$	$7.251 \pm 1.641^{*\#}$

*Significant difference ($p < 0.0001$) when compared with positive control.

##Significant difference ($p < 0.0001$) when compared with marketed formulation.

#Significant difference ($p < 0.01$) when compared with marketed formulation.

From the results, it was evident that loading the drugs into nanosponges has reduced the consumption amount of kaolin indicating lesser GI distress/ pica in the animals. This could be attributed to the improvement in solubility and overall bioavailability of both drugs. Another interesting observation made was that, on comparison of drugs-loaded NS with the marketed formulation. It could be seen that the values were statistically significant but the level of significance was lower than that observed for drugs-loaded MWNS. This observation is in tandem with that made during the PK studies.

Based on the in vivo tests, we can conclude that the nanosponges prepared by both techniques did show an improvement in the pharmacokinetic as well as the pharmacodynamic attributes of the drugs. With the two drugs chosen in this work, the improvement was more marked for CIN than DOM, And of the two methods of synthesis explored, the results of drugs-loaded MW-NS were found to be better than the ultrasound-assisted NS. Further exploration and studies with other drugs would be able to prove these observations as well as provide a justification for this occurrence.

Chapter 7

Summary and Conclusions

7. SUMMARY AND CONCLUSIONS

Nanosponges based on cyclodextrin are highly cross-linked polymers that have been arranged in three dimensional arrangements. CDNS have a spherical shape in addition to having a crystalline or amorphous structure. Different crosslinkers allow for the development of various NS. The polymer mesh size, polarity, and the release of trapped molecules could be altered by altering the strength and the type of cross-linking is used. They are the good choice for pharmaceutical application due to their biodegradability and modulated drug release. Nanosponges consisting of cyclodextrin can be complexed with a variety of hydrophilic and lipophilic compounds. By using nanosponges, poorly water-soluble molecules can be made more soluble in aqueous solutions, degradable substances can be protected and new delivery mechanisms can be realized in pharmaceuticals, cosmetics, protein/peptide delivery, and diagnostics.

The conventional methods of preparation of CDNS include the fusion/melt method and the solvent evaporation technique. These techniques had been the popular and the most used approach historically. Moreover, conventional methods produce nonuniform reactions due to brusque thermal variations in the bulk mixture, and complications arise during the processing steps. Because of the enormous solvent requirements and heat instability during the process, bulk scaling was particularly challenging using these traditional approaches. Other significant issues with conventional methods included their prolonged duration and low yield during synthesis. It was determined that the majority of investigations and research on nanosponges based on time-consuming conventional procedures, and the resulting product exhibited less crystallinity, resulting in less encapsulation of the molecule under study. It was vital to use more modern methods, such as microwave and ultrasonic-assisted synthesis of CDNS, and to investigate the effects of these newer synthetic techniques on the physical, morphological, and identify significant properties of nanosponges. This revolutionary idea could help a lot in the evolution of uncomplicated, economic, high-speed and expansible methods for the bulk fabrication of monodisperse, steady, and dimension/morphology- regulated NS.

Thus, the current project aimed to explore these methods for the synthesis of CDNS and to complex two drugs within its cavity to expand its application. The reason to study two drugs stemmed from the literature review, which pointed toward all work on CDNS being focused on entrapping one drug. Therefore, it was decided to investigate into the potential

of entrapping two drugs in the cavity of these nanosponges. This could expand the scope of work being done in this area.

The two drugs examined were domperidone and cinnarizine. Both have an ancient legacy of utilization in the management of Meniere's illness, that can cause vertigo, ringing in the ears, nausea, vomiting, and hearing loss. These drugs are plagued with low aqueous solubility and hence would be ideal candidates for the envisioned work. The motive to select these two molecules was based on two reasons. The primary reason was to explore the effect of entrapment in a CDNS on the enhancement of the in vitro and in vivo performances of drugs with different physicochemical properties. Thus, it was decided to use drugs belonging to BCS Class II which are plagued by poor aqueous solubility. BCS Class IV molecules weren't chosen as they also suffer from poor membrane permeability. Because of these reasons, the drugs of these categories often suffer from poor bioavailability. CDNS have the potential of improving the aqueous solubility by entrapping the drug and conveying it into the amorphous form and augmenting the membrane permeability owing to their small sizes. The two drugs were chosen, cinnarizine and domperidone, which are assigned to BCS Class II. The combination also made sense as the drugs work synergistically and are often prescribed concurrently.

The research began with preformulation assessments on the drugs and excipients, as well as the development and validation of an analytical and bioanalytical HPLC method that would be employed for the advancement of the project. In furthermore, calibration curves were constructed. The formulation development process was initiated with the selection of the optimal cyclodextrin. This was attained by phase solubility studies. The findings of the study indicated that β-cyclodextrin (β-CD) and hydroxypropyl-β-cyclodextrin are both suitable monomers for synthesis of CDNS for the selected drugs. Crosslinker selection was the second crucial step in the process. Diphenyl carbonate yielded a solid that was able to be separated and evaluated. Other advantages of diphenyl carbonate, such as its low cost, simplicity of handling, and ability to be transformed into a product with the desired properties, led to its selection.

The Box–Behnken blueprint was used to optimise the synthesis strategy as this one is appropriate for examining quadratic response surfaces and developing 2nd-order polynomial models. Both the microwave-assisted and ultrasonication-assisted processes were optimised with yield and particle size as the primary significant responses. The study design was found to be suitable and the design space was successfully identified.

The batches were scaled up without a hitch and evaluated. FTIR-ATR was used to identify the endpoint of the reaction.

The prepared nanosponges were loaded with the drugs using a lyophilization methodology. The microwave-assisted nanosponges (MW-NS), as well as the ultrasonication-assisted nanosponges (US-NS), were loaded with both drugs individually and in combination and evaluated for physicochemical characteristics, stability, pharmacokinetics and pharmacodynamics. The developed nanosponges have particle sizes ranging from 150 – 200 nm with a very narrow polydispersity index of 0.2 - 0.3. These Nanosponges' zeta potential was discovered to be about -10 mV. The percentage entrapment efficiency of MW-NS was determined to be 80%, while that of US-NS was 61%. FTIR, DSC, and XRD studies proved that the drug was encapsulated within the cavities of the nanosponges as opposed to surface adsorption. The porous nature of the nanocarrier was evident in the SEM scans. In vitro, drug release validated the hypothesis that these nanosponges could enhance the aqueous solubility of poorly water-soluble drugs and at the same time prolong their drug release to ensure better therapy and patient compliance. The dissolution of cinnarizine from each of the nanosponges followed first-order kinetics, whereas that of domperidone was found to be independent of the amount remaining to be released.

Both the nanosponges were successfully loaded into orally disintegrating tablets using Galen IQ 720 as the diluent and Primojel as the superdisintegrant. The prepared tablets had acceptable physicochemical attributes and disintegrated within 30 secs. Accelerated stability studies performed as per the guidelines laid down by ICH showed that the tablets were found to be unchanged for 6 months under both normal and exaggerated conditions. In-vivo pharmacokinetics study further cemented the hypothesis, wherein a 4-fold upsurge in the bioavailability of cinnarizine and a 2.75-fold surge in that of domperidone was observed. The results of all pharmacokinetics parameters were found to be statistically significant in comparison with the unformulated drug as well as the conventional commercial product. Upon performing a one-way ANOVA on the pharmacokinetic (PK) parameters and comparing the nanosponges prepared by both approaches, it was found that the parameters were improved more when using the nanosponges prepared by the microwave-assisted methodology. Similar observations were made while analysing the drug loading in vitro. The increase in the C_{max}, as well as AUC values, could be attributed to the molecular entrapment of the drugs, which when coming in contact with the gastrointestinal fluids dissolved completely, bypassing the

rate-limiting dissolution step. Another reason for the enhanced water solubility of the drugs would be improved wetting and interaction with the GI fluids. This happens due to the hydrophilic exterior of the CDNS.

From the results of the pharmacodynamic studies, it was evident that loading the drugs into nanosponges had reduced the consumption of an amount of kaolin, indicating lesser GI distress/ pica in the animals. This could be attributed to the improvement in solubility and overall bioavailability of both drugs. The observations made earlier were confirmed by the pharmacodynamic studies and revealed the microwave-assisted method to be superior to the ultrasound-assisted method of synthesis of nanosponges as it produced crystalline nanosponges with higher drug loading capacity that showed a prolonged residence time in the body. The AUC of both the drugs entrapped in MWNS was higher than that from USNS, validating the results of the in vitro characterisation.

Thus, the hypothesis that novel modes of synthesis of cyclodextrin-based nanosponges could be successfully developed to yield a more crystalline product with greater yield and lesser time, solvents, and cost, was emphatically proven by the experiments performed. Both the drugs displaying varied physicochemical properties could be successfully entrapped within the cavity of the nanosponges. This could make way for more work being done in this area thereby expanding the scope of CDNS. The analytical techniques used and the results obtained therefrom provided that scientific backup needed to guarantee the validity of the work. Loading two drugs simultaneously has also opened hitherto unexplored applications for nanocarriers. Thus, it could be concluded that the objectives set at the beginning of the work have been successfully met and that the aim has been achieved triumphantly.

Further work needs to be performed to scan various drugs, to streamline the drug selection and entrapment process. Although the study proves that multiple molecules could be entrapped simultaneously but there is a restriction on the size of the individual molecules. The cavities of the nanosponges have shown higher drug loading for drugs having a molecular size below 500 Da. The methods explored were greener as compared to the conventional methods, in terms of reduced use of solvents and shorter reaction time. But the nanosponges prepared by these methods too, produce toxic by-products like phenol as well as the presence of unreacted cross-linking agents. The removal of both of these required the use of organic solvents like ethanol or acetone, as well as, required a lengthy Soxhlet extraction. Thus, more work needs to be put in to shorten the time and effort required for the purification process. Although the raw materials used in the synthesis of the nanosponges enjoy the GRAS status, as well as extensive work, was done to purify the prepared nanosponges, acute as well as long-term toxicity studies need to be

performed to conclusively comment on the safety of these nanocarriers. Lastly, the work can be translated to the clinical testing stage to validate the results of the in vivo tests.

Chapter 8
Bibliography

REFERENCES

[1]   P. Fasinu, V. Pillay, V. M. K. Ndesendo, L. C. du Toit, and Y. E. Choonara, "Diverse approaches for the enhancement of oral drug bioavailability," *Biopharm. Drug Dispos.*, vol. 32, no. 4, pp. 185–209, 2011.

[2]   G. L. Amidon, H. Lennernäs, V. P. Shah, and J. R. Crison, "A theoretical basis for a biopharmaceutic drug classification: the correlation of in vitro drug product dissolution and in vivo bioavailability," *Pharm. Res.*, vol. 12, no. 3, pp. 413–420, 1995.

[3]   L. Di, P. V. Fish, and T. Mano, "Bridging solubility between drug discovery and development," *Drug Discov. Today*, vol. 17, no. 9–10, pp. 486–495, 2012.

[4]   F. Ditzinger *et al.*, "Lipophilicity and hydrophobicity considerations in bio-enabling oral formulations approaches–a PEARRL review," *J. Pharm. Pharmacol.*, vol. 71, no. 4, pp. 464–482, 2019.

[5]   J. Gajdziok, B. Vraníková, K. Kostelanská, D. Vetchỳ, J. Muselík, and R. Goněc, *Drug solubility and bioavailability improvement. Possible methods with emphasis on liquisolid systems formulation*. GRIN Verlag, 2018.

[6]   D. Nedra Karunaratne, I. R Ariyarathna, D. Welideniya, A. Siriwardhana, D. Gunasekera, and V. Karunaratne, "Nanotechnological strategies to improve water solubility of commercially available drugs," *Curr. Nanomedicine Former. Recent Pat. Nanomedicine*, vol. 7, no. 2, pp. 84–110, 2017.

[7]   B. T. Smith, *Remington education: physical pharmacy*. Pharmaceutical Press, 2015.

[8]   J.H. Kim, D.H. Shin, and J.S. Kim, "Preparation, characterization, and pharmacokinetics of liposomal docetaxel for oral administration," *Arch. Pharm. Res.*, vol. 41, no. 7, pp. 765–775, 2018.

[9]   M. Rao, A. Bajaj, I. Khole, G. Munjapara, and F. Trotta, "In vitro and in vivo evaluation of β-cyclodextrin-based nanosponges of telmisartan," *J. Incl. Phenom. Macrocycl. Chem.*, vol. 77, no. 1–4, pp. 135–145, 2013.

[10]   S. Swaminathan *et al.*, "Cyclodextrin-based nanosponges encapsulating camptothecin: Physicochemical characterization, stability and cytotoxicity," *Eur. J. Pharm. Biopharm.*, vol. 74, no. 2, pp. 193–201, 2010.

[11]   M. Laxmi, A. Bhardwaj, S. Mehta, and A. Mehta, "Development and characterization of nanoemulsion as carrier for the enhancement of bioavailability

of artemether," *Artif. Cells Nanomedicine Biotechnol.*, vol. 43, no. 5, pp. 334–344, 2015.

[12] Y. Gong, D. J. Grant, And H. G. Brittain, "Principles of solubility," in *Solvent systems and their selection in pharmaceutics and biopharmaceutics*, Springer, pp. 1–27,2007.

[13] K. T. Savjani, A. K. Gajjar, and J. K. Savjani, "Drug solubility: importance and enhancement techniques," *Int. Sch. Res. Not.*, vol. 2012, 2012.

[14] N. Shahrin, "Solubility and dissolution of drug product: a review," *Int. J. Pharm. Life Sci.*, vol. 2, no. 1, pp. 33–41, 2013.

[15] T. Welton and C. Reichardt, *Solvents and solvent effects in organic chemistry*. John Wiley & Sons, 2011.

[16] M. D. Rawlins, D. B. Henderson, and A. R. Hijab, "Pharmacokinetics of paracetamol (acetaminophen) after intravenous and oral administration," *Eur. J. Clin. Pharmacol.*, vol. 11, no. 4, pp. 283–286, 1977.

[17] J. Siepmann and F. Siepmann, "Mathematical modeling of drug dissolution," *Int. J. Pharm.*, vol. 453, no. 1, pp. 12–24, 2013.

[18] P. S. Mohanachandran, P. G. Sindhumol, and T. S. Kiran, "Superdisintegrants: an overview," *Int. J. Pharm. Sci. Rev. Res.*, vol. 6, no. 1, pp. 105–109, 2011.

[19] R. Duncan, "Nanomedicines in action," *Pharm J*, vol. 273, pp. 485–488, 2004.

[20] F. Trotta, M. Zanetti, and R. Cavalli, "Cyclodextrin-based nanosponges as drug carriers," *Beilstein J. Org. Chem.*, vol. 8, no. 1, pp. 2091–2099, 2012.

[21] D. Singh, G. C. Soni, and S. K. Prajapati, "Recent advances in nanosponges as drug delivery system: a review," *Eur J Pharm Med Res*, vol. 3, pp. 364–71, 2016.

[22] S. Kargozar and M. Mozafari, "Nanotechnology and Nanomedicine: Start small, think big," *Mater. Today Proc.*, vol. 5, no. 7, pp. 15492–15500, 2018.

[23] M. Nasrollahzadeh, M. S. Sajadi, M. Atarod, M. Sajjadi, and Z. Isaabadi, *An introduction to green nanotechnology*. Academic Press, 2019.

[24] B. Indira, S. S. Bolisetti, C. Samrat, S. M. Reddy, and R. Neerudu, "Nanosponges: a new era in drug delivery: review," *J. Pharm. Res.*, vol. 5, no. 12, pp. 5293–5296, 2012.

[25] S. Selvamuthukumar, S. Anandam, K. Krishnamoorthy, and M. Rajappan, "Nanosponges: A novel class of drug delivery system-review," *J. Pharm. Pharm. Sci.*, vol. 15, no. 1, pp. 103–111, 2012.

[26] B. Mognetti *et al.*, "In vitro enhancement of anticancer activity of paclitaxel by a Cremophor free cyclodextrin-based nanosponge formulation," *J. Incl. Phenom. Macrocycl. Chem.*, vol. 74, no. 1–4, pp. 201–210, 2012.

[27] P. Shende *et al.*, "Acute and repeated dose toxicity studies of different β-cyclodextrin-based nanosponge formulations," *J. Pharm. Sci.*, vol. 104, no. 5, pp. 1856–1863, 2015.

[28] F. Trotta, *Cyclodextrin nanosponges and their applications*. John Wiley & Sons, Inc.: Hoboken, NJ, 2011.

[29] M. Vij and P. Wadhwa, "Impacts of Nanotechnology on Pharmaceutical Sciences," in *Smart Nanotechnology with Applications*, CRC Press, pp. 273–278, 2020.

[30] T. C. Diniz *et al.*, "Cyclodextrins improving the physicochemical and pharmacological properties of antidepressant drugs: a patent review," *Expert Opin. Ther. Pat.*, vol. 28, no. 1, pp. 81-92, 2018.

[31] K. H. Frömming and J. Szejtli, "Pharmacokinetics and Toxicology of Cyclodextrins," in *Cyclodextrins in Pharmacy*, vol. 5, Dordrecht: Springer Netherlands, pp. 33–44, 1994.

[32] S. Pawar and P. Shende, "Dual drug delivery of cyclodextrin cross-linked artemether and lumefantrine nanosponges for synergistic action using 23 full factorial designs," *Colloids Surf. Physicochem. Eng. Asp.*, vol. 602, p. 125049, 2020.

[33] M. Tannous, F. Trotta, and R. Cavalli, "Nanosponges for combination drug therapy: state-of-the-art and future directions," *Nanomed.*, vol. 15, no. 7, pp. 643–646, 2020.

[34] F. Trotta and A. Mele, "Nanomaterials: Classification and Properties," in *Nanosponges*, F. Trotta and A. Mele, Eds. Weinheim, Germany: Wiley-VCH Verlag GmbH & Co. KGaA, pp. 1–26, 2019.

[35] F. Trotta, R. Cavalli, W. Tumiatti, O. Zerbinati, C. Roggero, and R. Vallero, "Ultrasound-assisted synthesis of cyclodextrin-based nanosponges," Sep. 04, 2008

[36] F. David, *Nanosponge drug delivery system more effective than direct injection,* 2011.

[37] S. Swaminathan, R. Cavalli, and F. Trotta, "Cyclodextrin-based nanosponges: a versatile platform for cancer nanotherapeutics development," *Wiley Interdiscip. Rev. Nanomed. Nanobiotechnol.*, vol. 8, no. 4, pp. 579–601, 2016.

[38] N. Richhariya, S. K. Prajapati, and U. K. Sharma, "Nanosponges: an innovative drug delivery system," *World J. Pharm. Res.*, vol. 4, no. 7, pp. 1751–1753, 2015.

[39] V. Singh *et al.*, "Ordered and disordered cyclodextrin nanosponges with diverse physicochemical properties," *RSC Adv.*, vol. 7, no. 38, pp. 23759–23764, 2017.

[40] G. V. Yadav and H. P. Panchory, "'Nanosponges' - A boon to the targeted drug delivery system," *J. Drug Deliv. Ther.*, vol. 3, no. 4, Art. no. 4, 2013.

[41] S. Pawar, P. Shende, and F. Trotta, "Diversity of β-cyclodextrin-based nanosponges for transformation of actives," *Int. J. Pharm.*, vol. 565, pp. 333–350, 2019.

[42] K. Tiwari and S. Bhattacharya, "The ascension of nanosponges as a drug delivery carrier: preparation, characterization, and applications," *J. Mater. Sci. Mater. Med.*, vol. 33, no. 3, p. 28, 2022.

[43] R. Pushpalatha, S. Selvamuthukumar, and D. Kilimozhi, "Cyclodextrin nanosponge based hydrogel for the transdermal co-delivery of curcumin and resveratrol: Development, optimization, in vitro and ex vivo evaluation," *J. Drug Deliv. Sci. Technol.*, vol. 52, pp. 55–64, 2019.

[44] M. Kamble, Z. Zaheer, S. Mokale, and R. Zainuddin, "Formulation Optimization and Biopharmaceutical Evaluation of Imatinib Mesylate Loaded β-cyclodextrin Nanosponges," *Pharm. Nanotechnol.*, vol. 7, no. 5, pp. 343–361, 2019.

[45] F. Caldera *et al.*, "Cyclic nigerosyl-1, 6-nigerose-based nanosponges: An innovative pH and time-controlled nanocarrier for improving cancer treatment," *Carbohydr. Polym.*, vol. 194, pp. 111–121, 2018.

[46] F. Trotta, C. Dianzani, F. Caldera, B. Mognetti, and R. Cavalli, "The application of nanosponges to cancer drug delivery," *Expert Opin. Drug Deliv.*, vol. 11, no. 6, pp. 931–941, 2014.

[47] C. P. Dora *et al.*, "Potential of erlotinib cyclodextrin nanosponge complex to enhance solubility, dissolution rate, in vitro cytotoxicity and oral bioavailability," *Carbohydr. Polym.*, vol. 137, pp. 339–349, 2016.

[48] S. Torne, S. Darandale, P. Vavia, F. Trotta, and R. Cavalli, "Cyclodextrin-based nanosponges: effective nanocarrier for Tamoxifen delivery," *Pharm. Dev. Technol.*, vol. 18, no. 3, pp. 619–625, 2013.

[49] S. J. Torne, K. A. Ansari, P. R. Vavia, F. Trotta, and R. Cavalli, "Enhanced oral paclitaxel bioavailability after administration of paclitaxel-loaded nanosponges," *Drug Deliv.*, vol. 17, no. 6, pp. 419–425, 2010.

[50] S. M. Omar, F. Ibrahim, and A. Ismail, "Formulation and evaluation of cyclodextrin-based nanosponges of griseofulvin as pediatric oral liquid dosage form for enhancing bioavailability and masking bitter taste," *Saudi Pharm. J.*, vol. 28, no. 3, pp. 349–361, 2020.

[51] R. Sharma, R. B. Walker, and K. Pathak, "Evaluation of the kinetics and mechanism of drug release from econazole nitrate nanosponge loaded carbapol hydrogel," 2011.

[52] S. Swaminathan, P. R. Vavia, F. Trotta, and S. Torne, "Formulation of betacyclodextrin based nanosponges of itraconazole," *J. Incl. Phenom. Macrocycl. Chem.*, vol. 57, no. 1, pp. 89–94, 2007.

[53] P. K. Shende, R. S. Gaud, R. Bakal, and D. Patil, "Effect of inclusion complexation of meloxicam with β-cyclodextrin-and β-cyclodextrin-based nanosponges on solubility, in vitro release and stability studies," *Colloids Surf. B Biointerfaces*, vol. 136, pp. 105–110, 2015.

[54] C. Conte *et al.*, "β-cyclodextrin nanosponges as multifunctional ingredient in water-containing semisolid formulations for skin delivery," *J. Pharm. Sci.*, vol. 103, no. 12, pp. 3941–3949, 2014.

[55] P. K. Shende, F. Trotta, R. S. Gaud, K. Deshmukh, R. Cavalli, and M. Biasizzo, "Influence of different techniques on formulation and comparative characterization of inclusion complexes of ASA with β-cyclodextrin and inclusion complexes of ASA with PMDA cross-linked β-cyclodextrin nanosponges," *J. Incl. Phenom. Macrocycl. Chem.*, vol. 74, no. 1–4, pp. 447–454, 2012.

[56] F. Trotta and R. Cavalli, "Characterization and applications of new hyper-cross-linked cyclodextrins," *Compos. Interfaces*, vol. 16, no. 1, pp. 39–48, 2009.

[57] R. Cavalli, F. Trotta, and W. Tumiatti, "Cyclodextrin-based nanosponges for drug delivery," *J. Incl. Phenom. Macrocycl. Chem.*, vol. 56, no. 1, pp. 209–213, 2006.

[58] R. Martin, I. Sánchez, R. Cao, and J. Rieumont, "Solubility and kinetic release studies of naproxen and ibuprofen in soluble epichlorohydrin-β-cyclodextrin polymer," *Supramol. Chem.*, vol. 18, no. 8, pp. 627–631, 2006.

[59] M. R. P. Rao, J. Chaudhari, F. Trotta, and F. Caldera, "Investigation of Cyclodextrin-Based Nanosponges for Solubility and Bioavailability Enhancement of Rilpivirine," *AAPS PharmSciTech*, vol. 19, no. 5, pp. 2358–2369, 2018.

[60]   M. R. Rao and C. Shirsath, "Enhancement of bioavailability of non-nucleoside reverse transciptase inhibitor using nanosponges," *AAPS PharmSciTech*, vol. 18, no. 5, pp. 1728–1738, 2017.

[61]   D. Lembo *et al.*, "Encapsulation of Acyclovir in new carboxylated cyclodextrin-based nanosponges improves the agent's antiviral efficacy," *Int. J. Pharm.*, vol. 443, no. 1–2, pp. 262–272, 2013.

[62]   P. R. Vavia, S. Swaminattan, F. Trotta, and R. Cavalli, *Applications of Nanosponges in Drug Delivery XIII International Cyclodextrin Symposium*. Turin, 2006.

[63]   A. Rezaei, J. Varshosaz, M. Fesharaki, A. Farhang, and S. M. Jafari, "Improving the solubility and in vitro cytotoxicity (anticancer activity) of ferulic acid by loading it into cyclodextrin nanosponges," *Int. J. Nanomedicine*, vol. Volume 14, pp. 4589–4599, 2019.

[64]   A. Singireddy and S. Subramanian, "Cyclodextrin nanosponges to enhance the dissolution profile of quercetin by inclusion complex formation," *Part. Sci. Technol.*, vol. 34, no. 3, pp. 341–346, 2016.

[65]   K. A. Ansari, P. R. Vavia, F. Trotta, and R. Cavalli, "Cyclodextrin-based nanosponges for delivery of resveratrol: in vitro characterisation, stability, cytotoxicity and permeation study," *Aaps Pharmscitech*, vol. 12, no. 1, pp. 279–286, 2011.

[66]   A. Deshpande and P. Patel, "Preparation and evaluation of cyclodextrin based atorvastatin nanosponges," *Am J PharmTech Res*, vol. 4, no. 3, pp. 2249–3387, 2014.

[67]   A. A. Olteanu, C.-C. Aramă, C. Radu, C. Mihăescu, and C.-M. Monciu, "Effect of β-cyclodextrins based nanosponges on the solubility of lipophilic pharmacological active substances (repaglinide)," *J. Incl. Phenom. Macrocycl. Chem.*, vol. 80, no. 1, pp. 17–24, 2014.

[68]   F. Trotta *et al.*, "Molecularly imprinted cyclodextrin nanosponges for the controlled delivery of L-DOPA: Perspectives for the treatment of Parkinson's disease," *Expert Opin. Drug Deliv.*, vol. 13, no. 12, pp. 1671–1680, 2016.

[69]   A. P. Sherje, A. Surve, and P. Shende, "CDI cross-linked β-cyclodextrin nanosponges of paliperidone: synthesis and physicochemical characterization," *J. Mater. Sci. Mater. Med.*, vol. 30, no. 6, p. 74, 2019.

[70] G. Yaşayan, B. Şatıroğlu Sert, E. Tatar, and İ. Küçükgüzel, "Fabrication and characterisation studies of cyclodextrin-based nanosponges for sulfamethoxazole delivery," *J. Incl. Phenom. Macrocycl. Chem.*, vol. 97, pp. 175–186, 2020.

[71] N. Rahi and K. Kumar, "Nanosponge: A new era of versatile drug delivery system," *UJPR*, vol. 2, pp. 31–39, 2017.

[72] R. Pushpalatha, S. Selvamuthukumar, and D. Kilimozhi, "Hierarchy analysis of different cross-linkers used for the preparation of cross-linked cyclodextrin as drug nanocarriers," *Chem. Eng. Commun.*, vol. 205, no. 6, pp. 759–771, 2018.

[73] T. S. Patil, N. A. Nalawade, V. K. Kakade, and S. N. Kale, "Nanosponges: A novel targeted drug delivery for cancer treatment," *Int. J. Adv. Res. Dev.*, vol. 2, no. 4, 2017.

[74] S. Shivani and K. K. Poladi, "Nanosponges-novel emerging drug delivery system: A review," *Int. J. Pharm. Sci. Res.*, vol. 6, no. 2, Art. no. 2, 2015.

[75] S. Shrestha and S. Bhattacharya, "Versatile use of nanosponge in the pharmaceutical arena: a mini-review," *Recent Pat. Nanotechnol.*, vol. 14, no. 4, pp. 351–359, 2020.

[76] K. Tiwari and S. Bhattacharya, "The ascension of nanosponges as a drug delivery carrier: preparation, characterization, and applications," *J. Mater. Sci. Mater. Med.*, vol. 33, no. 3, pp. 1–21, 2022.

[77] F. van de Manakker, T. Vermonden, C. F. van Nostrum, and W. E. Hennink, "Cyclodextrin-Based Polymeric Materials: Synthesis, Properties, and Pharmaceutical/Biomedical Applications," *Biomacromolecules*, vol. 10, no. 12, pp. 3157–3175, 2009.

[78] M. Shringirishi, S. K. Prajapati, A. Mahor, S. Alok, P. Yadav, and A. Verma, "Nanosponges: a potential nanocarrier for novel drug delivery-a review," *Asian Pac. J. Trop. Dis.*, vol. 4, pp. S519–S526, 2014.

[79] E. K. Patel and R. J. Oswal, "Nanosponge and micro sponges: a novel drug delivery system," *Int. J. Res. Pharm. Chem.*, vol. 2, no. 2, pp. 2281–2781, 2012.

[80] E. Setijadi, L. Tao, J. Liu, Z. Jia, C. Boyer, and T. P. Davis, "Biodegradable star polymers functionalized with β-cyclodextrin inclusion complexes," *Biomacromolecules*, vol. 10, no. 9, pp. 2699–2707, 2009.

[81] S. Swaminathan *et al.*, "In vitro release modulation and conformational stabilization of a model protein using swellable polyamidoamine nanosponges of

β-cyclodextrin," *J. Incl. Phenom. Macrocycl. Chem.*, vol. 68, no. 1, pp. 183–191, 2010.

[82]   G. Tejashri, B. Amrita, and J. Darshana, "Cyclodextrin based nanosponges for pharmaceutical use: A review," *Acta Pharm.*, vol. 63, no. 3, pp. 335–358, 2013.

[83]   S. Swaminathan and F. Trotta, "Cyclodextrin Nanosponges," in *Nanosponges*, F. Trotta and A. Mele, Eds. Weinheim, Germany: Wiley-VCH Verlag GmbH & Co. KGaA, pp. 27–57, 2019.

[84]   F. Caldera, M. Tannous, R. Cavalli, M. Zanetti, and F. Trotta, "Evolution of Cyclodextrin Nanosponges," *Int. J. Pharm.*, vol. 531, no. 2, pp. 470–479, 2017.

[85]   R. Lala, A. Thorat, and C. Gargote, "Current trends in β-cyclodextrin based drug delivery systems," *Int J Res Ayur Pharm*, vol. 2, no. 5, pp. 1520–1526, 2011.

[86]   S. Tang, L. Kong, J. Ou, Y. Liu, X. Li, and H. Zou, "Application of cross-linked β-cyclodextrin polymer for adsorption of aromatic amino acids," *J. Mol. Recognit. Interdiscip. J.*, vol. 19, no. 1, pp. 39–48, 2006.

[87]   M. Ferro *et al.*, "Anomalous diffusion of Ibuprofen in cyclodextrin nanosponge hydrogels: an HRMAS NMR study," *Beilstein J. Org. Chem.*, vol. 10, no. 1, pp. 2715–2723, 2014.

[88]   A. Alsbaiee, B. J. Smith, L. Xiao, Y. Ling, D. E. Helbling, and W. R. Dichtel, "Rapid removal of organic micropollutants from water by a porous β-cyclodextrin polymer," *nature*, vol. 529, no. 7585, pp. 190–194, 2016.

[89]   P. Patel, A. Deshpande, and S. Nmims, "Patent review on cyclodextrin based nanosponges prepared by different methods: physicochemical characterization, factors influencing formation and applications," *World Journal of Pharmaceutical Sciences.*, 2(4), 380–385, 2014.

[90]   A. Vyas, S. Saraf, and S. Saraf, "Cyclodextrin based novel drug delivery systems," *J. Incl. Phenom. Macrocycl. Chem.*, vol. 62, no. 1–2, pp. 23–42, 2008.

[91]   M. M. Momin, Z. Zaheer, R. Zainuddin, and J. N. Sangshetti, "Extended release delivery of erlotinib glutathione nanosponge for targeting lung cancer," *Artif. Cells Nanomedicine Biotechnol.*, vol. 46, no. 5, pp. 1064–1075, 2018.

[92]   S. Panda, S. V. Vijayalakshmi, S. Pattnaik, and R. P. Swain, "Nanosponges: A novel carrier for targeted drug delivery," *Int. J. Pharmatech Res.*, vol. 8, pp. 213–24, 2015.

[93]   M. Tebyetekerwa, X. Wang, Y. Wu, S. Yang, M. Zhu, and S. Ramakrishna, "Controlled synergistic strategy to fabricate 3D-skeletal hetero-nanosponges with

high performance for flexible energy storage applications," *J. Mater. Chem. A*, vol. 5, no. 40, pp. 21114–21121, 2017.

[94]   J. Guineo-Alvarado *et al.*, "Degree of crosslinking in β-cyclodextrin-based nanosponges and their effect on piperine encapsulation," *Food Chem.*, vol. 340, p. 128132, 2021.

[95]   H. Mashaqbeh, R. Obaidat, and N. Al-Shar'i, "Evaluation and Characterization of Curcumin-β-Cyclodextrin and Cyclodextrin-Based Nanosponge Inclusion Complexation," *Polymers*, vol. 13, no. 23, Art. no. 23, 2021.

[96]   I. K. Jasim, S. N. Abd Alhammid, and A. A. Abdulrasool, "Synthesis and evaluation of B-cyclodextrin Based Nanosponges of 5- Fluorouracil by Using Ultrasound Assisted Method," *Iraqi J. Pharm. Sci. P-ISSN 1683 - 3597 E-ISSN 2521 - 3512*, vol. 29, no. 2, Art. no. 2, 2020.

[97]   A. Matencio *et al.*, "Study of oxyresveratrol complexes with insoluble cyclodextrin based nanosponges: Developing a novel way to obtain their complexation constants and application in an anticancer study," *Carbohydr. Polym.*, vol. 231, p. 115763, 2020.

[98]   S. Allahyari *et al.*, "Preparation and characterization of cyclodextrin nanosponges for bortezomib delivery," *Expert Opin. Drug Deliv.*, vol. 17, no. 12, pp. 1807–1816, 2020.

[99]   G. Yaşayan, B. Şatıroğlu Sert, E. Tatar, and İ. Küçükgüzel, "Fabrication and characterisation studies of cyclodextrin-based nanosponges for sulfamethoxazole delivery," *J. Incl. Phenom. Macrocycl. Chem.*, vol. 97, pp. 175–186, 2020.

[100]   A. Rezaei, J. Varshosaz, M. Fesharaki, A. Farhang, and S. M. Jafari, "Improving the solubility and in vitro cytotoxicity (anticancer activity) of ferulic acid by loading it into cyclodextrin nanosponges," *Int. J. Nanomedicine*, vol. Volume 14, pp. 4589–4599, 2019.

[101]   S. Kumar, Pooja, F. Trotta, and R. Rao, "Encapsulation of Babchi Oil in Cyclodextrin-Based Nanosponges: Physicochemical Characterization, Photodegradation, and In Vitro Cytotoxicity Studies," *Pharmaceutics*, vol. 10, no. 4, Art. no. 4, 2018.

[102]   M. F. Zidan, H. M. Ibrahim, M. I. Afouna, and E. A. Ibrahim, "In vitro and in vivo evaluation of cyclodextrin-based nanosponges for enhancing oral bioavailability of atorvastatin calcium," *Drug Dev. Ind. Pharm.*, vol. 44, no. 8, pp. 1243–1253, 2018.

[103]   R. Zainuddin, Z. Zaheer, J. N. Sangshetti, and M. Momin, "Enhancement of oral bioavailability of anti-HIV drug rilpivirine HCl through nanosponge formulation," *Drug Dev. Ind. Pharm.*, vol. 43, no. 12, Art. no. 12, 2017.

[104]   A. Singireddy, S. Rani Pedireddi, S. Nimmagadda, and S. Subramanian, "Beneficial effects of microwave assisted heating versus conventional heating in synthesis of cyclodextrin based nanosponges," *Mater. Today Proc.*, vol. 3, no. 10, pp. 3951–3959, 2016.

[105]   S. Sapino *et al.*, "Photochemical and antioxidant properties of gamma-oryzanol in beta-cyclodextrin-based nanosponges," *J. Incl. Phenom. Macrocycl. Chem.*, vol. 75, no. 1–2, pp. 69–76, 2013.

[106]   S. S. Darandale and P. R. Vavia, "Cyclodextrin-based nanosponges of curcumin: formulation and physicochemical characterization," *J. Incl. Phenom. Macrocycl. Chem.*, vol. 75, no. 3–4, pp. 315–322, 2013.

[107]   S. Swaminathan *et al.*, "Structural evidence of differential forms of nanosponges of beta-cyclodextrin and its effect on solubilization of a model drug," *J. Incl. Phenom. Macrocycl. Chem.*, vol. 76, no. 1–2, pp. 201–211, Jun. 2013.

[108]   A. P. Sherje, B. R. Dravyakar, D. Kadam, and M. Jadhav, "Cyclodextrin-based nanosponges: A critical review," *Carbohydr. Polym.*, vol. 173, pp. 37–49, 2017.

[109]   S. Anandam and S. Selvamuthukumar, "Optimization of microwave-assisted synthesis of cyclodextrin nanosponges using response surface methodology," *J. Porous Mater.*, vol. 21, no. 6, pp. 1015–1023, 2014.

[110]   D. Singh, G. C. Soni, and S. K. Prajapati, "Recent advances in nanosponges as drug delivery system: a review," *Eur J Pharm Med Res*, vol. 3, pp. 364–71, 2016.

[111]   A. Kumari, A. Jain, P. Hurkat, A. Verma, and S. K. Jain, "Microsponges: a pioneering tool for biomedical applications," *Crit. Rev. Ther. Drug Carr. Syst.*, vol. 33, no. 1, 2016.

[112]   A. Jain, S. K. Prajapati, A. Kumari, N. Mody, and M. Bajpai, "Engineered nanosponges as versatile biodegradable carriers: An insight," *J. Drug Deliv. Sci. Technol.*, vol. 57, p. 101643, 2020.

[113]   R. A. Osmani, P. Kulkarni, S. Manjunatha, R. Vaghela, and R. Bhosale, "Cyclodextrin nanosponge-based systems in drug delivery and nanotherapeutics: Current progress and future prospects," *Org. Mater. Smart Nanocarriers Drug Deliv.*, pp. 659–717, 2018.

[114] S. Wolfgang, "Sample preparation," *Light Scatt. Polym. Solut. Nanoparticle Dispers.*, pp. 43–44, 2007.

[115] S. Shen, Y. Wu, Y. Liu, and D. Wu, "High drug-loading nanomedicines: progress, current status, and prospects," *Int. J. Nanomedicine*, vol. 12, p. 4085, 2017.

[116] S. M. Omar, F. Ibrahim, and A. Ismail, "Formulation and evaluation of cyclodextrin-based nanosponges of griseofulvin as pediatric oral liquid dosage form for enhancing bioavailability and masking bitter taste," *Saudi Pharm. J.*, vol. 28, no. 3, pp. 349–361, 2020.

[117] J. Alongi, M. Poskovic, P. nM Visakh, A. Frache, and G. Malucelli, "Cyclodextrin nanosponges as novel green flame retardants for PP, LLDPE and PA6," *Carbohydr. Polym.*, vol. 88, no. 4, pp. 1387–1394, 2012.

[118] G. A. Stephenson, "Applications of X-ray powder diffraction in the pharmaceutical industry," *Rigaku J*, vol. 22, no. 1, pp. 2–15, 2005.

[119] H. G. Brittain, S. J. Bogdanowich, D. E. Bugay, J. DeVincentis, G. Lewen, and A. W. Newman, "Physical characterization of pharmaceutical solids," *Pharm. Res.*, vol. 8, no. 8, pp. 963–973, 1991.

[120] V. Cinà, M. Russo, G. Lazzara, D. C. Martino, and P. L. Meo, "Pre-and post-modification of mixed cyclodextrin-calixarene co-polymers: a route towards tunability," *Carbohydr. Polym.*, vol. 157, pp. 1393–1403, 2017.

[121] I. Mallard *et al.*, "Polydisperse methyl β-cyclodextrin–epichlorohydrin polymers: variable contact time 13C CP-MAS solid-state NMR characterization," *Beilstein J. Org. Chem.*, vol. 11, no. 1, pp. 2785–2794, 2015.

[122] G. Crini *et al.*, "Solid-state NMR characterization of cyclomaltoheptaose (β-cyclodextrin) polymers using high-resolution magic angle spinning with gradients," *J. Appl. Polym. Sci.*, vol. 75, no. 10, pp. 1288–1295, 2000.

[123] G. Yurtdaş, M. Demirel, and L. Genç, "Inclusion complexes of fluconazole with β-cyclodextrin: physicochemical characterization and in vitro evaluation of its formulation," *J. Incl. Phenom. Macrocycl. Chem.*, vol. 70, no. 3–4, pp. 429–435, 2011.

[124] K. A. Connors and T. Higuchi, "Phase solubility techniques," *Adv Anal Chem Instrum*, vol. 4, no. 2, 1965.

[125] N. Abbas *et al.*, "Development and evaluation of scaffold-based nanosponge formulation for controlled drug delivery of naproxen and ibuprofen," *Trop. J. Pharm. Res.*, vol. 17, no. 8, pp. 1465–1474, 2018.

[126] P. Srinivas and A. Jahnavi Reddy, "Formulation and evaluation of isoniazid loaded nanosponges for topical delivery," *Pharm. Nanotechnol.*, vol. 3, no. 1, pp. 68–76, 2015.

[127] S. Kumar, P. Dalal, and R. Rao, "Cyclodextrin nanosponges: a promising approach for modulating drug delivery," in *Colloid Science in Pharmaceutical Nanotechnology*, IntechOpen, 2019.

[128] Y. Zhang, F.-C. Meng, Y.-L. Cui, and Y.-F. Song, "Enhancing effect of hydroxypropyl-β-cyclodextrin on the intestinal absorption process of genipin," *J. Agric. Food Chem.*, vol. 59, no. 20, pp. 10919–10926, 2011.

[129] Y. Zhang, Y.-L. Cui, L.-N. Gao, and H.-L. Jiang, "Effects of β-cyclodextrin on the intestinal absorption of berberine hydrochloride, a P-glycoprotein substrate," *Int. J. Biol. Macromol.*, vol. 59, pp. 363–371, 2013.

[130] P. Kumari, P. Singh, and A. Singhal, "Cyclodextrin-based nanostructured materials for sustainable water remediation applications," *Environ. Sci. Pollut. Res.*, vol. 27, no. 26, pp. 32432–32448, 2020.

[131] S. Nazerdeylami, J. B. Ghasemi, G. M. Ziarani, A. Amiri, and A. Badiei, "Direct monitoring of diclofenac using a supramolecular fluorescent approach based on β-cyclodextrin nanosponge," *J. Mol. Liq.*, vol. 336, p. 116104, 2021.

[132] S. Baboota, R. Khanna, S. P. Agarwal, J. Ali, and A. Ahuja, "Cyclodextrins in drug delivery systems: An update," *Pharm. Inf.*, no. 58, pp. 73–74, 2003.

[133] A. Vishwakarma, P. Nikam, R. Mogal, and S. Talele, "Review on nanosponges: A benefication for novel drug delivery," *Int J PharmTech Res*, vol. 6, pp. 11–20, 2014.

[134] A. Matencio *et al.*, "Study of oxyresveratrol complexes with insoluble cyclodextrin based nanosponges: Developing a novel way to obtain their complexation constants and application in an anticancer study," *Carbohydr. Polym.*, vol. 231, p. 115763, 2020.

[135] R. Sharma and K. Pathak, "Polymeric nanosponges as an alternative carrier for improved retention of econazole nitrate onto the skin through topical hydrogel formulation," *Pharm. Dev. Technol.*, vol. 16, no. 4, pp. 367–376, 2011.

[136] S. Shivani and K. K. Poladi, "Nanosponges-novel emerging drug delivery system: A review," *Int. J. Pharm. Sci. Res.*, vol. 6, no. 2, p. 529, 2015.

[137] F. Trotta, P. Shende, and M. Biasizzo, "Method for preparing dextrin nanosponges," *PCT Pat Appl WO2012147069 A*, vol. 1, 2012.

[138]   D. Lembo, F. Trotta, and R. Cavalli, *Cyclodextrin-based nanosponges as vehicles for antiviral drugs: challenges and perspectives*. Future Medicine, 2018.

[139]   R. Cavalli, A. K. Akhter, A. Bisazza, P. Giustetto, F. Trotta, and P. Vavia, "Nanosponge formulations as oxygen delivery systems," *Int. J. Pharm.*, vol. 402, no. 1–2, pp. 254–257, 2010.

[140]   D. Schwartz, S. Sofia, and W. Friess, "Integrity and stability studies of precipitated rhBMP-2 microparticles with a focus on ATR-FTIR measurements," *Eur. J. Pharm. Biopharm.*, vol. 63, no. 3, pp. 241–248, 2006.

[141]   J. Li and X. J. Loh, "Cyclodextrin-based supramolecular architectures: syntheses, structures, and applications for drug and gene delivery," *Adv. Drug Deliv. Rev.*, vol. 60, no. 9, pp. 1000–1017, 2008.

[142]   H. Wang *et al.*, "A Supramolecular Approach for Preparation of Size-Controlled Nanoparticles," *Angew. Chem.*, vol. 121, no. 24, pp. 4408–4412, 2009.

[143]   Desai, C. T., & Prabhakar, B. R., *Cyclodextrin nanosponges,In Encyclopaediaof biomedical polymers and polymeric biomaterials. pp. 1–12. Taylor & Francis.2014*.

[144]   N. Blanchemain *et al.*, "Polyester vascular prostheses coated with a cyclodextrin polymer and activated with antibiotics: cytotoxicity and microbiological evaluation," *Acta Biomater.*, vol. 4, no. 6, pp. 1725–1733, 2008.

[145]   J. Zhang and P. X. Ma, "Host–guest interactions mediated nano-assemblies using cyclodextrin-containing hydrophilic polymers and their biomedical applications," *Nano Today*, vol. 5, no. 4, pp. 337–350, 2010.

[146]   V. Budhwar, "Cyclodextrin complexes: An approach to improve the physicochemical properties of drugs and applications of cyclodextrin complexes," *Asian J. Pharm. AJP*, vol. 12, no. 02, 2018.

[147]   A. Gonzalez Pereira, M. Carpena, P. García Oliveira, J. C. Mejuto, M. A. Prieto, and J. Simal Gandara, "Main applications of cyclodextrins in the food industry as the compounds of choice to form host–guest complexes," *Int. J. Mol. Sci.*, vol. 22, no. 3, p. 1339, 2021.

[148]   J. R. Lakkakula and R. W. Maçedo Krause, "A vision for cyclodextrin nanoparticles in drug delivery systems and pharmaceutical applications," *Nanomed.*, vol. 9, no. 6, pp. 877–894, 2014.

[149] S. Swaminathan and F. Trotta, "Cyclodextrin Nanosponges," in *Nanosponges*, F. Trotta and A. Mele, Eds. Weinheim, Germany: Wiley-VCH Verlag GmbH & Co. KGaA, pp. 27–57, 2019.

[150] A. Singireddy, S. Rani Pedireddi, S. Nimmagadda, and S. Subramanian, "Beneficial effects of microwave assisted heating versus conventional heating in synthesis of cyclodextrin based nanosponges," *Mater. Today Proc.*, vol. 3, no. 10, pp. 3951–3959, 2016.

[151] S. A. Kumari and S. M. Naga, "Validated RP-HPLC method for simultaneous estimation of Cinnarizine and Domperidone in bulk and pharmaceutical dosage form," *J Pharm Sci. Innov.*, vol. 2, no. 2, pp. 46–50, 2013.

[152] R. Khursheed *et al.*, "Development and validation of RP-HPLC method for simultaneous determination of curcumin and quercetin in extracts, marketed formulations, and self-nanoemulsifying drug delivery system," *Re GEN Open*, vol. 1, no. 1, pp. 43–52, 2021.

[153] R. Kumar *et al.*, "Development and validation of RP-HPLC method for estimation of fisetin in rat plasma," *South Afr. J. Bot.*, vol. 140, pp. 284–289, 2021.

[154] T. Higuchi and K. A. Connors, "Phase Solubility Techniques," *Adv. Anal. Chem. Instrum.*, vol. 4, pp. 117–212, 1965.

[155] S. Anandam and S. Selvamuthukumar, "Optimization of microwave-assisted synthesis of cyclodextrin nanosponges using response surface methodology," *J. Porous Mater.*, vol. 21, no. 6, pp. 1015–1023, 2014.

[156] S. M. Omar, F. Ibrahim, and A. Ismail, "Formulation and evaluation of cyclodextrin-based nanosponges of griseofulvin as pediatric oral liquid dosage form for enhancing bioavailability and masking bitter taste," *Saudi Pharm. J.*, vol. 28, no. 3, pp. 349–361, 2020.

[157] S. Sharma, T. Sharma, M. Deep, and A. Sharma, "Techniques to Determine Powder Flow Properties".

[158] M. P. Paarakh, P. A. Jose, C. M. Setty, and G. P. Christoper, "Release kinetics–concepts and applications," *Int J Pharm Res Technol*, vol. 8, no. 1, pp. 12–20, 2018.

[159] R. Khursheed *et al.*, "Development and validation of RP-HPLC based bioanalytical method for simultaneous estimation of curcumin and quercetin in rat's plasma," *South Afr. J. Bot.*, 2021.

[160] A. Police *et al.*, "Development and validation of an RP-HPLC method for the quantitation of odanacatib in rat and human plasma and its application to a pharmacokinetic study," *Biomed. Chromatogr.*, vol. 29, no. 11, pp. 1664–1669, 2015.

[161] Y. Harahap, N. Azizah, and R. Andalusia, "Simultaneous Analytical Method Development of 6-Mercaptopurine and 6-Methylmercaptopurine in Plasma by High Performance Liquid Chromatography-Photodiode Array.," *J. Young Pharm.*, vol. 9, 2017.

[162] Madhuri Dinde, "Development and Evaluation of Cinnarizine Loaded Nanosponges: Pharmacodynamic and Pharmacokinetic Study on Wistar Rats," *Int J Pharm Sci Rev Res*, vol. 65 (2), pp. 96–105, 2020.

[163] G. J. Sanger, J. D. Holbrook, and P. L. Andrews, "The translational value of rodent gastrointestinal functions: a cautionary tale," *Trends Pharmacol. Sci.*, vol. 32, no. 7, pp. 402–409, 2011.

[164] N. Takeda, S. Hasegawa, M. Morita, and T. Matsunaga, "Pica in rats is analogous to emesis: an animal model in emesis research," *Pharmacol. Biochem. Behav.*, vol. 45, no. 4, pp. 817–821, 1993.

[165] R. J. McCaffrey, "Appropriateness of kaolin consumption as an index of motion sickness in the rat," *Physiol. Behav.*, vol. 35, no. 2, pp. 151–156, 1985.

[166] K. Yamamoto, S. Matsunaga, M. Matsui, N. Takeda, and A. Yamatodani, "Pica in Mice as New Model for the Study of Emesis.," *Methods Find. Exp. Clin. Pharmacol.*, vol. 24, no. 3, pp. 135–138, 2002.

[167] N. Sirisha and S. Kumari, "Validated RP-HPLC method for simultaneous estimation of sinnarizine and domperidone in bulk and pharmaceutical dosage form," *J. Pharm. Sci. Innov.*, vol. 2, no. 2, pp. 46–50, 2013.

[168] M. M. Abdelrahman, "Simultaneous determination of Cinnarizine and Domperidone by area under curve and dual wavelength spectrophotometric methods," *Spectrochim. Acta. A. Mol. Biomol. Spectrosc.*, vol. 113, pp. 291–296, 2013.

[169] B. Javali *et al.*, "Development and Validation of UV Spectrophotom- etric Method for Simultaneous Estimation of Omeprazole and Domperidone in Capsule Dosage forms," *Glob. J. Pharm. Pharm. Sci.*, vol. 1, no. 2, 2017.

[170] S. Raghuvanshi and K. Pathak, "Recent advances in delivery systems and therapeutics of cinnarizine: a poorly water soluble drug with absorption window in stomach," *J. Drug Deliv.*, vol-2, 2014.

[171] X. Chai *et al.*, "Fused Deposition Modeling (FDM) 3D Printed Tablets for Intragastric Floating Delivery of Domperidone," *Sci. Rep.*, vol. 7, no. 1, Art. no. 1, 2017.

[172] C. H. Gu, D. Rao, R. B. Gandhi, J. Hilden, and K. Raghavan, "Using a novel multicompartment dissolution system to predict the effect of gastric pH on the oral absorption of weak bases with poor intrinsic solubility," *J. Pharm. Sci.*, vol. 94, no. 1, pp. 199–208, 2005.

[173] R. Paus, E. Hart, Y. Ji, and G. Sadowski, "Solubility and Caloric Properties of Cinnarizine," *J. Chem. Eng. Data*, vol. 60, no. 8, pp. 2256–2261, 2015.

[174] A. Aboutaleb, S. Abdel-Rahman, M. Ahmed, and M. Younis, "Improvement of Domperidone Solubility and Dissolution Rate by Dispersion in Various Hydrophilic Carriers," *J. Appl. Pharm. Sci.*, pp. 133–139, 2016.

[175] B. A. Daihom, E. R. Bendas, M. I. Mohamed, and A. A. Badawi, "Development and in vitro evaluation of domperidone/Dowex resinate embedded gastro-floatable emulgel and effervescent alginate beads," *J. Drug Deliv. Sci. Technol.*, vol. 59, p. 101941, 2020.

[176] E. M. M. Del Valle, "Cyclodextrins and their uses: a review," *Process Biochem.*, vol. 39, no. 9, pp. 1033–1046, 2004.

[177] T. Jarvinen, K. Järvinen, N. Schwarting, and V. J. Stella, "beta-cyclodextrin derivatives, SBE4-beta-CD and HP-beta-CD, increase the oral bioavailability of cinnarizine in beagle dogs," *J. Pharm. Sci.*, vol. 84, no. 3, pp. 295–299, 1995.

[178] M. Patel and R. Hirlekar, "Multicomponent cyclodextrin system for improvement of solubility and dissolution rate of poorly water soluble drug," *Asian J. Pharm. Sci.*, vol. 14, no. 1, pp. 104–115, 2019.

[179] J. Guineo-Alvarado *et al.*, "Degree of crosslinking in β-cyclodextrin-based nanosponges and their effect on piperine encapsulation," *Food Chem.*, vol. 340, p. 128132, 2021.

[180] M. Shringirishi, A. Mahor, R. Gupta, S. K. Prajapati, K. Bansal, and P. Kesharwani, "Fabrication and characterization of nifedipine loaded β-cyclodextrin nanosponges: An in vitro and in vivo evaluation," *J. Drug Deliv. Sci. Technol.*, vol. 41, pp. 344–350, 2017.

[181] F. Trotta and A. Mele, *Nanosponges: Synthesis and Applications*. John Wiley & Sons, 2019.

[182] N. Rahi and K. Kumar, "Nanosponges: a new era of versatile drug delivery system," *Univers. J. Pharm. Res.*, vol. 2, no. 3, 2017.

[183] S. Bhattacharjee, "DLS and zeta potential – What they are and what they are not?," *J. Controlled Release*, vol. 235, pp. 337–351, 2016.

[184] S. A. Khan *et al.*, "β-Cyclodextrin-based (IA-co-AMPS) Semi-IPNs as smart biomaterials for oral delivery of hydrophilic drugs: Synthesis, characterization, in-Vitro and in-Vivo evaluation," *J. Drug Deliv. Sci. Technol.*, vol. 60, p. 101970, 2020.

[185] S. Pawar and P. Shende, "Dual drug delivery of cyclodextrin cross-linked artemether and lumefantrine nanosponges for synergistic action using 23 full factorial designs," *Colloids Surf. Physicochem. Eng. Asp.*, vol. 602, p. 125049, 2020.

[186] F. Caldera, M. Tannous, R. Cavalli, M. Zanetti, and F. Trotta, "Evolution of Cyclodextrin Nanosponges," *Int. J. Pharm.*, vol. 531, no. 2, pp. 470–479, 2017.

[187] V. Singh *et al.*, "Ordered and disordered cyclodextrin nanosponges with diverse physicochemical properties," *RSC Adv.*, vol. 7, no. 38, pp. 23759–23764, 2017.

[188] D. Mitchell, J. D. Laycock, and W. F. Stephens, "Motion sickness-induced pica in the rat," *Am. J. Clin. Nutr.*, vol. 30, no. 2, pp. 147–150, 1977.

Dated: 06 Dec 2019

Mohit Vij
Registration Number: 41800748
Programme Name: Doctor of Philosophy (Pharmaceutics)

Subject: Letter of Candidacy for Ph.D.

Dear Candidate,

We are very pleased to inform you that the Department Doctoral Board has approved your candidacy for the Ph.D. Programme on 06 Dec 2019 by accepting your research proposal entitled: "Formulation, characterization and evaluation of nanosponge-based drug delivery system for poorly soluble drugs"

As a Ph.D. candidate you are required to abide by the conditions, rules and regulations laid down for Ph.D. Programme of the University, and amendments, if any, made from time to time.

We wish you the very best!!

In case you have any query related to your programme, please contact Centre of Research Degree Programmes.

Head

Centre for Research Degree Programmes

Note:-This is a computer generated certificate and no signature is required. Please use the reference number generated on this certificate for future conversations.

LIST OF PUBLICATIONS

1. Vij Mohit, Wadhwa Pankaj*, Microwave-Assisted Fabrication of Cyclodextrin-Based Nanosponges for Solubility Enhancement, ECS Trans. 2022; Vol-107, 1214. DOI 10.1149/10701.12143ecst.

2. Wadhwa Pankaj*, Vij Mohit and Dand Neha, Wave-Assisted Techniques, a Greener and Quicker Alternative to Synthesis of Cyclodextrin-Based Nanosponges: A Review, Recent Patents on Nanotechnology 2023; 17(). https://dx.doi.org/10.2174/1872210516666220928114103.

3. Vij Mohit, Dand Neha and Wadhwa Pankaj *, A Review on the Applications of Nano-medicines in Treatments of Metabolic Diseases, Recent Innovations in Chemical Engineering 2021; 14(4). DOI: 10.2174/2405520414666210121160001.

4. Vij Mohit, Wadhwa Pankaj*, Impacts of Nanotechnology on Pharmaceutical Sciences, Smart Nanotechnology with Applications 2020; (pp.273-278). DOI:10.1201/9781003097532-17.

5. Vij Mohit, Neha Dand, Lalit Kumar, Amardeep Ankalgi, Pankaj Wadhwa, Sultan Alshehri, Faiyaz Shakeel, Mohammed M. Ghoneim, Prawez Alam, and Shahid Ud Din Wani, RP-HPLC-Based Bioanalytical Approach for Simultaneous Quantitation of Cinnarizine and Domperidone in Rat Plasma, Separations 2023; 10(3):159. https://doi.org/10.3390/separations10030159.

6. Vij Mohit, Neha Dand, Lalit Kumar, Pankaj Wadhwa, Shahid Ud Din Wani, Wael A. Mahdi, Sultan Alshehri, Prawez Alam, and Faiyaz Shakeel, Optimisation of a Greener-Approach for the Synthesis of Cyclodextrin-Based Nanosponges for the Solubility Enhancement of Domperidone, a BCS Class II Drug, Pharmaceuticals 2023; 16(4):567. https://doi.org/10.3390/ph16040567.

IEC
UNIVERSITY
THE KNOWLEDGE EXPERTS

HIMACHAL PRADESH

INTERNATIONAL CONFERENCE CUM RESEARCHER'S SUMMIT-2021

ON

RESEARCH & DEVELOPMENT IN PHARMACEUTICAL SCIENCES: UPDATES AND PERSPECTIVES

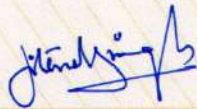Organized by **IEC School of Pharmacy**

10th-11th September, 2021

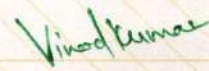**IEC UNIVERSITY**, Himachal Pradesh

THIS IS TO CERTIFY THAT

MOHIT VIJ

**PARTICIPATED IN THE CONFERENCE AND
PRESENTED POSTER/ORAL PRESENTATION ON**

Solubility enhancement of Annarizine by fabrication of cyclo-dextrin - based Nanosponges employing a microwave -assisted method.

and got _____ award on recommendation of the evaluation panel

Professor (Dr) Jitender Singh
Vice-chancellor I/c

Er. Vinod Kumar
Registrar

CONFERENCE SUPPORT

Biozenta | innova CAPTAB | BIOSAFE | HP-PERC |

IEC UNIVERSITY

Pinjore -Nalagarh National Highway Atal Shiksha Nagar, Kallujhanda, Baddi, District Solan, Himachal Pradesh

Certificate of Poster Presentation

AICTE Sponsored
Online National Conference on
"Precision Medicine : Current
Scenario and Future Aspects"
24th-25th September 2021.

PHARMACY: ALWAYS
TRUSTED FOR YOUR
HEALTH.

Sri Aurobindo
Institute of Pharmacy

AICTE
All India Council for Technical Education

SAIPNC 2021

Sri Aurobindo Institute of Pharmacy, Indore (M.P.)

hereby declares that

Mohit Vij
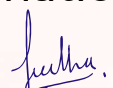
has presented the following abstract as author:

Solubility Enhancement Of Cinnarizine By Fabrication Of Cyclodextrin-Based Nanosponges Employing An Ultrasound-Assisted Method

As a poster during the online national conference 2021.

Convenor	Co-Convenor	Coordinator	Organizing Secretary
Prof. S. C. Chaturvedi	Dr. Gaurav Kant Saraogi	Dr. (Mrs.) Sudha Vengurlekar	Mr. Sunil Kumar Dwivedi

Ref. No- PBRI/IAEC/2022032

Date: 28/03/22

CERTIFICATE

It is hereby certified that animal experimentation of research work entitled **"Formulation, characterization and evaluation of nanosponge-based drug delivery system for poorly soluble drugs"** of **Mr. Mohit Vij** is approved by Institutional Animal Ethics Committee (IAEC) of Pinnacle Biomedical Research Institute (PBRI),Bhopal (Reg.No. PBRI/462).

Approval No: PBRI/IAEC/29-03/010

Species: Albino Wistar rats

No of animals sanctioned/utilized: 30

Sex: Male

Manager
Research and Development

Pinnacle Biomedical Research Institute (PBRI)

Bharat Scout and Guide Campus, Near Depot Square, Shanti Marg, Shamla Hills, Bhopal (M.P.) – 462003
Contact No.– 0755-2665174;+9194258-90029   e-mail.–pbrinstitute@gmail.com   Web:www.pbri.in

Ref. No-PBRI/Cer/2022035

CERTIFICATE

This is to certify that preclinical studies of research work entitled **"Formulation, characterization and evaluation of nanosponge-based drug delivery system for poorly soluble drugs"** assigned to **Mr. Mohit Vij** was completed from Pinnacle Biomedical Research Institute (PBRI), Bhopal.

15April 2022
Bhopal

Manager
Research & Development